

Spring 1-1-2013

Improved Modeling of Residential Air Conditioners and Heat Pumps for Energy Calculations

Dylan Spencer Cutler

University of Colorado at Boulder, dylancutler@yahoo.com

Follow this and additional works at: https://scholar.colorado.edu/cven_gradetds



Part of the [Architectural Engineering Commons](#), and the [Civil Engineering Commons](#)

Recommended Citation

Cutler, Dylan Spencer, "Improved Modeling of Residential Air Conditioners and Heat Pumps for Energy Calculations" (2013). *Civil Engineering Graduate Theses & Dissertations*. 272.

https://scholar.colorado.edu/cven_gradetds/272

This Thesis is brought to you for free and open access by Civil, Environmental, and Architectural Engineering at CU Scholar. It has been accepted for inclusion in Civil Engineering Graduate Theses & Dissertations by an authorized administrator of CU Scholar. For more information, please contact cuscholaradmin@colorado.edu.

**Improved Modeling of Residential Air Conditioners and
Heat Pumps for Energy Calculations**

by

Dylan S. Cutler

B.A., Middlebury College, 2004

A thesis submitted to the
Faculty of the Graduate School of the
University of Colorado in partial fulfillment
of the requirements for the degree of
Masters Of Science
Department of Civil, Environmental and Architectural Engineering

2013

This thesis entitled:
Improved Modeling of Residential Air Conditioners and Heat Pumps for Energy Calculations
written by Dylan S. Cutler
has been approved for the Department of Civil, Environmental and Architectural Engineering

Michael Brandemuehl

Moncef Krarti

Jon Winkler

Date _____

The final copy of this thesis has been examined by the signatories, and we find that both the content and the form meet acceptable presentation standards of scholarly work in the above mentioned discipline.

Cutler, Dylan S. (M.S.)

Improved Modeling of Residential Air Conditioners and Heat Pumps for Energy Calculations

Thesis directed by Prof. Michael Brandemuehl

This thesis provides the capability for improved predictions of the annual energy use of residential air conditioners and heat pumps. The annual simulation engine - EnergyPlus - was used to evaluate the effects that manufacturers data has on predicted annual energy consumption. A new approach to modeling residential air conditioners and heat pumps (inside of the framework of EnergyPlus) was developed and is presented here. The new approach has updated system information and involves a reduced number of user inputs. This approach was also adjusted for use with the simulation engine, DOE-2.

To inform this research, manufacturer data was collected for the majority of currently available air conditioners and heat pumps. This data was parsed and written into a SQLite database that was used to generate full sets of model inputs for over 450 heat pumps and air conditioners. The predicted performance of these different units was evaluated through annual simulation in EnergyPlus. Inspection of the simulation results led to questions regarding the quality of data coming from the manufacturers. The combination of questionable data and the benefits of simplified model inputs led to a sensitivity analysis on the various model inputs.

The results of this sensitivity analysis showed limited impact from the complex regression curve-fits on the expanded performance tables, especially for single speed units. Representative curves were selected and a parametric study was performed in various climates that demonstrated the impact of using the selected curves in place of individual unit curves. Rated values were the cause of most of the variability observed in the initial simulations. Rated values were evaluated through a comparison with AHRI published data. Results from the sensitivity study and the rated value comparison led to recommendations for best modeling practices. Information on how the manufacturers' data impacted predicted energy use can be used to inform future reporting standards.

Acknowledgements

The author would like to thank the US Department of Energy and the National Renewable Energy Lab (NREL) for supporting this research effort.

Special thanks go out to my advisor at the University of Colorado: Mike Brandemuehl, and my technical lead at NREL: Craig Christensen. Their knowledge, patience, and guidance throughout the entire research effort made this work possible.

I would like to extend special thanks to Neal Kruis and Jon Winkler for their continual support and advice throughout the project. They were always available to discuss difficult research questions and provided excellent advice on research methodology. I would also like to thank Moncef Krarti, and Jon Winkler for agreeing to be a part of my defense committee; I appreciate your advice and comments.

Finally, I would like to thank the entire BSP faculty and students for providing an amazing and stimulating graduate education. It was a great experience.

Contents

Chapter	
1	Introduction 1
1.1	Motivation 1
1.2	Objectives 3
1.3	Methodology 5
2	Background and Literature Review 9
2.1	Unitary System Overview 9
2.2	Overview of Equipment Efficiency Metrics 11
2.3	Key Characteristics of Direct Expansion Systems 14
2.3.1	Capacity 14
2.3.2	Efficiency 15
2.3.3	Cycling Losses 16
2.3.4	Defrost Cycle 18
2.3.5	Indoor Fan 19
2.4	Literature Review 20
3	Data Review and Compilation 24
3.1	Discussion of Data: Availability, Acquisition, and Formatting 24
3.2	AHRI Data 25
3.2.1	Required Testing Conditions 25

3.2.2	Access to AHRI Data	26
3.2.3	Acceptable Tolerances in AHRI Data	27
3.3	Manufacturer’s Expanded Performance Tables	27
3.3.1	Processing of the Expanded Performance Tables	32
4	In Depth Model Descriptions	35
4.1	EnergyPlus and DOE-2 Split System Models	35
4.1.1	EnergyPlus - Single Speed: Cooling	35
4.1.2	EnergyPlus - Multi Speed: Cooling	39
4.1.3	EnergyPlus - Single Speed: Heating	42
4.1.4	EnergyPlus - Multi Speed: Heating	44
4.1.5	Differences in DOE-2	44
4.2	Summary of Model Assumptions	49
5	Generating Model Inputs and Data Evaluation	51
5.1	Generating Model Inputs	51
5.2	Data Evaluation Process	55
5.2.1	Visual Inspection	55
5.2.2	Calculation of Bypass Factor	57
5.2.3	Replication of the EnergyPlus Algorithms Through Engineering Equation Solver (EES)	61
5.2.4	Visualization of the Generated Curve Fits	66
5.3	Conclusions From Data Evaluation	70
6	Sensitivity Study on Model Inputs	72
6.1	Batch Run Methodology	73
6.1.1	Generating the Input Files	73
6.1.2	Description of Building Used in the Input File	74
6.1.3	Removing Nominal Capacity from the Picture	74

6.1.4	Part Load	75
6.2	Initial Results	76
6.3	Sensitivity Study	80
6.3.1	Curve Sensitivity Results - Temperature Curves	81
6.3.2	Curve Sensitivity Results - Flow Fraction Curves	83
6.4	Summary of Curve Sensitivity Results	88
6.5	Two Stage Sensitivity	89
6.6	Selecting Representative Curves	91
6.7	Impact of Using Fixed Curves	92
6.8	Curve Coefficients for Energy Modeling (SI and IP)	99
7	Rated Values - SEER/HSPF Comparisons	103
7.1	Single Speed Rated Values	104
7.2	Two Stage Rated Values	108
7.3	Discussion and Modeling Methodology	114
8	Heat Pumps - Notable Differences(Curves and Rated Values)	117
8.1	Curve Data	119
8.2	Rated Values	124
8.3	Conclusions From Heat Pumps	128
9	Conclusions and Future Work	130
9.1	Conclusions	130
9.2	Future Work	133

Bibliography	135
---------------------	-----

Appendix

A Example Python Script	137
B SEER and HSPF calculations	145
B.1 SEER Calculation Procedures	145
B.1.1 Single Stage Units	145
B.1.2 Two Stage Units	146
B.2 HSPF Calculation Procedures	149
B.2.1 Single Stage Units	149
B.2.2 Two Stage Units	153

Tables

Table

3.1	Required Test Conditions as Defined by AHRI 210/240	26
3.2	Common Independent and Dependent Variables	28
3.3	Dependent Variables Reported on by Manufacturer (Cooling)	30
3.4	Independent Variables Reported on by Manufacturer (Cooling)	30
3.5	Dependent Variables Reported on by Manufacturer (Heating)	31
3.6	Independent Variables Reported on by Manufacturer (Heating)	31
5.1	Errors in calculated exiting conditions	59
5.2	Comparison of SHR Calculated by EES Program to EPT SHR (for Carrier SEER 14)	63
5.3	Comparison of SHR Calculated by EES Program to EPT SHR (for Goodman SEER 14)	64
5.4	Comparison of EPT SHRs to Both Versions of EES Calculations	65
6.1	Error due to using a single set of curves for each manufacturer - Houston	95
6.2	Error due to using a single set of curves for each manufacturer - Atlanta	95
6.3	Error due to using a single set of curves for each manufacturer - Phoenix	95
6.4	Error due to using a single set of curves for each manufacturer - Chicago	95
6.5	Error due to using a single set of curves all manufacturers - Houston	96
6.6	Error due to using a single set of curves all manufacturers - Atlanta	96
6.7	Error due to using a single set of curves all manufacturers - Phoenix	96
6.8	Error due to using a single set of curves all manufacturers - Chicago	96

6.9	Error due to using fixed low and high curves for each manufacturer - Houston	98
6.10	Error due to using fixed low and high curves for each manufacturer - Atlanta	98
6.11	Error due to using fixed low and high curves for each manufacturer - Phoenix	98
6.12	Error due to using fixed low and high curves for each manufacturer - Chicago	98
6.13	Curves coefficients for air conditioners (IP units)	99
6.14	Curves coefficients for air conditioners (SI units)	100
6.15	Curves coefficients for heat pumps - cooling (IP units)	100
6.16	Curves coefficients for heat pumps - cooling (SI units)	100
6.17	Curves coefficients for heat pumps - heating (IP units)	101
6.18	Curves coefficients for heat pumps (SI units)	101

Figures

Figure

1.1 Residential Site Energy Consumption by End Use [6]	2
2.1 Ideal Vapor Compression Cycle (http://refrigerationcycleexperiment.blogspot.com)	10
2.2 Binning for SEER rating procedure	12
2.3 Hourly weighted load profile for SEER	13
3.1 2008 Market Share for Air Conditioners and Heat Pumps [6]	33
4.1 Multi-Speed Run Time Example: Top - High speed only. Bottom - Optimal Low Speed Operation	41
4.2 Two versions of DOE-2's EIR-fPLR curve	48
5.1 Measurement points for net and gross capacity calculation for a blow through configuration	53
5.2 Data Entry Error in Carrier's SEER 21 Line	56
5.3 Data Entry Error in York's SEER 15 Line	57
5.4 Two Common Errors in the BF Calculation	58
5.5 Region of the Psychrometric Chart for Air Conditioner Exiting Conditions	60
5.6 Visualization of Biquadratic Curves: Four Manufacturers	68
5.7 Alteration of the Rating Point in York Capacity Curve	70
6.1 $\overline{COP}_{net,ss}$ of all single stage air conditioners evaluated	77
6.2 $\overline{COP}_{net,ss}$ of all two stage air conditioners evaluated	79

6.3	The progression of the curve sensitivity study	81
6.4	Effects of letting only $Q_{f(T)}$ vary	82
6.5	Effects of letting both $Q_{f(T)}$ and $EIR_{f(T)}$ vary	83
6.6	Effects of letting only $Q_{f(FF)}$ vary - fixed fan speed of 350 CFM/Ton	84
6.7	Effects of letting only $Q_{f(FF)}$ vary - fixed fan speed of 450 CFM/Ton	85
6.8	Effects of letting both flow fraction curves vary - fixed fan speed of 350 CFM/Ton	86
6.9	Effects of letting both flow fraction curves vary - fixed fan speed of 450 CFM/Ton	87
6.10	Effects of having all units use their unit specific curve inputs (all curves vary)	88
6.11	Comparison of low stage to high stage performance	90
6.12	Change in Cooling Energy Due to Using Fixed Curves - Carrier, Houston, 400 CFM/Ton	93
7.1	Comparison of EER_A - AHRI versus database values	105
7.2	C_d values calculated from the SEER equation	107
7.3	Comparison of two stage EER_{A_2} - AHRI versus database values	109
7.4	Comparison of $SEER_{CALC}$ to $SEER_{AHRI}$ with variation of C_d included	110
7.5	Comparison of $SEER_{CALC}$ to Simulation Results	112
7.6	SA_{eff} of the different units	113
8.1	Initial results for all single stage heat pumps	118
8.2	Initial results for all two stage heat pumps	119
8.3	Impact on $\overline{COP}_{net,ss,h}$ due to changing the heating set point	121
8.4	Variation due to temperature curves	122
8.5	Variation due to flow fraction curves (350CFM/Ton)	122
8.6	Variation due to flow fraction curves (450CFM/Ton)	123
8.7	Graph depicting integrated capacity as a function of outdoor dry bulb [3]	125
8.8	Comparison of $HSPF_{CALC}$ and $HSPF_{AHRI}$	126
8.9	Simulation results for the matching Carrier units	126
8.10	Comparison of AHRI and Database COP_{47} values	127

8.11 Comparison of AHRI and Database COP₁₇ values 128

B.1 Binning for SEER rating procedure 146

B.2 Hourly weighted load profile for SEER 147

B.3 Binning for HSPF rating procedure 150

Chapter 1

Introduction

1.1 Motivation

Air conditioning has become practically ubiquitous across the United States and is becoming common place in most countries around the world. The vapor compression cycle that is the most common way of providing chilled air to an indoor environment is run off of electricity. This makes air conditioning especially energy intensive on a source energy basis.

In the residential sector air conditioning is now found in $\approx 90\%$ of new single family homes (up from 75% in 1991). Heat pumps have also been on a steady rise over the last 20 years. The presence of a heat pump as the primary heating system in new homes rose from 22% in 1991 to 37% in 2009 [6].

In 2008 residential air conditioning accounted for $\approx 9\%$ (see figure 1.1) of the site energy consumed and 14% of the source energy in the US residential housing stock. The associated electricity costs accounted for $\approx 13\%$ of the end-use expenditures. The energy and costs associated with heat pumps are more difficult to disaggregate due to the various heating technologies that could account for the space heating end use. Yet, if we take the fact that $\approx 9\%$ of total existing households use a heat pump as the primary heating source and multiply that by the 45% site energy for heating, that gives 4.1% of site energy consumption for heat pumps. This equates to 13% of residential end-use consumption accounted for by air conditioners and heat pumps as of 2010. With residential buildings accounting for roughly 22% of the United States energy use, this implies that $\approx 2.9\%$ of total US annual energy (or 2.9 quads) is consumed by residential air conditioners and heat pumps [6]. This is significant portion of our total energy consumption and will continue to rise as

indicated by the upward trends in heat pump and air conditioner use.

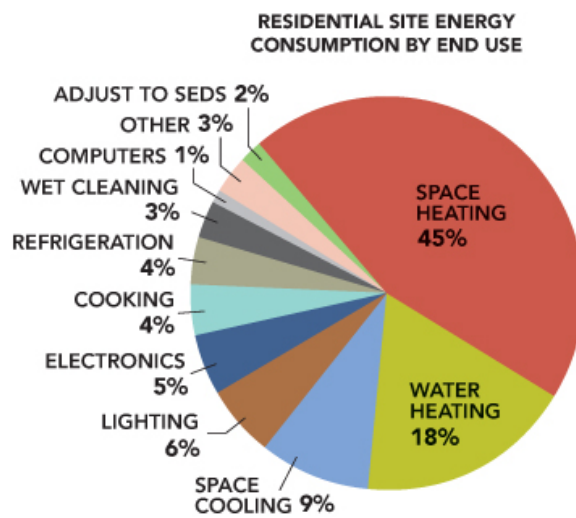


Figure 1.1: Residential Site Energy Consumption by End Use [6]

In order to recommend efficient designs and reduce the energy consumption of air conditioners and heat pumps it is first necessary to accurately quantify both the energy consumption of the units and the relative efficiencies of different units. The principal metrics used to quantify the energy efficiency of air conditioners and heat pumps are the Seasonal Energy Efficiency Ratio (SEER) and Heating Seasonal Performance Factor (HSPF) respectively. These metrics consist of a single value used to quantify the seasonal energy efficiency of a unit. These metrics do not vary with respect to: climate, building type, or specific unit characteristics. The consensus from the research community is that these are convenient yet inaccurate metrics for quantifying annual energy use [5] [7] [13]. SEER and HSPF also provide only very rough estimates of actual consumption and are really meant only as a ranking method for different levels of efficiency (though even this ranking has been shown to be inaccurate for different climates and different units [5] [12]).

An alternative approach to quantifying annual energy consumption is through whole-building annual simulation software. These programs provide the capability to capture complex interactions between buildings, climate, and occupants. The simulation engines provide the capability to evaluate energy use trends across different equipment lines and across different buildings and climates. Though it is unlikely that manufacturers and the marketplace will discard the SEER/HSPF metrics in exchange for annual simulation,

the use of annual simulation tools can inform designers, policy makers, and any future improvements to the SEER and HSPF rating procedures.

The split-system direct expansion units that are used for the vast majority of air conditioning and all heat pumps discussed here are very difficult to model in a computer simulation. To accurately model the complexities of two-phase refrigerant flow in the evaporator and the condenser, one needs not just a complete mass and energy balance, but also descriptions of the fluid dynamics within the coils. The complexities of the cycle combined with the large variation in equipment characteristics makes a first principals model very difficult to construct and very time consuming to run. For these reasons, the air conditioner and heat pump models in annual simulation tools are surrogate (or regression-based) models that utilize data that characterizes performance at various operating conditions. Regression analysis is performed on this data and the resulting curve fits are used to predict performance at off-rated operating conditions during the simulation.

The surrogate models are dependent on the performance characteristics that are input into the models. Therefore, for accurate predictions of energy consumption and performance, it is crucial to understand the nature of the data being used and how that data interacts with the algorithms contained in the model.

1.2 Objectives

This research will focus on split-system residential air conditioners and heat pumps. There will also be a focus towards the high-efficiency, two stage models that have recently become more prevalent in the market. Single speed models will also be thoroughly analyzed as they are the most commonly used equipment. The combination of single stage and two stage air conditioners and heat pumps will provide a comprehensive evaluation of the currently available split systems in the marketplace.

The main objectives of this research are:

- (1) To provide accurate means of evaluating annual energy use for a large variety of currently available air conditioners and heat pumps
 - In any climate

- In any building
- (2) To evaluate the relative performance of different units and compare this to the industry standard values of SEER and HSPF
 - (3) To determine the necessary (significant) inputs to simulation engines to accurately represent heat pumps and air conditioners

To achieve objective 1 it is necessary evaluate a unit under various climatic conditions and in various buildings. To achieve objective 2, it is necessary to repeat objective 1 for a wide variety of units and compare their performance to the nominal unit efficiencies. The number of combinations involved with these two goals makes it impossible to perform actual unit testing. Whole-building annual simulation is considered to be the best available method to capture the complex interactions of: equipment, building, and climate. It also provides the ability to compare the different units without actually having to swap out physical units and monitor their performance. The whole-building annual simulation approach provides a method for analyzing performance and achieving objectives 1 and 2.

Even utilizing the simplified, regression-based models that are employed by the simulation tools (described above and in more detail in chapter 4), the simulation engines require many inputs to the model. A large portion of these inputs are coefficients to quadratic or biquadratic regression fits. The complexity of these inputs limits the ability of any but the most experienced user from inputting their own user-defined characteristics (e.g. modeling a specific unit from a specific manufacturer). Even for the highly experienced user who is able to generate his/her own curve fits, is unclear how their inputs inform their model. This brings us to objective number 3 and the research questions that immediately follow from that objective:

- How do the inputs compare between different AC/HP units?
- What is the quality of the data used to generate these inputs?
- Will these inputs model a unit that is comparable to a SEER 13? A SEER 21?
- How much variation is there between the current model and other models of the same nominal SEER/HSPF level?

- Which of these various, complex inputs have the most effect on the results?

It is the goal of this research to answer these questions for the modeling community. To realize that goal, this research aims to provide accurate information on the effect and relative importance of the model inputs, and then define how they relate to the more generally utilized metrics: SEER and HSPF. This will make it possible to quantify the energy consumption (both relative and absolute) of air conditioners and heat pumps. The ability to quantify annual energy consumption for any climate, house, and equipment type will allow for accurate ranking of efficiency across a range of important variables. Utilization of this capability can lead to better implementation of codes and designs and ultimately lead to a reduction in the energy consumed by heat pump and air conditioner use.

1.3 Methodology

In order to accomplish the goals outlined above, it was necessary to develop a scope and methodology for the project. The methodology described here outlines the general framework and process that was followed throughout the course of the research. The detailed methodology that was utilized in specific parts of the research (i.e. the input sensitivity study, Chapter 6) will be discussed in their respective sections.

To accomplish objectives 1 and 2, it was necessary to define the tools that would be used for the analysis and the methods that would be employed in order to ensure accurate representation of performance. The first major question in outlining the research process was which tool/s to use in the research. One of the principal goals (objective 1) was to provide a method for assessing air conditioner and heat pumps energy usage across different climates and different buildings. It was considered critical to be able to provide a more complete, national picture of air conditioner and heat pump energy usage. The lack of climate and building interaction is one of the short-comings that has been identified in SEER and HSPF rating procedures. To better inform national (or even local) policy on split system energy use it was considered crucial to incorporate these components into the analysis. With this requirement in mind, it was decided to utilize the whole-building, annual simulation tools EnergyPlus and DOE-2. Some consideration was given to alternative annual simulation tools such as: TRNSYS, Trane TRACE, and ENERGY-10. EnergyPlus and

DOE-2 were eventually selected due to their prominent position within the energy modeling community and their flexibility with regards to user inputs.

Both DOE-2 and EnergyPlus provide the capability to capture the interaction between climate, building, occupant, and systems. The decision to utilize both simulation engines in this analysis was taken for a number of reasons. Most importantly it would provide comparison and verification between the two simulation models. The two simulation engines utilize similar yet distinct algorithms and it was considered beneficial to be able to compare between results and evaluate some of the differing assumptions between the two algorithms. The dual model approach was also beneficial to development of a residential modeling and optimization software, BEopt, developed in the residential buildings group at the National Renewable Energy Laboratory (NREL) where this research was completed.

BEopt is a residential specific modeling software that provides a graphical front end for EnergyPlus and DOE-2, an integrated cost database, and a cost-based optimization capability for annual simulations. It provides the Department of Energy's (DOE) Building America program with the capability to model potential energy saving technologies and to select the optimal package of energy conservation measures based on either cost-savings or energy-savings. BEopt supports both EnergyPlus and DOE-2 as options for annual simulation engines, therefore it was considered beneficial to utilize both simulation engines during the research effort.

Initially, the scope also included the possibility of incorporating a component based model such as the model developed by Wassmer in [21] or the Heat Pump Design Model developed by Oak Ridge National Laboratory [19]. A component based model was attractive due to the fact that it would not be necessary to compile manufacturers' performance data and it would provide a first-principals based approach to the modeling problem. After literature review and considerable discussion, the component based model approach was discarded for a number of reasons, including:

- The complexity and runtime required for an accurate model
- The continued need for complicated and hard-to-access inputs describing the physical characteristics (albeit, different inputs than the regression based models)

- The lack of applicability for the general simulation community (most people in the modeling community use EnergyPlus or DOE-2)
- The need to create an independent model for BEopt usage that would be called during the simulation (most likely increasing runtime significantly)

After deciding upon using annual simulation tools for the research, it was then decided to focus in on EnergyPlus as the simulation used for the majority of the research. DOE-2 was used for comparative analysis and many of the findings of this research applied to DOE-2 as well due to the similarity between the two tools. This decision to use EnergyPlus as the main research tool was due to EnergyPlus's position as the most current simulation engine (with on-going development), improved split-system algorithm (see chapter 4), and improved capture of the interaction between conditioned space and HVAC systems.

Once it was decided to use EnergyPlus as the simulation tool for the research, it was necessary to define how to proceed in providing improved modeling capabilities (objective 3). From analysis of the simulation engine algorithms (described in chapter 4), it was determined that the first step in the research would be the compilation of a database containing all of the performance data on currently available air conditioner and heat pump units. This process is described in chapter 3. This database was used to generate the necessary inputs for the simulation engines, therefore enabling comparison across the different available units. It also enabled the evaluation of how the model inputs generated from this data affected the annual simulation results. Physical data regarding the type of compressor, size and configuration of coil, refrigerant type, etc. was also gathered. This data was compared against the annual simulation results in order to identify any correlations between predicted use and physical characteristics.

The last portion of the initial methodology was to evaluate the pros and cons of offering a database of complete simulation inputs for every make and model with currently available performance data. This option was compared against the other extreme of generalizing (and simplifying) the inputs across a given SEER line. Both of these approaches would accomplish the goal of providing improved usability of the simulation models. With the make/model option, the user would be able to select a specific unit from the database and receive all of the necessary inputs for the simulation. Alternatively, with a generalized model the user

would be able to enter in some accessible, key characteristics of a unit that would define any variation seen while assessing the larger set of options in the database. This option would provide increased accessibility to users that did not want to select an exact unit, and would also not require continuous updating of the database whenever the market available units changed. The decision between these competing options would be determined due to availability and quality of data.

Finally, the selected approach would be used to evaluate the SEER and HSPF rating systems through parametric analysis across various climates and various units.

Chapter 2

Background and Literature Review

2.1 Unitary System Overview

The first modern air conditioning system was invented in 1902 by Willis Carrier. By sending air over coils filled with cold water he was able to both lower the temperature of the air and control humidity in the space. This process is based on the thermodynamic Carnot Cycle proposed much earlier (1824) by Sadi Carnot. Yet Carrier's air conditioning system was the first time that the vapor compression cycle was used to change the properties of air for the purpose of conditioning a space or building.

The vapor compression cycle consists of a working fluid (refrigerant) that interacts with four components: a compressor, an evaporator, an expansion device, and a condenser. In refrigeration mode, the working fluid will enter the compressor as saturated vapor and be compressed isentropically to a superheated vapor state. The work done by the compressor heats the working fluid up beyond the temperature of the outdoor environment (T_H). Upon entering the condenser, the gas begins to transfer heat to the cooler outdoor temperature until it reaches saturation point and condenses at T_H . It is important to note that even though the outdoors is likely warmer than the indoor environment, the refrigerant will still reject heat to this hot reservoir, relying on the work of the compressor to raise the temperature of the refrigerant appropriately. The refrigerant leaves the condenser as a saturated liquid. The refrigerant now undergoes isenthalpic expansion to a two-phase liquid vapor state with a temperature equal to that of the indoor environment (T_C). Finally, the refrigerant passes through the evaporator and the remaining fluid is evaporated by absorbing heat from the indoor environment. This leaves the refrigerant as fully saturated vapor and the cycle begins again with

the compressor [16].

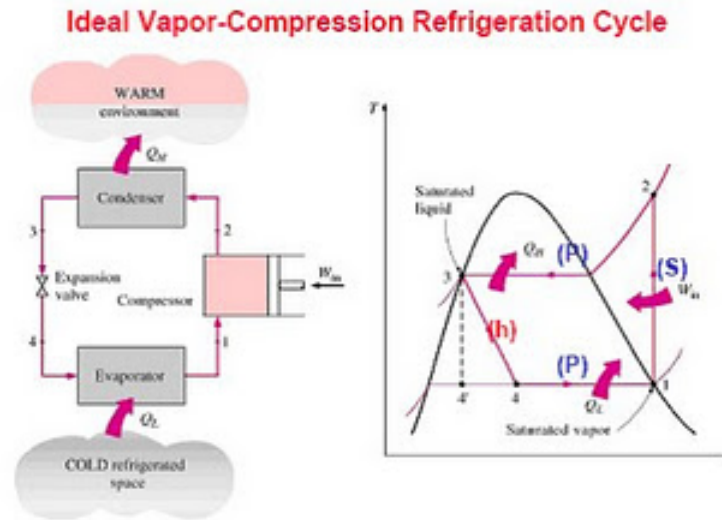


Figure 2.1: Ideal Vapor Compression Cycle (<http://refrigerationcycleexperiment.blogspot.com>)

This idealized cycle is not possible in a real world scenario. In the actual vapor compression cycle, the heat transfer is not reversible and therefore the refrigerant must be compressed to a higher temperature than the ambient temperature and it must be cooled to a temperature below the indoor, controlled environment. The compression is also not able to be accomplished isentropically requiring a greater input of work to reach the same constant pressure line. Finally, there is the necessary superheat (evaporator exit, to avoid wet compression) and subcool (condenser exit, to avoid any vapor mixed in during expansion process). These are the significant deviations from the ideal vapor compression cycle, there are other factors such as pressure drop in the coils that also play a role in reducing the overall efficiency of the cycle.

The unitary split-system that is seen today has an outdoor cabinet that houses the condenser and compressor. The compressor is either a single speed or two stage compressor (and some variable speed drives are have recently come online). The condenser is assisted by a condenser fan that blows the air over the coil. These components are connected to the indoor section by refrigerant piping. The indoor section consists of the expansion valve, the evaporator, and the evaporator fan (often the furnace fan). Expansion valves are one of the areas of improvement in recent years. There are the older fixed type of expansion devices (capillary

tube or orifice) and newer, modulating valves (either thermostatic expansion valves (TXV) or electronic expansion valves (EEV)). These modulating expansion valves provide better control of the charge in the system and associated superheat at the evaporator outlet. This provides better efficiency to the system and less refrigerant migration. Placement of a solenoid valve between the condenser outlet and the throttling valve can also reduce refrigerant migration.

The split system can essentially be run in reverse by inclusion of the appropriate reversing valve. This allows the system to change the location of the heat source and the heat sink, thus enabling the system to provide heat to the indoor environment. With this reversing valve, proper controls, and a defrost system, an air conditioning unit is essentially converted into a heat pump.

2.2 Overview of Equipment Efficiency Metrics

The two key metrics used by industry to define the efficiency of air conditioners and heat pumps are the Seasonal Energy Efficiency Rating (SEER) and the Heating Seasonal Performance Factor (HSPF). These metrics attempt to define the efficiency of the heating or cooling system over the course of the year, taking into account part load effects that come from operation at off-peak conditions (cycling effects). The SEER and HSPF metrics combine steady state efficiencies (defined as capacity divided by power consumption) at various fixed operating conditions and incorporate cycling losses proportional to the expected part load performance at those operating conditions. The calculation methods for SEER and HSPF are defined by the Air-Conditioning Heating and Refrigeration Institute (AHRI), and are outlined in detail in AHRI/ANSI 210-240 [1]. The general methodology of the metric is described below and details are presented here in Appendix B. For further discussion of the steady state efficiency and part load performance, see sections 2.3.2 and 2.3.3 (respectively) in the following sections of this chapter.

The single stage SEER calculation takes into account the rated efficiency at 82°F outdoor dry bulb, 80°F indoor dry bulb and 67°F indoor wet bulb and assumes a part load factor (PLF) of 0.5 at 82°F. These two assumptions taken together imply that the SEER rating procedure assumes that 82°F is the average operating point for the entire cooling season and that the air conditioner or heat pump sees a load that is half of the rated capacity (rated at 95°F outdoor dry bulb) at those conditions.

One other aspect of the rating procedure that is worth noting is the indoor conditions at which the units are tested. All cooling tests are performed at 80°F indoor dry bulb and 67°F indoor wet bulb. This essentially assumes that the cooling set point is 80°F which is significantly higher than most people keep their thermostats in the summertime. This should not effect the relative rating of units, but it does lead to higher steady state efficiencies than would actually be encountered under more realistic operating conditions.

The two stage SEER calculation is very different than the single speed calculation outlined above. The first significant difference is that it uses a temperature binning to describe the climatic temperature distribution. There are eight different bins with each bin containing 5°F: 67, 72, 77, 82, 87, 92, 97, 102. The bins are referenced as $j = 1, \dots, 8$.

Bin Number, j	Bin Temperature Range °F	Representative Temperature for bin °F	Fraction of Total Temperature Bin Hours, N_j/N
1	65-69	67	0.214
2	70-74	72	0.231
3	75-79	77	0.216
4	80-84	82	0.161
5	85-89	87	0.104
6	90-94	92	0.052
7	95-99	97	0.018
8	100-104	102	0.004

Figure 2.2: Binning for SEER rating procedure

The two stage SEER process defines a building load term ($BL(T_j)$) that defines the load the unit is required to meet as a function of temperature, defined as:

$$BL(T_j) = \frac{(T_j - 65)}{95 - 65} * \frac{\dot{Q}^{k=2}(95)}{1.1} \quad (2.1)$$

Where 1.1 is a sizing factor and $\dot{Q}^{k=2}(95)$ is the capacity at the A₂ test (steady state test point at 95°F outdoor dry bulb, 80°F indoor dry bulb and 67°F indoor wet bulb). It can be seen that 95°F is defined as the design temperature for the SEER process and 65°F is the balance temperature (or zero load temperature).

When T_j (the bin temperature) is equal to 65°F the equation evaluates to 0, implying zero load. When T_j equals 95°F the load is equal to the capacity of the unit indicating that this was the temperature designed for at full capacity.

This building load is used to weight the contribution of every temperature bin. This is to indicate the higher demand on the air conditioner unit at higher temperatures, even though there may be more total hours spent at lower temperatures. The combination of building load weighting and bin weighting is shown in figure 2.3.

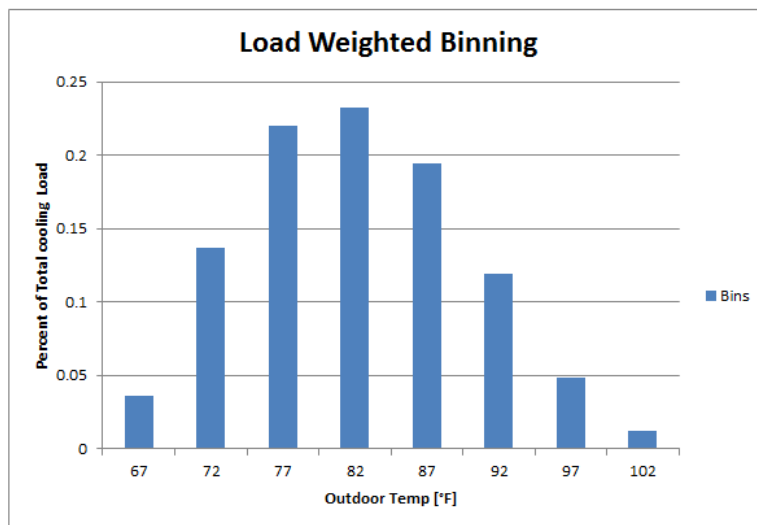


Figure 2.3: Hourly weighted load profile for SEER

It can be noted that even though the climate described by the bins in figure 2.2 has the highest fractional hours in the 72°F bin, the load is centered at 82°F. This is the same as in the single speed SEER procedure. Both the most common temperature bin and the center of the load distribution are at relatively cool temperatures. This generally skews the efficiencies to higher values than would actually be seen in hotter climates such as Houston or Phoenix.

The seasonal efficiency of the unit is then calculated using the capacity and power values that were gathered at the rated testing conditions and weighting them both by the hours spent in that bin, the approximated load in that bin, and the estimated part load effects at that bin. For actual calculation procedures of both the single and two stage SEER values, the reader is referred to Appendix B.

It should be noted that in both the single stage and the two stage SEER calculations there is no consideration of the climate or the building construction/efficiency. There is only one temperature binning for the SEER calculation. One of the goals of the current research is to enable accurate modeling of air conditioners and heat pumps so that the design and research communities are able to evaluate performance of these units across a wide variety of climates and in various building types.

The HSPF calculations for single stage and two stage heat pumps are very similar to the calculation procedure for two stage air conditioners. It utilizes temperature binning and the capacity and power results of the steady state rating points to estimate annual efficiency of the unit. In the HSPF calculation there are actually six different binning profiles that describe different types of climates, yet only one of those six binnings is actually required to be reported.

2.3 Key Characteristics of Direct Expansion Systems

2.3.1 Capacity

The capacity of the system is the rate of cooling (or heating) energy the system can provide at a given set of operating conditions. Capacity is always measured once the system has reached steady state operation. It can be measured in watts, Btu/h, or in Tons (equivalent to 12,000 Btu/h). Most of residential systems come in capacities ranging from 1.5 to 5 Tons. Two stage units will have two separate capacities, one at the high speed and one at the low speed of the compressor.

The total capacity which is described above is then broken down into sensible capacity and latent capacity. The sensible capacity is the portion of the total capacity that reduces the dry bulb temperature of the air. There is also the latent component which reduces the total moisture content of the air. Humidity reduction is accomplished by achieving a coil surface temperature that is below the dew point temperature of the air. This causes condensation on the coil surface which then proceeds to drain off the coil into a drain pan. The energy associated with the phase change from vapor to liquid is the latent capacity of the system. The sensible heat ratio (*SHR*) is defined as $SHR = Q_{sens}/Q_{tot}$.

The nominal capacity of a system is the steady state capacity at a certain rating point. This allows

installers/consumers to compare an equivalent value across different makes and models. The agreed upon rating point for total cooling capacity, as dictated by AHRI, is 95°F outdoor dry bulb, 80°F indoor dry bulb, and 67°F indoor wet bulb. The rating point for total heating capacity is 47°F outdoor dry bulb, 70°F indoor dry bulb, and 60°F indoor wet bulb.

The total capacity of a system changes as the ambient conditions deviate from that rating point. The capacity of an air conditioner increases as the outdoor dry bulb temperature decreases. This is due to the lower ambient temperature which allows the compressor to operate more efficiently, providing more efficient heat exchange with the outdoors. At lower ambient conditions, losses are also reduced. The capacity also increases at higher entering wet bulb temperatures. This is due to the increased differential between dewpoint and coil surface temperature. This increases the latent capacity at only a slightly reduced sensible capacity, resulting in a greater total capacity. For heat pumps, a decrease in outdoor dry bulb causes a decrease in capacity for similar reasons. Wet bulb temperatures do not significantly effect the performance of a heat pump due to the fact that heating is a sensible-only process

A final detail to note when discussing capacity is the difference between “net” and “gross” capacities. The capacity reported by AHRI is what is called a “net” capacity. This means that the heat produced by the fan motor is included in the air stream. Therefore the air is actually heated up a certain amount from the rating point yet the reported capacity is calculated as the amount of heat removed from the rated conditions to achieved exiting conditions at a certain airflow rate. A “gross” capacity is the capacity delivered by the refrigerant. This would be the air-side capacity measured from just before the coil to just after the coil (fan heat not included). Both simulation engines require gross capacities for their capacity inputs. For a more detailed discussion of net and gross, see section 5.1.

2.3.2 Efficiency

The efficiency of the system is defined as how much cooling (or heating) energy is generated by the system (the capacity) divided by the electrical energy that is input into the system. Again, efficiency is reported at steady state conditions. Efficiency is usually denoted as Energy Efficiency Ratio (EER) for cooling efficiencies and as Coefficient of Performance (COP) for heating efficiencies. EER takes the units

[Btuh/W] and COP takes the units [W/W] (dimensionless). It can therefore be seen that one can easily convert between EER and COP by the formula: $EER = COP * 3.413$. A commonly used input in simulation engines is Energy Input Ratio (EIR) which is defined as $1/COP$.

The efficiency of a unit is reported for the same cooling and heating set points denoted above (95/80/67 cooling, and 47/70/60 heating). The efficiency of an air conditioner increases at lower outdoor dry bulb temperatures due to the fact that the compressor does not need to work as hard to drive the working fluid to a temperature above ambient. The efficiency also increases at higher entering wet bulbs, again due to the larger temperature differential between the dew point of the air and the coil surface temperature.

As with capacity, the difference between net and gross is equally important with efficiency metrics. All efficiencies reported by the manufacturers (either EER or COP) are net values, meaning that they are using a net capacity as defined above and a net power (including the power drawn by the indoor fan in the input power value). The efficiencies required by the simulation engines require a gross efficiency value. This is because the fan is modeled completely separately than the heating or cooling coil.

2.3.3 Cycling Losses

All of the unitary discussion up to this point has been focused on steady state operation. Capacity and efficiency are defined as steady state values and are reported as such by the manufacturers. They are also expected to be steady state values by the simulation engines. That being said, part load degradation is a significant component of air conditioner and heat pump performance. Part load degradation occurs due to the fact that these systems have a minimum turn-down (low speed for two stage units and the only available speed for single-speed units). Therefore, if the load in the space is ever lower than the lowest available capacity for the unit, the unit has to cycle between off and low (“on” for single speed) to maintain setpoint. During cycling it takes a certain amount of time to reach steady state capacity even though the power consumption from the fan and compressor are relatively constant throughout the on-time of the unit. The level of impact that cycling has on performance depends on two characteristics of the unit:

- (1) Start-up delays in the system (determined by the time constant, τ , of the system)

(2) The cycling rate of the system (usually determined by the thermostatic control)

These two components are taken into consideration in the cycling test prescribed by AHRI 210/240 [1]. The cycling test requires that the unit be turned off (after reaching steady state) for 24 minutes. It is then forced on for 6 minutes. This cycle is repeated a minimum of 2 times. The total cooling energy delivered and the total energy consumed is recorded and then C_d is calculated as:

$$C_d = \frac{1 - \frac{EER_{cyc,dry}}{EER_{ss,dry}}}{1 - CLF} \quad (2.2)$$

Where:

- $EER_{cyc,dry}$ is the cycling efficiency under dry coil conditions, defined as 80°F indoor dry bulb, 57°F indoor wet bulb, and 82°F outdoor dry bulb
- $EER_{ss,dry}$ is the steady state efficiency under those same conditions
- CLF being defined as,

$$CLF = \frac{Q_{cyc,dry}}{\dot{Q}_{ss,dry} * \Delta\tau_{cyc,dry}} \quad (2.3)$$

- $\Delta\tau_{cyc,dry}$ is the full on/off cycle time in hours.

The C_d value must be greater than zero and if the cycling test is not performed or if the C_d value is greater than 0.25, than it is set to the default of 0.25.

It can be noted that the AHRI test holds the on-time of the unit fixed at 0.2 (6 min/30 min). This makes sense due to the fact that the cycling rate is a function of the thermostatic control, not of the unit which is being tested and therefore should remain constant across all different air conditioner and heat pump tests. This is not the case in real implementations.

The delay in reaching steady state performance is caused by refrigerant migration in the system and by the time it takes to overcome the thermal mass of the heat exchangers. The time to cool/heat the coils cannot be significantly improved, yet refrigerant migration can be reduced and there has been significant improvements in this cause of part load losses in the recent years. Refrigerant migration occurs in the off-cycle due to pressure differentials in the system. The high pressure refrigerant (vapor and liquid) tends to

migrate to the low pressure suction line and crankcase. The refrigerant is soluble in the crankcase oil and will end up needing to be redistributed into the system and vaporized out of the oil upon system restart. These effects can be reduced either by crankcase heating (reducing the driving pressure differential) or by a liquid solenoid valve and a pump down routine where the refrigerant is stored in the condenser side of the system during off cycle. The implementation of the liquid solenoid solution has significantly dropped the part load losses to where C_d values of 0.02-0.1 are common in most units.

2.3.4 Defrost Cycle

The defrost cycle is the term given to the period of time when a heat pump warms up the outdoor coil so as to melt off and eliminate any frost that may have built up during heating operation. Due to the fact that the outdoor coil must be driven to a lower temperature than the ambient air (so as to absorb heat from the outdoor air), it is common for the surface temperature of the outdoor coil to fall below the dew point of the ambient air. When this situation occurs, the ambient air will condense on the surface of the coil (much like the indoor coil during cooling mode). If the outdoor coil surface temperature is below freezing, then this condensate will freeze on the coil. This ice build-up can drastically lower the efficiency and capacity of the coil due to: lower surface area, higher pressure drop, and degraded heat exchange between the coil and the ambient air.

In order to rid the coil of frost build-up, one of two approaches are usually implemented: resistive defrost or reverse cycle defrost. The first method (resistive defrost) is when a resistive element is incorporated into the outdoor coil which can be turned on to heat up the coil and melt off the frost. The second (and more common) approach - reverse cycle defrost - is to periodically run the heat pump in cooling mode. During the cooling mode operation the refrigerant is compressed and heated before traveling to the outdoor coil and this hot fluid warms the outdoor coil from the inside, again causing the coil to shed any frost layers. During the reverse cycle operation either the indoor fan is turned off or the backup element is required to operate to heat up the cold air that is being generated by the indoor coil now that it is in cooling mode (fan operation in defrost is dependent on specific unit controls). In general it is more energy efficient to use the reverse cycle defrost due to the improved COP when using a vapor compression cycle over resistive heating.

There are two main types of control for the defrost cycle: timed or on-demand. Timed defrost operates exactly as it sounds, dependent on the outdoor temperature the unit will be put into defrost mode for a set period of time. On-demand defrost depends on a sensor to let the system know when a defrost cycle is required.

2.3.5 Indoor Fan

The indoor fan provides the airflow over the indoor coil and distributes either the cool or warm air throughout the residence. The indoor fan is generally sold separately from the air conditioner or heat pump unit and therefore is not described in the expanded performance data on the air conditioner or heat pump. For air conditioners it is common to utilize the furnace fan to provide the required air flow. In the case of heat pumps, the fan is generally included with the indoor coil, yet the specific combination of indoor and outdoor unit (mix and match) is not specified by the manufacturer.

There are two main types of motors used with supply fans in residential applications: permanent split capacitors (PSC) and brushless permanent magnets (BPM). Both of these motors are able to offer multiple speeds. PSC motors are really single speed motors that accomplish multi speed operation by using “speed taps” that weaken the circuit and cause the fan to run at lower speeds than normal when loaded. BPM motors are actual variable speed motors that can be controlled electronically to turn down to match the required air flow rate. PSC motors are less efficient than BPM motors, especially at lower speed, and require a relatively constant power input across different “speeds” and different static pressures. BPM motors use much less power at lower speeds, more closely following the cubed fan law.

Due to the fact that air conditioners are not generally paired with an indoor coil/fan (heat pumps generally do have a recommended indoor unit), the SEER and HSPF rating procedures allow the unit to either be tested with a specific fan or to use a default power rating of 365 Watts per 1000 CFM. The SEER and HSPF ratings use net capacity and efficiency values in their calculations. Therefore, most expanded performance tables report net values, yet the simulation engines require gross values due to the indoor fan being modeled separately. The fact that the actual fan and its power consumption at different speeds is not reported by the manufacturers presents a number of problems in generating the gross inputs required by

EnergyPlus and DOE-2. These concerns and how they were addressed will be discussed in section 5.1.

2.4 Literature Review

The literature review for this research began with a general review of previous work on modeling split system air conditioners in annual simulations. As noted in the objectives section 1.2, the central goal of this research was to provide accurate evaluation of air conditioner and heat pump energy consumption utilizing the simulation engines DOE-2 and EnergyPlus. Therefore, the focus of the literature review was on previous research on split system modeling in these two simulation engines.

The most complete description encountered regarding the DOE-2 model was provided by A. Courtney in his 2006 Master's thesis, *Assessing the Effectiveness of SEER as a Predictor of Seasonal Cooling Efficiency* [5]. In his research Courtney used the DOE-2 model to evaluate seasonal cooling energy use for 56 different air conditioner models. The inputs for these 56 units were generated by the Southern California Edison research effort headed up by J.J. Hirsch and Associates [11]. The seasonal cooling energy predicted by the DOE-2 simulations was compared to the nominal SEER values for all 15 of the US IECC climate zones. He then takes some of the typical units and evaluates their deviation from the nominal SEER value at all 216 continental US TMY locations. From this climate correction factors were calculated for all climate zones. The research also includes assessment of the 2-speed DOE-2 model inputs and some of the assumptions implicit in that model: the effect of using one set of curves for high and low speed, the shape of the EIR-fPLR curve, and the effect of duct transients on cooling energy.

The research by Courtney was based on an initial study commissioned by the California utility, Southern California Edison and carried out by J.J. Hirsch and Associates [12]. This study evaluated SEER as an energy predictor for all the different climate zones in California. In support of this research, the 2-speed air conditioner model was added to DOE-2 by Steve Gates. This research effort looked at the predicted energy consumption of a large number of air conditioners and heat pumps (data initially gathered by the California Energy Commission(CEC)) throughout the different climate zones of California. They provide detailed discussion of all of the assumptions inherent in the SEER rating procedure and use the DOE-2 model to demonstrate a large amount of variation in energy use across different climates (for all SEER levels) and

variation across different units (for the same nominal SEER level). The results of this research indicated that energy consumption predicted with the nominal SEER value could only be considered accurate within $\pm 25\%$, and that to eliminate possible overlap in performance between different SEER values one would need to increase the SEER value by two SEER points or more.

This effort also produced full sets of DOE-2 inputs for ≈ 90 air conditioner units from which “representative” units were selected each nominal SEER level. The units used in the study were selected from the CEC database based on availability of performance data and then by visual inspection of performance maps and elimination of obvious data error. From that subset of units the “representative” units were selected based on median EER and C_d values. This final set of air conditioners and their DOE-2 inputs were subsequently used in the Courtney study. The “representative” units selected in the Hirsch study were the inputs utilized in the first version of BEopt.

Kruis was the first to look in depth at the differences between the simulation algorithms in DOE-2 and EnergyPlus. In his paper, “Reconciling Differences Between Residential DX Cooling Models in EnergyPlus and DOE-2”, Kruis provides detailed descriptions of the model algorithms and provides methods for conversion between DOE-2 inputs and EnergyPlus inputs. The conversion methods that are laid out in the paper show good agreement when comparing exiting air conditions, heat extraction, and power consumption. This research was done for single speed air conditioners.

All of the other research performed on the simulation algorithms was carried out by looking at the engineering manuals (well-maintained in EnergyPlus and out of date for DOE-2, see [17] and [23] respectively). Further investigation and verification of the engineering manuals was carried out through inspection of the simulation engine source code. The inspection of source code was especially important in the DOE-2 case due to the fact that the two stage air conditioner model was implemented as part of the Hirsch effort described above [12], yet this occurred long after the last version of the DOE-2 engineering manual was published in 1982 [19].

One of the first examples of research into the effects of the actual simulation inputs was carried out by Henderson et al. in their 2000 report on improving part-load energy use predictions and latent removal predictions in DOE-2 by user defined functions [9]. In this study they provide a summary of previous work

on part load degradation, beginning with the original work by Parken et al. on part load that led to the development of the cycling test component of the SEER calculation. They then summarize the current state of physical approximation of part load losses. It has been shown by [18] and [8] that the start-up characteristics can be modeled effectively by first order, linear time-invariant system. Solutions to this ordinary differential equation take the form: $x(t) = c_0 + c_1 * e^{-t/\tau}$ where τ is the time constant. This theoretical model of the start-up effects was combined with the maximum cycling rate of the system (N_{max} , in cycles/hr) by Henderson and Rengarajan in [8] to give the following formula for part load factor as a function of part load ratio (note: $PLF = \frac{PartLoadEfficiency}{SteadyStateEfficiency}$, and successive substitution is required to solve the equation):

$$PLF_{i+1} = 1 - \alpha * (1 - e^{-1/\alpha}) \quad (2.4)$$

Where:

$$\alpha = 4 * \tau * N_{Max} * (1 - \frac{PLR}{PLF_i}) \quad (2.5)$$

Henderson et al. utilize this theoretical function to generate a part load curve which is then compared to the current DOE-2 default curves. This is one of the few examples where the validity of the curve fits are tested and comparisons are generated between the default curves and potentially improved curves.

The second portion of this paper suggests some improvements to the way that DOE-2 deals with sensible/latent performance. These improvements are based on the constant bypass factor, ADP/BF approach (discussed in detail in section 4.1.1). The improvements were implemented via user defined functions in DOE-2.1; the user defined function option was not carried over into DOE-2.2, so this approach does not currently work with DOE-2.2. The development team for EnergyPlus however did incorporate the approach suggested in this paper by Henderson et al. into the DX cooling model in EnergyPlus. This is the cause for the differences between the two simulation engines in their current states.

Two other models were originally considered as potential options for simulating the air conditioner and heat pump performance. These were the component based model developed by Wassmer in [21] and the Heat Pump Design Model (HPDM) developed by Oak Ridge National Laboratory, [19]. The Wassmer model provides a component based model that relies mostly on “first principals” to evaluate steady state

performance. The part load performance is modeled based on the algorithms described above from Henderson et al. The HPDM is a fully developed model that performs complete energy balances on the air and refrigerant sides of the vapor compression loop, and also models complex fluid mechanics processes in the coils. The HPDM does not account for any cycling losses and only models steady state performance. Both of these models require complex sets of inputs (very detailed in the case of the HPDM) and they are not integrated into an annual simulation tool.

This literature review has given an overview of the various approaches to split system modeling, and has provided a comprehensive summary of the work done on the annual simulation models EnergyPlus and DOE-2. Two critical gaps were identified during the course of the literature review: analysis of the effects of the expanded performance data on annual simulations, and research on the implementation of the EnergyPlus model (especially in the case of two stage or multi-speed operation). The research done by Hirsch and Associates, Courtney, and Wassmer all pointed to short-comings in the manufacturers' data. They noted: lack of available data, errors in data entry, potential data adjustment, and inaccurate exiting conditions [10], [21], [5]. Despite the observation of many potential short-comings in the data, the impacts that those issues had on the simulation engines was left unexplored. This could have large impacts in the accuracy of the simulations and effect results of future research. There was also a dearth of research on the EnergyPlus algorithms, especially the multi-speed model. Krus provided a discussion of the single speed algorithm and how it correlated with DOE-2, yet a complete evaluation of the algorithm had not been documented. There also had not been any research on the use of expanded performance data in EnergyPlus, nor how that performance compares to DOE-2 predictions. The research described here has filled the two gaps identified during the literature review. The research has evaluated and quantified the impact of the expanded performance data on annual simulations. It has also provided methods for limiting the negative impacts of some of the error in the expanded performance data. It has also provided a complete analysis and documentation of the EnergyPlus simulation model (for both single and two stage operation). The combination of these two accomplishments have gone a long way in improving the accuracy and consistency of split system modeling.

Chapter 3

Data Review and Compilation

3.1 Discussion of Data: Availability, Acquisition, and Formatting

As discussed in section 1.2, it is the objective of this research to provide a means of assessing the currently available air conditioners and heat pumps, both in terms of total energy use and in terms of relative order of efficiency. Whole building, annual simulation tools provide the capability to evaluate a large number of units, across a wide variety of climates and building types. In order to utilize whole building, annual simulations to evaluate the different air conditioners and heat pumps, it was first necessary to generate the inputs that are needed to run those simulations. The split-system direct expansion models in both DOE-2 and EnergyPlus are based on performance data. They first define performance at a set of rated conditions. Performance at off-rated conditions is then predicted by multiple curves that scale the rated values according to the specific conditions for each time step in the annual simulation. These curves are regression fits to data on performance at off-rated conditions. The combination of the rated conditions and the curve-fits allow the simulation engine to predict performance at all of the different conditions during a full annual simulation.

In order to generate these model inputs, the user must either perform extensive testing at a large number of indoor/outdoor conditions or the user must use existing published data. Due to the incredibly large amount of time and money required to test an air conditioner or heat pump unit, the testing route is almost never utilized. This leaves published data as the source for model inputs. The two main sources for published performance data on air conditioners and heat pumps are: the Air-Conditioning, Heating and Refrigeration Institute (AHRI), and individual manufacturers' expanded performance tables. This section

evaluates the pros and cons of these two different data sources, and then discusses the generation of a database containing the vast majority of the current manufacturers expanded performance tables

3.2 AHRI Data

AHRI is an HVAC trade association that oversees and authorizes the large majority of the certifications for air conditioners and heat pumps in the United States. AHRI was recently named a certification body by the Environmental Protection Agency (EPA). This development places them as the certification body governing Energy Star certification and associated rebates. They dictate all testing procedures and define the SEER and HSPF rating systems in the performance rating document: ANSI/AHRI 210/240 [1]. Therefore all units that are certified by AHRI must undergo certain test procedures as outlined in ANSI/AHRI 210/240. This implies that there exists a certain amount of testing data resultant from the AHRI testing requirements. There are two problems with using AHRI data to inform the simulation models: lack of sufficient test points, and limited access to the full data sets.

3.2.1 Required Testing Conditions

A summary of the required test conditions for air conditioners and heat pumps is presented in table 3.1. For a full description of all possible tests, see [1]. For information on how these test points are used in the SEER and HSPF calculation procedures, see Appendix B. In addition to the tests listed in table 3.1, a cycling test to evaluate part load performance is usually performed due to the below-average default value prescribed by 210/240 of $C_d = 0.25$.

It can be noted that there are only two required test conditions for a single-speed unit in cooling mode and four required for a two stage unit in cooling mode. All of these tests have identical indoor conditions, only varying outdoor conditions. There are three tests required for a single-speed in heating mode and seven tests for a two stage unit in heating mode. Again all of the heating mode tests only vary the conditions on the outdoor coil. This makes sense for AHRI testing, in that they are really only certifying the outdoor unit (mix-and-match of different indoor coils is not considered; the SEER rating for a specific unit only requires the highest sales volume combination of indoor and outdoor coils). Yet these tests do not provide adequate

Table 3.1: Required Test Conditions as Defined by AHRI 210/240

Mode	Test	Outdoor Dry Bulb	Indoor Dry Bulb	Indoor Wet Bulb	Compressor Capacity
Single Speed Cool	A	95	80	67	-
	B	82	80	67	-
Two Speed Cool	A2	95	80	67	High
	B2	82	80	67	High
	B1	82	80	67	Low
	F1	82	80	67	Low
Single Speed Heat	H1	47	70	60	-
	H2	35	70	60	-
	H2	17	70	60	-
Two Speed Heat	H0 ₁	62	70	60	Low
	H1 ₂	47	70	60	High
	H1 ₁	47	70	60	Low
	H2 ₂	35	70	60	High
	H2 ₁	35	70	60	Low
	H3 ₀	17	70	60	High
	H3 ₁	17	70	60	Low

data to generate the EnergyPlus and DOE-2 model inputs. In order to generate the model inputs, one needs to know how unit performance varies with outdoor dry bulb, indoor wet bulb, and airflow over the coil. The only independent variable that is varied in the required AHRI tests is outdoor dry bulb. This makes producing the full set of required curve fits impossible.

3.2.2 Access to AHRI Data

Despite the fact that the AHRI data does not contain enough information for adequate model inputs, the data can still be useful in air conditioner and heat pump research. It can be used in verifying other data sources, in comparing against predicted performance, and potentially as a standard set of inputs in simplified models. Data from the AHRI testing procedures is made available in two forms: an online directory, and as a database (with an annual subscription fee of \$2000).

The main limiting factor with the AHRI data is that they do not publish the full list of test results. The only data published is: SEER, EER, and Capacity at the A test (95/80/67) rating point for cooling, and Capacity, COP (at high and low test points), and HSPF for heating. This limited set of reported data makes it difficult to use the data to verify performance at various outside conditions. It also makes it impossible to

evaluate the way that a specific unit achieves its SEER or HSPF rating. Due to the limited data published in the database it was not considered worthwhile to purchase access to that resource. The online directory can be queried for different indoor and outdoor coil combinations, yet it is not possible to export data for a large number of units at once.

Ideally, AHRI would make available both the other required test points and the coefficient of degradation (C_d), if the cycling test was performed. The C_d value would be the most beneficial piece of AHRI data, due to the fact that part-load degradation can be estimated using this metric. For a further discussion of part-load degradation, see section 2.3.3.

3.2.3 Acceptable Tolerances in AHRI Data

Even though the data provided by AHRI is limited in scope, it is certainly the most reliable data regarding the performance of air conditioners and heat pumps. This is due to the fact that all of the tests that AHRI reports on (as well as the tests not reported, yet used in the SEER and HSPF calculations) are subject to strict testing procedures and are monitored by an independent and objective third party: AHRI. This allows for comparison between other data sources (discussed below) and the AHRI data for verification of data quality. Yet, in order to compare other data sources to the AHRI data, it is necessary to first quantify the uncertainty in AHRI data and their testing procedures.

ANSI/AHRI 210/240 describes the acceptable tolerance very clearly in section 6.5 of the document. In this section they state that: “To comply with this standard, measured test results shall not be less than 95% of Published Ratings for performance ratios and capacities” [1]. This indicates that AHRI accepts error of $< 5\%$ in both the performance ratios (SEER and rated EER values) and rated capacities. Therefore it is only reasonable to expect agreement to $\pm 5\%$ of the AHRI data. Conclusions drawn about percent error less than 5% is within the uncertainty of the data and cannot be conclusive.

3.3 Manufacturer’s Expanded Performance Tables

This leads to the data provided by individual manufacturers. Even though they are not required to provide performance data, the large majority of manufacturers publish expanded performance tables (EPTs)

in which they characterize a units performance at a wide range of conditions. The EPTs are mostly generated to assist contractors and installers with unit selection. Once design conditions have been determined, the contractor is able to evaluate how different units perform at those specific design conditions. This large range of conditions is also exactly what is required to generate the necessary model inputs. Thus the EPTs were considered the best available data for the current research. The common sets of independent and dependent variables are listed in Table 3.2. A complete list of the independent variables for cooling and their ranges by manufacturer is given in table 3.4. A complete list of the dependent variables for cooling and their ranges by manufacturer is given in table 3.3. The comparable tables for heating are provided in tables 3.5 and 3.6. The majority of EPTs report all values as net not gross. This implies that they include fan power in the reported power consumption and fan heat in the reported capacity.

Table 3.2: Common Independent and Dependent Variables

Independent Variables (Cooling)	Dependent Variables (Cooling)
Outdoor Dry Bulb	Total Capacity
Indoor Dry Bulb	Sensible Capacity
Indoor Wet Bulb	Power
Air Flow Rate	
Independent Variables (Heating)	Dependent Variables (Heating)
Outdoor Dry Bulb	Total Capacity
Indoor Dry Bulb	Integrated Capacity
Air Flow Rate	Power

The EPTs contain performance data at a large number of operating conditions, yet there is no governing standard that regulates how this information is reported, in what ranges it is reported, and in what format it is reported. This lack of standardization leads to a wide variety in reporting standards across manufacturers. EPTs are currently found in PDF, HTML, and hard copy (either as excel files on a compact disc upon request or in paper format upon request) depending on the manufacturer. It also leads to a wide variation in both the dependent variables that are reported on, and in the ranges over which independent variables are varied. Table 3.3 shows the ranges of dependent variables for different manufacturers. Table 3.4 shows the independent variables (operating conditions) that are reported for the same set of manufacturers. It is also important to note that the EPTs are not representative of actual testing data. The EPTs are

generated by the manufacturers in-house computer models. These models usually take in the test data from the AHRI test points and then proceed to generate model based predictions of performance at all other conditions. Therefore, while this data is the best that is currently available, it must be noted that it is only as good as the models produced by the individual manufacturers.

Table 3.3: Dependent Variables Reported on by Manufacturer (Cooling)

Manufacturer	Sensible Capacity [Mbtu/h]	Latent Capacity [Mbtu/h]	Total Capacity [Mbtu/h]	System Power [kW]	S/T Ratio	Amps [Amps]	Hi Pressure [psi]	Low Pressure [psi]	Compressor Power [kW]
Carrier	✓		✓	✓					
Goodman			✓	✓	✓	✓	✓	✓	
Trane	✓		✓	✓					
Lennox			✓	✓	✓				✓
Rheem		✓	✓	✓			✓	✓	✓
York	✓		✓	✓					
Nordyne	✓		✓	✓					

Table 3.4: Independent Variables Reported on by Manufacturer (Cooling)

Manufacturer	Outdoor Dry Bulb [°F]	Entering Dry Bulb [°F]	Entering Wet Bulb [°F]	CFM [CFM/Ton]
Carrier	75—85—95—105—115—125	80	57—62—63—67—72	Approx 350-450
Goodman	65—75—85—95—105—115	70—75—80—85	59—63—67—71	Approx 350-450
Trane	85—95—105—115	70—72—78—80	59—63—67—71	Approx 350-450
Lennox	85—95—105—115	75—80—85	63—67—71	Approx 350-450
Rheem	55—75—95—105—115	80	57—63—67—75	Approx 400
York	65—75—85—95—105—115—125	80	57—62—63—67—72	Approx 350-450
Nordyne	60—70—80—90—95—100—110—120	80	62—63—67—72	Approx 350-450

Table 3.5: Dependent Variables Reported on by Manufacturer (Heating)

Manufacturer	Total Capacity [Mbtu/h]	System Power [kW]	Compressor Power kW	Integrated Capacity [kW]	COP	ΔT [°F]	Amps [Amps]	Hi Pressure [psi]	Low Pressure [psi]
Carrier	✓	✓		✓					
Goodman	✓	✓			✓	✓	✓	✓	✓
Lennox	✓	✓	✓						
Rheem	✓	✓	✓	✓	✓			✓	✓
Trane	✓	✓							
York	✓	✓			✓				

Table 3.6: Independent Variables Reported on by Manufacturer (Heating)

Manufacturer	Outdoor Dry Bulb [°F]	Entering Dry Bulb [°F]	CFM [CFM/Ton]
Carrier	-3-7-17-27-37-47-57-67	65-70-75	Approx 350-450
Goodman	-10--5-0-5-10-15-17-20-25-30-35-40-45-47-50-55-60-65"	70	Approx 400
Lennox	-15-5-25-45-65	70	Approx 350-450
Rheem	17-35-47	60-70-80	Approx 400
Trane	2-7-12-17-22-27-32-37-42-47-52-57-62-67-72	60-70-75-80	Approx 400
York	10-17-30-40-47-60	60-70-80	Approx 350-450

Tables 3.3 to 3.6 demonstrate the wide variety of reported variables and the operating conditions under which they are reported. For air conditioners, the variation is significant but it is more of an inconvenience (in dealing with different operating ranges) than a paucity of data. The heat pump reporting on the other hand, has limitations with regards to completeness for certain manufacturers. Only two of the manufacturers (Carrier and Rheem) provide data on integrated capacity; capacity including effects of the defrost cycle. Only two of the manufacturers (Carrier and York) report data at **both** various entering dry bulb and various CFMs. This limits the usability of the data for generating full sets of simulation inputs.

3.3.1 Processing of the Expanded Performance Tables

One of the first main challenges in the research process was compiling all of the available performance data into a usable resource for generating the model inputs. To adequately look at the performance of the current collection of air conditioners and heat pumps, it was necessary to put all of the available EPTs into a standard format. This would allow for equal comparison across different manufacturers and would also allow for efficient production of model inputs across a large number of individual units.

The process of compiling these documents was made difficult due to: wide variability in ease of access (both in locating and processing the files), and the wide variation in variables reported on (see tables 3.3 to 3.6 above). An exhaustive search of all of the top market shareholders resulted in portable document format (PDF) EPTs for Carrier, Goodman, Lennox, and York (representing 62% of the market share), Excel format for Rheem and Nordyne (21% of market share), and HTML format for Trane (14% of market share). The total market share evaluated during data collection was 97% (see figure 3.1).

The Nordyne data was only provided for limited model lines and therefore was not processed and included in the final database. The performance data on the Nordyne IQ drive did prove to be useful and was utilized to approximate multi-speed performance in the latest BEopt release. Rheem did not provide access to their EPTs, yet upon contacting their engineering department they agreed to collect performance data on all their top sales volume units. They provided the data in excel format and the data included actual test results. The data points they reported were not sufficient for generating the curve fits required for EnergyPlus simulation, therefore the data was used mostly as a form of verification of trends that

Buildings Energy Data Book: 5.3 Heating, Cooling, and Ventilation Equipment		March 2011	
5.3.6 2008 Unitary Air-Conditioner/Heat Pump Manufacturer Market Shares (Percent of Products Produced)			
<u>Company</u>	<u>Market Share (%)</u>	Total Units Shipped:	5,833,354 (1)
UTC/Carrier	27%		
Goodman (Amana)	14%		
American Standard (Trane)	14%		
York	12%		
Nordyne	12%		
Rheem	9%		
Lennox	9%		
Others	3%		
Total	100%		
Note(s): 1) Does not include water-source or ground-source heat pumps.			
Source(s): Appliance Magazine, U.S. Appliance Industry: Market Share, Life Expectancy & Replacement Market, and Saturation Levels, January 2010, p. 5.			

Figure 3.1: 2008 Market Share for Air Conditioners and Heat Pumps [6]

developed throughout the research process. They were the only manufacturer that provided degradation coefficient values (C_d) and W/CFM values for the indoor fans. This data was used to inform the selection of appropriate C_d values and fan power consumption for BEopt options.

This left the four manufacturers publishing in PDF and Trane in HTML as the main data sources for the research effort. This data all had to be compiled and converted into a common format. It was therefore necessary to transfer the PDF files into a useable data format. To accomplish this transformation, the PDF files were copied and pasted into text files. The Trane data ended up being easily copied into Excel format. Individual Python scripts were then written to parse the text files for each of the other four manufacturers. Python is a free, open-source programming language (though it is most often used for scripting purposes). Python is also the language being utilized for the upcoming BEopt 2.0 release. Therefore the methods used in compiling this database will be applicable/compatible with future BEopt releases. This leaves the door open to possible direct integration of the database into BEopt runs in version 2.0 and forward.

It was necessary to write ten different scripts due to the fact that the five manufacturers all used different table formats in the EPTs and also between air conditioners and heat pumps. An example script that was used for parsing the text files can be found in Appendix A. The Python scripts were used to output the tables into a comma separated value format (CSV). The Trane files in HTML format proved to be easily converted into similar CSV files. All of these CSV files were then read (via another Python

script) into a SQLite database. This process resulted in a fully-searchable database with thousands of data points describing performance characteristics for approximately 260 currently available air conditioner units and 200 currently available heat pump units. This was the first database created that brought together performance data from all of the different manufacturers into one useable format. This database was used to produce the simulation model inputs for all units contained in the database (see section 5.1). It is possible that this database could inform future research into other aspects of air conditioner and heat pump research and it has been made available within the residential buildings group at NREL.

Chapter 4

In Depth Model Descriptions

4.1 EnergyPlus and DOE-2 Split System Models

This section will look in depth at the structure of the two split system models evaluated for the current research: EnergyPlus and DOE-2. The model for cooling mode will be discussed first and then followed by the heating coil model. The focus will generally be on EnergyPlus's model, with secondary evaluation of the DOE-2 model. EnergyPlus was chosen as the principal model for this investigation for a number of reasons:

- A more simple and theoretically sound model than DOE-2
- Lower numbers of inputs and less complex inputs
- Much improved documentation as compared to DOE-2
- EnergyPlus's position as the most current/advanced simulation engine with on-going development

The DOE-2 model has some significant differences to the EnergyPlus implementation. These differences will be noted and commented upon in section 4.1.5. For details on the conversion process between DOE-2 and EnergyPlus, please see N. Kruis's paper, Reconciling Differences Between Residential Cooling Models in DOE-2 and EnergyPlus [15].

4.1.1 EnergyPlus - Single Speed: Cooling

EnergyPlus's model is a surrogate model based on regression curve-fits of manufacturer's data. It uses performance data at rated conditions (AHRI A-test conditions of 95 outdoor dry bulb, 80/67 indoor

dry bulb/wet bulb) combined with curve-fits to simulate performance at off-rated conditions. The required information at **rated** conditions consists of:

- Total capacity
- Sensible heat ratio (SHR)
- Coefficient of performance (COP)
- Airflow over the indoor coil (CFM)

Capacity and COP are required to be gross values (without effects of indoor fan heat or power). This is due to the fact that the indoor fan is modeled separately in EnergyPlus. The rated values listed above are modified by five separate **curves** that describe performance at off-rated conditions:

- Total Capacity - function of entering wet bulb and outdoor dry bulb ($Q_{f(T)}$)
- Energy Input Ratio (EIR - inverse of COP) - function of entering wet bulb and outdoor dry bulb ($EIR_{f(T)}$)
- Total Capacity - function of flow fraction ($Q_{f(FF)}$)(FF defined as \dot{m}/\dot{m}_{rated})
- EIR - function of flow fraction ($EIR_{f(FF)}$)
- Part Load Fraction (PLF) - function of part load ratio (PLR)

The total capacity and EIR curves that are a function of entering wet bulb and outdoor dry bulb are both bi-quadratic curve fits. They take the form, $y = a + b(T_{ewb}) + c(T_{ewb})^2 + d(T_{odb}) + e(T_{odb})^2 + f(T_{ewb}) * (T_{odb})$, where *ewb* is entering wet bulb and *odb* is outdoor dry bulb. The total capacity and EIR curves that are a function of flow fraction are both quadratic curve fits; they take the form, $y = a + b(FF) + c(FF)^2$. The part load fraction as a function of part load ratio curve is a quadratic curve fit of the form $y = a + b(PLR) + c(PLR)^2$. Part load ratio is defined as the ratio of sensible cooling load to total sensible capacity for the current time step in the simulation. The output of the part load fraction curve is used to modify the part load ratio of the unit for that time step and defines the run time. The run time fraction

(RTF) is modified as $RTF = PLR/PLF$. Thus, if the output of the part load fraction curve is less than one, it causes an increase in the run time for that time step. This adjustment accounts for the part load losses of the unit. It should be noted that all of the capacity and power calculations are assumed to be at steady state, therefore part load is accounted for by extending the total run time (at steady state) of the unit.

There are a few interesting assumptions that are inherent in the way that the EnergyPlus curve inputs are defined. The first is that total capacity and efficiency are assumed to be independent of entering dry bulb temperature. This assumption clearly follows from the way the modifying curves are defined; there is no curve that varies with entering dry bulb. The second is that variation with temperature and flow rate happens independently. The fact that EnergyPlus defines two separate curves implies that the model assumes that there is no interaction between these variables.

The part load ratio is how EnergyPlus defines the runtime for a unit at each time step. It calculates the load on the zone for that time step, and the desired outlet temperature from the coil to meet that load. The algorithm then iterates (using a regula falsi/false position method) on a residual function of the difference between the desired outlet temperature and the current outlet temperature. The variable that the iteration varies to reduce the residual is the part load ratio. Thus, EnergyPlus converges on a portion of the time step that the unit must run at steady state to meet a calculated delivery temperature for the time step. This part load ratio is used as the input to the part load fraction curve (as described above) and then modified by the output of that curve to determine the final run time for the time step.

Finally, the power consumption for the time step is calculated:

$$P = EIR * Q_{Total} * RTF \quad (4.1)$$

Where EIR and Q_{Total} are calculated by the equations (4.2) and (4.3) respectively:

$$EIR = EIR_{rated} * EIR_{f(T)} * EIR_{f(FF)} \quad (4.2)$$

$$Q_{Total} = Q_{Total,Rated} * Q_{f(T)} * Q_{f(FF)} \quad (4.3)$$

Where $EIR_{f(T)}$ and $Q_{f(T)}$ are the curves for EIR and Total Capacity as a function of entering wet bulb and outdoor dry bulb and $EIR_{f(FF)}$ and $Q_{f(FF)}$ are the curves for EIR and Total Capacity as a function

of flow fraction.

The preceding discussion describes how EnergyPlus evaluates total capacity and power. EnergyPlus also must quantify the sensible and latent performance of the unit for each time step. To calculate the sensible and latent portions, EnergyPlus utilizes the rated SHR and the apparatus dew point (ADP)/bypass factor (BF) model. The ADP is defined as fully saturated air with a dew point temperature equal to the temperature at the surface of the coil. The ADP can be calculated using a psychrometrics chart by plotting both the entering and exiting conditions and drawing a straight line through those two points; where that line intersects that 100% saturation curve is the ADP. The BF describes the fraction of the incoming air that exits the coil at exactly the same conditions as it entered. The rest of the air is assumed to exit the coil fully saturated with temperature equal to the ADP (ADP conditions). This process is outlined below: First calculate the exiting air conditions at AHRI rated conditions (95/80/67) by using the total and sensible heat equations:

$$h_o = h_i - \frac{Q_{Total,Rated}}{\dot{m}} \quad (4.4)$$

$$T_{o,db} = T_{i,db} - \frac{Q_{Sens,Rated}}{\dot{m}} \quad (4.5)$$

$$\omega_o = \omega(h_o, T_{o,db}) \quad (4.6)$$

Then calculate the temperature and humidity ratio at ADP by simultaneously solving equations (4.7) and (4.8):

$$\frac{\omega_i - \omega_0}{T_{i,db} - T_{o,db}} = \frac{\omega_i - \omega_{ADP}}{T_{i,db} - T_{ADP,db}} \quad (4.7)$$

$$\omega_{ADP} = \omega(T_{ADP,db}, \phi = 100\%) \quad (4.8)$$

With ω_{ADP} and $T_{ADP,db}$ defined, the ADP enthalpy can be calculated:

$$h_{ADP} = h(\omega_{ADP}, T_{ADP,db}) \quad (4.9)$$

Finally, calculate the bypass factor according to the definition (4.10):

$$BF = \frac{h_i - h_o}{h_i - h_{ADP}} \quad (4.10)$$

The ADP/BF method is a way of calculating the effectiveness of a cross-flow heat exchanger; it can be seen from the definition of BF (4.10) that it is ratio of the change in enthalpy from entering to exiting conditions over the change in enthalpy from the entering conditions to the theoretical APD state. This makes the BF analogous to $1-\epsilon$, where ϵ is the effectiveness of the coil. Therefore BF can equivalently be described in terms of number of transfer units (NTU), $BF = e^{-NTU} = e^{-\frac{UA/C_p}{\dot{m}}} = e^{-\frac{A_o}{\dot{m}}}$. It can be noted that for a fixed coil geometry, BF only varies with flow rate (\dot{m}) over the coil.

EnergyPlus's model uses the rated SHR and total capacity to calculate the BF at rated conditions (as outlined above). It then uses the rated mass flow rate and this rated BF to calculate the A_o value. A_o is used with the actual flow rate at each time step to calculate the BF for the current time step. The current BF is then used with the total capacity, indoor conditions, and ambient conditions for the time step to back into the sensible and latent capacities.

4.1.2 EnergyPlus - Multi Speed: Cooling

The inputs for EnergyPlus's multi-speed model are very similar to the single-speed model. The model requires the user to define how many speeds are being modeled (acceptable values are 1 to 4). A full set of the model inputs (rated values and curve-fits) defined for the single-speed model is then required for each individual speed.

At the beginning of each time step, if there is a need for cooling, EnergyPlus checks the available capacity at each speed (beginning with the lowest speed). This is done using the rated capacity for that speed along with its associated temperature and flow fraction curves evaluated at the current conditions. If the tested speed does not have the required capacity to meet the load, then the next speed is tested and so on until a speed is found that has more capacity than the required load. If the highest speed is reached and

the load is still higher than the capacity, then the unit will run the entire time step and the time step will be included in the hours cooling load not met metric.

Once the speed required to meet the load has been determined, the simulation engine determines what portion of the time step will be spent at that speed and what portion will be spent at the speed below. For the rest of the discussion the unit will be assumed to be a two speed unit with only a high and low speed. This will simplify terminology to only include high and low speed, without sacrificing any complexity since the algorithm between speeds is exactly the same, independent of number of speeds (2, 3, or 4). To determine the portion of time spent at high and low speed, EnergyPlus does not allow cycling (between low and off) when the load falls between the low and high capacity. This assumption implies ideal control of the unit such that the low speed operates for the maximum portion of the time step such that the load can be exactly met by the high speed operating for the remaining portion of the time step. EnergyPlus then linearly interpolates between the high and low speeds to establish the performance for the time step. To better illustrate the method EnergyPlus uses to calculate run time, a simple example is presented.

Assume that the high speed has a normalized capacity of 1.0 and that the low speed has a normalized capacity of 0.5. The load for the current step is 0.75 (normalized to the high speed). To fully meet this load there is a spectrum of high and low run time combinations. At one end of the spectrum, the high speed could run for 75% of the time step and then the unit could shut off for the remaining 25% (shown in Figure 4.1 - Top). At the other end of the spectrum the high speed could run for 50% of the time step and the low speed could run for the other 50% (shown in Figure 4.1 - Bottom). Note that any more than 50% run time at the low speed would make the unit unable to meet the load with the high speed operating the rest of the time step. There are theoretically an infinite number of other combinations in between those two extremes that would suffice; essentially the problem is under-defined. EnergyPlus solves this problem by requiring run time at high speed plus run time at low speed equal 1: $Runtime_{HIGH} = 1 - Runtime_{LOW}$. This disallows all combinations except for the combination shown in Figure 4.1 - Bottom. This also implies that there is no cycling allowed when the load is between high and low capacities (all of the other combinations require the unit shutting off for some portion of the time step). Essentially EnergyPlus assumes ideal control of unit's compressor. This assumption should be valid for properly installed/controlled air conditioner and heat

pump units.

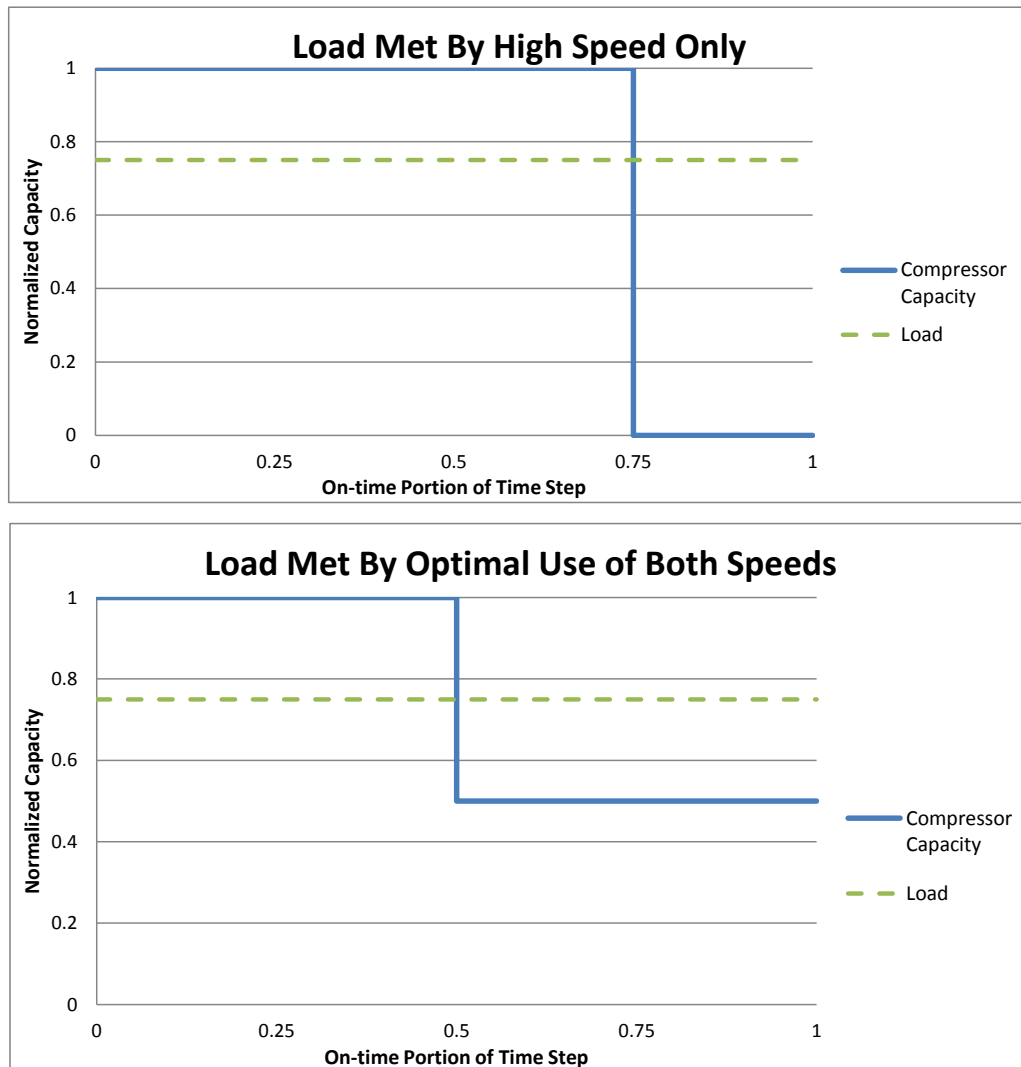


Figure 4.1: Multi-Speed Run Time Example: Top - High speed only. Bottom - Optimal Low Speed Operation

Once the runtime has been determined, the performance is linearly interpolated between the high and low speeds using the run time as the weighting factor. The power consumed during that time step is calculated: $P_{Cool} = Q_{HIGH} * EIR_{HIGH} * RTF + Q_{LOW} * EIR_{LOW} * (1 - RTF)$. Capacity and EIR are evaluated using the inputs for their respective speeds.

In multi speed operation, part load can either be evaluated at each speed (useful when simulating multiple compressors, as in a staged system), or only during cycling below low speed and off. Due to the

fact that the two stage units being modeled in this study were utilizing a single compressor, part load effects were only modeled during cycling. The modeling of low speed operation (or cycling between low speed and off) is identical to the single speed cooling model described above ¹ .

4.1.3 EnergyPlus - Single Speed: Heating

The single speed heat pump model that EnergyPlus uses is very similar to the cooling model. It uses a combination of rated values (at the H₁ test, 47/70/60) and curves to predict performance at a variety of conditions. The required values are listed below.

Rated:

- Total capacity
- Coefficient of performance (COP)
- Airflow over the indoor coil (CFM)

Curves:

- Total Capacity - function of entering dry bulb and outdoor dry bulb ($Q_{f(T)}$)
- Energy Input Ratio (EIR - inverse of COP) - function of entering dry bulb and outdoor dry bulb ($EIR_{f(T)}$)
- Total Capacity - function of flow fraction ($Q_{f(FF)}$)
- EIR - function of flow fraction ($EIR_{f(FF)}$)
- Part Load Fraction (PLF) - function of part load ratio (PLR)

It should be noted that the capacity and EIR as a function of temperature curves can either be biquadratic (function of entering dry bulb and outdoor dry bulb) or quadratic (function of outdoor dry bulb only).

¹ There are slight differences if the fan is modeled as running continuously, yet for this study the fan was assumed to cycle with the compressor (comparable to the standard control strategy), thus making the single speed model identical to the low speed operation here

The DX heating object also requires some inputs with regards to the defrost cycle. The first is what type of defrost cycle is being implemented: reverse cycle of resistive. If the user selects a resistive defrost cycle, s/he must define the capacity of the resistive element. If the reverse cycle defrost is selected, the user must define a defrost-EIR curve that is a function of outdoor dry bulb and entering wetbulb. This is essentially like the EIR curve that is required for cooling mode. This makes sense in that that is exactly what the unit is doing in reverse cycle: cooling. The one difficulty with this input is that none of the cooling data remotely approaches the low ambient temperatures that are required to generate this curve. For this study this curve was assumed to be constant a constant generated from the cooling-EIR curve at 60 drybulb and 60 wet bulb. This is exactly where DOE-2 evaluates the same curve for reverse cycle efficiency, making the comparison more exact between models. It is also unlikely that there are large changes in efficiency at the low ambient temperatures seen during defrost cycles.

Along with the type of defrost, the user must define the control strategy: timed or on-demand. If the timed control strategy is selected the user must define the length of the defrost cycle. If it is an on-demand cycle, EnergyPlus calculates an approximate outdoor coil surface temperature and then evaluates a $\Delta\omega$ function to estimate a required on-time for the defrost cycle. Once the required on-time is calculated, capacity and efficiency multipliers are calculated. During this process the added load due to cooling the building in reverse cycle is calculated and added to the runtime defined by PLR. For more information on the methods used for calculating the multipliers or runtime, see [17].

The power consumption is then calculated as follows:

$$P = \frac{Q_{Total} * EIR * PLR}{PLF} \quad (4.11)$$

Where:

$$EIR = EIR_{Rated} * EIR_{f(T)} * EIR_{f(FF)} * EIR_{DefrostAdjust} \quad (4.12)$$

$$Q_{Total} = Q_{Total,Rated} * Q_{f(T)} * Q_{f(FF)} * Q_{DefrostAdjust} \quad (4.13)$$

$$PLF = a + b * PLR + c * PLR^2 \quad (4.14)$$

It can be noted that the calculations for heating mode are very similar to the cooling mode calculations

except for some differences regarding defrost cycle. The lack of any latent calculations also simplifies the calculation procedure.

4.1.4 EnergyPlus - Multi Speed: Heating

The multi-speed heating algorithm operates almost exactly as described in the multi speed cooling section. In fact both the multi-speed cooling coil and the multi-speed heating coil can only be used within the same parent object: UnitaryHeatPump:AirToAir:MultiSpeed. The multi-speed heating coil uses the single speed heating algorithm described above and utilizes a separate set of inputs for each of 2-4 speeds. Again, part load losses were only considered to impact the unit when cycling between low and off.

4.1.5 Differences in DOE-2

On a macro scale, the DOE-2 model employs a very similar methodology to the EnergyPlus model; it uses rated values (defined at the same 95/80/67 AHRI A rating point) and modifies those values with various curve fits. Yet upon closer inspection, many of the actual inputs and algorithms utilized are quite different between the two simulation engines. The significant deviations are addressed below. For a complete discussion of the DOE-2 model and its inputs, please refer to Appendix B in [5].

- Requires explicit definition of bypass factor (rated value and curve fit) in the required inputs
- Calculation method for the sensible capacity
- Calculation of run time between speeds (multi-speed operation)
- Assumes that total capacity, sensible capacity and EIR do not vary with flow rate (no flow fraction curves)

DOE-2 requires that the user input both a rated BF and a curve defining BF as a function of entering wet bulb and outdoor dry bulb. The sensible capacity is then calculated as:

$$Q_{sens} = Q_{sens,rated} * Q_{sens,f(T)} + \dot{m} * C_p * (1 - BF) * (T_{db,i,rated} - T_{db,i}) \quad (4.15)$$

Where $Q_{sens,f(T)}$ is the sensible curve as a function of indoor wet bulb and outdoor dry bulb and BF is defined using both the rated value and the BF curve (as a function of indoor wet bulb and outdoor dry bulb).

From the previous discussion of the ADB/BF model, it can be seen that the required inputs for DOE-2 result in an over-defined model (it should not be necessary to define both sensible and BF values). The fact that the model is both over-defined and requires the user to provide complicated inputs such as a BF curve were some of the main factors in deciding to use EnergyPlus as the principal simulation engine.

The way in which DOE-2 handles multi-speed operation is another large difference between DOE-2 and EnergyPlus. DOE-2 deals with multiple speed by defining an EIR curve that is a function of part load ratio (EIR-fPLR). This curve is used to define the EIR at loads less than the high speed capacity. The EIR-fPLR curve is used in conjunction with the COOL-STAGES variable that defines the rated capacities at lower speeds. COOL-STAGES is a comma-separated array that defines that ratio of rated capacity at each speed to the rated high speed capacity. Thus, an entry of [0.7,1] would define a two stage compressor with the low stage operating at 70% of the high stage capacity. The EIR-fPLR curve is used between a PLR of 1.0 and the MIN-UNLOAD-RATIO (usually the lowest of the COOL-STAGES) and is used to capture both the reduction in runtime at lower part loads and any improvement in efficiency at lower speeds. For part load ratios below the MIN-UNLOAD-RATIO the unit is assumed to cycle, and a different curve (COOL-CLOSS-FPLR) is used to capture the effects of those cycling losses. The fact that the EIR-fPLR curve describes both the runtime of the unit and the improvement in efficiency at lower speeds makes this curve quite complicated. This complication is required because the equation that DOE-2 uses to calculate energy consumption by the air conditioner does not contain a specific term that defines runtime. A description of SDSF subroutine that is called by the VARVOL routine in DOE-2 is described below. This discussion specifically focuses on the operation between speeds. The power is calculated in this subroutine as:

$$P_{Cool} = QCT * EIR * NOWFRC * PCTON \quad (4.16)$$

The term *NOWFRC* is initialized as 1, and never reassigned a value (except in the RESSYS routine which is not used here). The final term of this equation, *PCTON* is defined as:

$$PCTON = Min(1, CLPLR/CLCOR) \quad (4.17)$$

Where:

$$CLPLR = CFMCYC * AMIN1(PLRC/(hgmin + .001), 1.0) \quad (4.18)$$

$$CLCOR = CVAL(< COOL - CLOSS - FPLR >, CLPLRM, CLPLRM) \quad (4.19)$$

$$CLPLRM = AMAX1(CLPLR, < COOL - CLOSS - MIN >) \quad (4.20)$$

The key term here is the CFMCYC term. From the engineering description of the Staged Flow/Capacity DX Cooling/Heating algorithm which is used within the VARVOL subroutine, it can be noted that CFMCYC is the fraction of the hour that the fan is running. When the unit is between speeds it is defined as 1. Therefore, $CLPLR = 1 * AMIN1(PLRC/(hgmin+.001), 1.0)$, yet if the unit is between speeds, PLRC must be greater than hgmin. This implies that $CLPLR = 1$ for between speed operation. Since $CLPLR = 1$, it follows that the COOL-CLOSS-FPLR curve will be evaluated at one and $CLCOR = 1$. This shows that $PCTON = 1$ during between speed operation. Thus, between speeds (4.16) simplifies to² :

$$P_{Cool} = QCT * EIR \quad (4.21)$$

Where:

- *QCT* is total capacity defined by, $QCT = Q_{Rated} * QM1$
 - * Q_{Rated} is the user input for rated total capacity
 - * $QM1 = Q_{f(ODB,EWB)}$ is the user input for the curve evaluated at the current conditions
- *EIR* is energy input ratio defined by, $EIR = EIR_{Rated} * EIRM1 * EIRM2$
 - * EIR_{Rated} is the user input for the rated EIR
 - * $EIRM1$ is the first EIR curve modifier, $EIRM1 = EIR_{f(ODB,EWB)}$

² Note that this equation only holds for operation between speeds

* $EIRM2$ is the second EIR curve modifier, $EIRM2 = EIR_f(PLRCC)$

* $PLRCC = \text{Max}(\text{MinUnloadRatio}, PLRC)$

* $PLRC = Q_{load} / (Q_{capacity} * CFMCYC)$

Evaluation of this series of equations shows that the run time for the unit is defined by $PLRC$, which is then used to evaluate the $EIR - fPLR$ curve. Therefore, this curve must both define the improvement in efficiency at the low speed (reduced EIR) and the reduction in the run time at the high speed capacity. To demonstrate the dual effects of this curve, let us consider the simplified case where the unit has the same efficiency at high speed and low speed. One might assume that the curve would be constant in this case; essentially saying that EIR does not vary with PLR. Yet, upon evaluation of (4.21), it is clear that a constant value curve would not reflect the reduction in required capacity at lower PLRs. The QCT term of (4.21) would not change at all. Therefore, if $EIRM2$ curve was constant, there would be no difference in P_{Cool} between a time step where the load was equal to the capacity and a time step where the load was half the capacity. To correctly model a unit with a constant EIR at high and low speed it is necessary to set $EIR - fPLR = PLR$ (essentially a $y = x$ relationship). To capture the fact that two stage air conditioner units actually have a lower EIR at the low stage, the curve must then return a value below the $y = x$ line at reduced PLRs. These two cases (the simplified, constant EIR case and the more realistic reduced EIR case) are shown in figure 4.2.

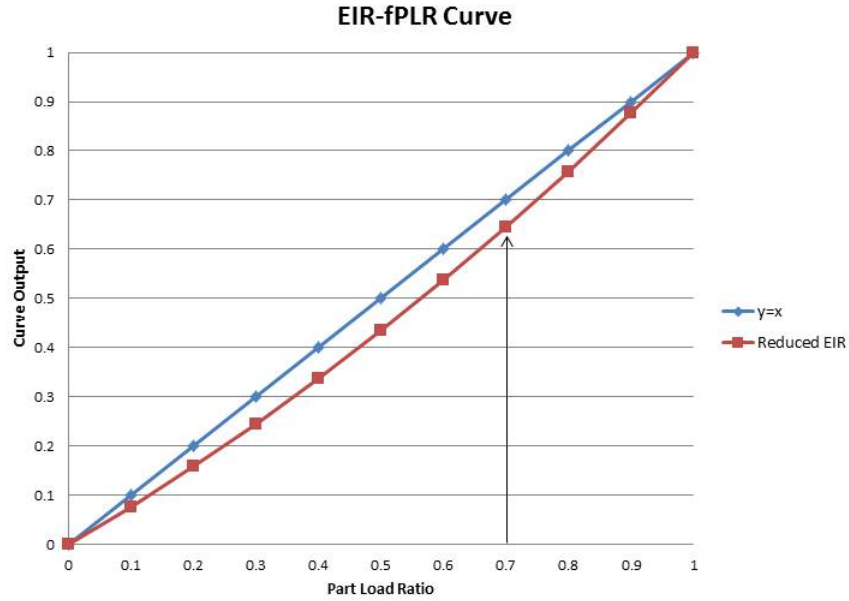


Figure 4.2: Two versions of DOE-2's EIR-fPLR curve

A second (more concerning) complication with the DOE-2 algorithm curve is the fact that $PLRC$ which has just been identified as the runtime portion of the DOE-2 algorithm (when between speeds) is evaluated as the ratio between the total load and the total capacity for the time step. This clearly follows from the observation that CFM_{CYC} is equal to 1 between speeds; therefore $PLRC = Q_{total,load}/Q_{total,capacity}$. This is not consistent with the fact that air conditioner units are controlled with a thermostat, which is a sensible-only device ³.

This apparent error in the DOE-2 algorithm causes erroneous results when modeling two stage units. The combination of the unnecessary complexity in user inputs and the use of total loads when defining runtime were the final components in the decision to use EnergyPlus as the simulation engine for the research carried out for this thesis ⁴.

³ A humidity set point can be implemented, yet that is handled with a separate algorithm in DOE-2

⁴ The single speed model and operation between off and low stage both use a mix of sensible and total loads and capacities for run time calculations.

4.2 Summary of Model Assumptions

This chapter has discussed both of the simulation engine algorithms extensively. They are both regression based models that use a combination of rated values and curves to simulate coil performance. This section is included simply to give a summary of the distinguishing characteristics of each simulation engine, their overlap, and their main differences. This list is not assumed to be complete, rather it is presented as a summary of the points highlighted in the previous sections of the chapter.

EnergyPlus

- Total capacity and efficiency are modified by enter wet bulb and outdoor dry bulb
- Total capacity and efficiency are modified by flow fraction
- Assumes that total capacity and efficiency are not affected by indoor dry bulb
- Assumes that flow fraction and temperature effects are independent (separate curves)
- Utilizes ADP/BF to calculate sensible capacity
- Assumes that BF is constant for all indoor/outdoor conditions (varies only with flow fraction)
- Part load losses modeled with a curve that increases runtime at lower part load fractions
- Utilizes a second set of inputs for each speed (multi-speed operation)
- Allows for separate sets of curves at different operating speeds
- Linearly interpolates between speeds to determine capacity and efficiency for loads that fall between high and low capacity

DOE-2

- Total capacity and efficiency are modified by enter wet bulb and outdoor dry bulb
- Assumes that total capacity and efficiency are do not vary with flow rate over the coil (no flow fraction curves)

- Assumes that total capacity and efficiency are not affected by indoor dry bulb
- Requires rated values and curves for both sensible capacity and BF
- Utilizes a combination of those inputs to calculate sensible capacity
- Multi-speed operation modeled by combining capacity ratios and an EIR-fPLR curve
- EIR-fPLR curve captures both improved efficiency and lower runtime at lower loads
- Runtime between speeds is calculated as the ratio of total load to total capacity (should be based on sensible load and capacity)

It is essential to understand the way that the simulation algorithms operate so as to generate accurate input values from the data. It is also important when evaluating the effects that different inputs have on the results produced during an annual simulation. The following chapter looks at the data that was collected into the database and evaluates that quality of the data from a variety of angles. The assumptions listed above will be crucial in understanding how some of the inconsistencies outlined in the following chapter will effect the results and can inform research into how to limit the impact of these inconsistencies.

Chapter 5

Generating Model Inputs and Data Evaluation

5.1 Generating Model Inputs

Through the evaluation of all available data sources on air conditioners and heat pumps (see section 3.1), it became clear that the manufacturer's expanded performance tables (EPTs) were the only resource that would provide adequate information for producing all of the model inputs required by EnergyPlus. The SQLite database that was generated as part of this research effort now provided the capability to generate model inputs for over 460 air conditioners and heat pumps. There are many more than 460 air conditioner and heat pump models on the market. The reason that they are not all represented here is that most manufacturers only publish expanded performance data for a single indoor/outdoor combination. This fact (along with the access issues described in chapter 3) brings the number of units with available data down to the 460 denoted above. These combinations are generally the highest sales volume combination which is the only combination for which testing is required under the SEER rating procedure.

The specific model inputs were generated by querying the database using SQL. The SQL queries were implemented within a loop in a python script. This allowed for iteration through the entire database with the necessary inputs being written out to a file at the end of every step in the loop. The least squares regression necessary to produce the biquadratic (and quadratic) curve fits was performed by the python method: `linalg.lstsq`. The step-by-step process for each individual unit is outlined below:

- (1) Use a SQL query to read in all of the data for the given unit
- (2) Loop through the data and place the operating conditions in one array and the corresponding

capacities and EIRs in separate arrays

- (3) During the loop, when the operating conditions were equal to the rated conditions, write all of those values to another array (rated values)
- (4) Correlate the capacity and EIR arrays to the operating conditions array using least squares regression (generates curve fit coefficients)
- (5) Write both the curve fit coefficients and the rated values to an output file
- (6) Repeat with the next unit

This process resulted in full model inputs for 260 individual air conditioner units and 200 individual heat pump units.

An important difference to note between the data reported in the EPTs and the required model inputs is the difference between net and gross values. Figure 5.1 demonstrates the difference between net and gross capacity. The net value measurement evaluates the entering conditions before the fan and the exiting conditions leaving the coil. This does not take into account the heat introduced into the air stream by the fan motor. Thus the load removed by the air conditioning coil (the gross value) is actually larger than the calculated net value due to the fact that it removes the fan motor heat in addition to the change from entering to exiting conditions. In both DOE-2 and EnergyPlus the fan and the coil are each modeled separately. Therefore, the simulation engines require all of the model inputs to be gross values.

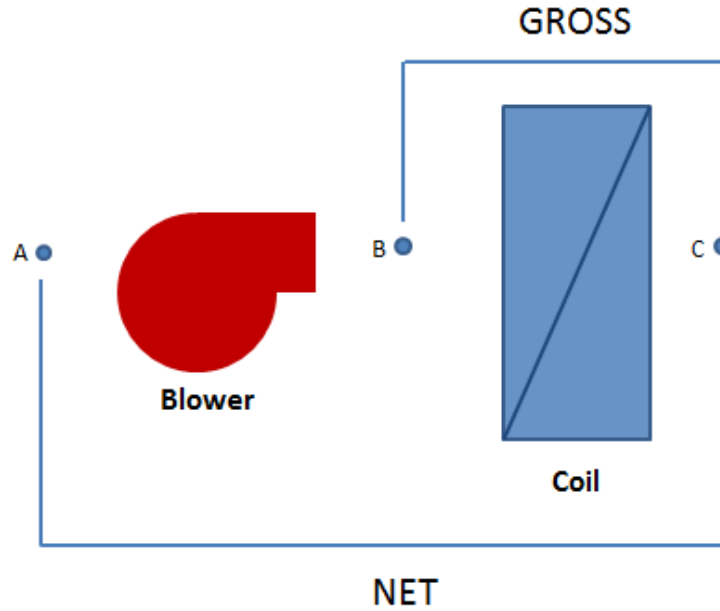


Figure 5.1: Measurement points for net and gross capacity calculation for a blow through configuration

It was considered beneficial to store the actual reported (net) data in the database in case the database was used in future research. Therefore, all of the manufacturer's data was stored exactly as reported and the conversion to gross values was performed in the python script that generated the model inputs. To make the conversion from net to gross, an assumption was required on the amount of fan power [W] per volume of air moved over the coil [CFM]. This was required because manufacturers do not report what type of fan was used for the specific tests. Often the coil is actually installed in combination with a furnace and utilizes the furnace fan for the required airflow. For this reason, AHRI provides a default value of 365 W/1000 CFM for coils tested without a specific indoor fan. This default of 0.365 W/CFM was used for the conversion from net to gross in this study. There have been some studies that maintain that the default value of 0.365 W/CFM is below the average fan power encountered in buildings today [14], [22], though it might be a roughly accurate number for the low static pressure that AHRI prescribes for the testing procedure (0.1-0.2 in static). For this research, fan power was not central to the research topic and therefore was not deeply investigated, and for all coils that were tested without an air-handler (a significant portion), the default value from AHRI is what they are required to use in their reporting. This made the default value of 0.365 W/CFM the best

assumption given the information at hand. The equations used for converting from net to gross are shown below:

$$\dot{Q}_{Net} = \begin{cases} \dot{Q}_{Gross} - \dot{V} * 0.365 * 3.413 & \text{if in cooling mode} \\ \dot{Q}_{Gross} + \dot{V} * 0.365 * 3.413 & \text{if in heating mode} \end{cases} \quad (5.1)$$

$$\dot{P}_{Net} = \dot{P}_{Gross} + \dot{V} * 0.365 \quad (5.2)$$

Where \dot{Q}_{Net} and \dot{P}_{Net} are the capacity (in Btu) and power (in Watts) values from the manufacturer and \dot{V} is the volumetric flow rate for that data point expressed in CFM.

The gross capacity is larger than the net in cooling due to the fact that the coil sees a larger load if the entering conditions are measured after the fan due to the added heat in the air stream (whereas in heating the added fan heat makes the net capacity larger). The power calculation is more intuitive in that it is simply subtracting the fan power out of the net value in order to get a gross value.

To calculate the gross COP required by the simulation engines it was necessary to convert the net capacity and power reported by the manufacturers as follows (shown for cooling). If we let F equal to the required CFM/Btu of capacity, then $\dot{V} = F * \dot{Q}_{gross}$ and equations (5.1) and (5.2) can be combined into:

$$EER = \frac{\dot{Q}_{Net}}{\dot{P}_{Net}} = \frac{\dot{Q}_{Gross} - F * \dot{Q}_{Gross} * 0.365 * 3.413}{\dot{P}_{Gross} + F * \dot{Q}_{Gross} * 0.365} \quad (5.3)$$

Rearranged,

$$\dot{P}_{Gross} = \frac{\dot{Q}_{Gross} - F * \dot{Q}_{Gross} * 0.365 * 3.413}{EER} - F * \dot{Q}_{Gross} * 0.365 \quad (5.4)$$

Dividing through by \dot{Q}_{Gross} one gets,

$$EIR = \frac{1}{COP} = \frac{\dot{P}_{Gross}}{\dot{Q}_{Gross}} = \frac{1 - F * 0.365 * 3.413}{EER} - F * 0.365 \quad (5.5)$$

Equation (5.5) allows for COP (a gross value) to be expressed only in terms of EER (net) and a CFM/Btu of capacity number (F , assumed to be 400CFM/12,000Btu). This allows for easy conversion back

and forth between net and gross efficiencies. Equation (5.5) is for cooling, the minus sign in the top of the fraction (after the last equal sign) would need to be switched to a plus sign for heating.

5.2 Data Evaluation Process

Before the generated sets of model inputs were used in the research, the data and resulting inputs were evaluated for quality and consistency. The data evaluation was accomplished using a number of different methods:

- (1) Visual inspection for data entry errors
- (2) Calculation of the BF for each set of reported conditions
- (3) Replication of the EnergyPlus ADP/BF algorithms through Engineering Equation Solver (EES) programs
- (4) Visualization of the curves generated and evaluation of these curves across manufacturers and across different models/capacities

Each of these evaluation methods produced interesting results that informed decisions on the final recommendations presented here for optimal modeling of split system air conditioners and heat pumps, given the current data opportunities and annual simulation models. The results from each of these evaluations are presented below.

5.2.1 Visual Inspection

Visual inspection was limited in its use due to the quantity of data that was collected. It was utilized during the writing of the python scripts to make sure that the data was being processed accurately and transferred to the database correctly. It was initially expected that a certain number of errors would be generated through the data parsing. This did not turn out to be the case. The scripts proved to be quite robust and parsed the remaining files smoothly (after being tuned to a specific text file).

Data inspection was most often precipitated by unexpected or suspicious results during evaluation of model inputs or simulation results. These unexpected results would require inspection of both the database

and the EPTs themselves. As mentioned above, the unexpected results would most often trace back to the EPTs. The results of the visual inspection did uncover a number of data entry errors in the tables. A sample of these errors is highlighted in Figures 5.2 and 5.3.

DETAILED COOLING CAPACITIES

EVAPORATOR AIR		CONDENSER ENTERING AIR TEMPERATURES deg F																		
CFM	EWB	75			85			95			105			115			125			
		Capacity MBtu/h	Total System KW**	Sens†	Capacity MBtu/h	Total System KW**	Sens†	Capacity MBtu/h	Total System KW**	Sens†	Capacity MBtu/h	Total System KW**	Sens†	Capacity MBtu/h	Total System KW**	Sens†	Capacity MBtu/h	Total System KW**	Sens†	
24ANA124A30 Outdoor Section With FESANB004 Indoor Section - High Stage																				
700	72	31.17	16.07	1.44	29.97	15.63	1.42	1.60	28.69	15.17	1.78	27.29	14.67	1.97	25.76	14.13	2.18	24.05	13.53	2.42
	67	28.22	19.46	1.42	27.12	19.04	1.58	25.94	18.60	1.76	24.67	18.12	1.95	23.26	17.59	2.16	21.67	17.01	2.40	
	62	26.17	18.84	1.40	25.15	18.42	1.57	24.05	17.97	1.74	22.95	17.48	1.93	21.53	16.95	2.14	20.05	16.36	2.38	
750	72	25.56	22.82	1.40	24.56	22.43	1.58	23.48	22.00	1.74	22.31	21.54	1.93	21.04	21.01	2.14	19.90	19.90	2.38	
	67	24.41	24.41	1.39	23.68	23.68	1.55	22.89	22.89	1.73	22.01	22.01	1.92	21.02	21.02	2.14	19.89	19.89	2.38	
	62	23.06	25.06	1.40	24.30	24.30	1.58	23.47	23.47	1.74	22.56	22.56	1.93	21.53	21.53	2.15	20.36	20.36	2.39	
800	72	28.64	20.17	1.43	27.51	19.74	1.59	26.29	19.29	1.76	24.98	18.81	1.95	23.53	18.26	2.17	21.91	17.70	2.41	
	67	26.57	19.51	1.41	25.51	19.08	1.57	24.38	18.63	1.75	23.14	18.13	1.94	21.79	17.60	2.15	20.27	17.00	2.39	
	62	25.95	23.77	1.41	24.92	23.37	1.57	23.81	22.94	1.74	22.62	22.46	1.93	21.53	21.53	2.15	20.36	20.36	2.39	
800	72	32.04	16.98	1.46	30.76	16.54	1.62	29.40	16.06	1.79	27.93	15.56	1.99	26.32	15.01	2.20	24.53	14.41	2.44	
	67	29.01	20.86	1.43	27.85	20.43	1.60	26.60	19.98	1.77	25.25	19.49	1.96	23.77	18.96	2.17	22.11	18.37	2.41	
	62	26.30	24.70	1.41	25.24	24.30	1.58	24.12	23.85	1.75	23.06	23.06	1.94	22.00	22.00	2.16	20.78	20.78	2.40	
57	25.67	25.67	1.41	24.88	24.88	1.57	24.01	24.01	1.75	23.06	23.06	1.94	22.00	22.00	2.16	20.78	20.78	2.40		
CONDENSER ENTERING AIR TEMPERATURES deg F																				
CFM	EWB	75			85			95			105			115			125			
		Capacity MBtu/h	Total System KW**	Sens†	Capacity MBtu/h	Total System KW**	Sens†	Capacity MBtu/h	Total System KW**	Sens†	Capacity MBtu/h	Total System KW**	Sens†	Capacity MBtu/h	Total System KW**	Sens†	Capacity MBtu/h	Total System KW**	Sens†	
24ANA124A30 Outdoor Section With FESANB004 Indoor Section - Low Stage																				
700	72	25.69	14.00	0.95	24.27	13.44	1.09	22.81	12.87	1.24	21.27	12.28	1.42	19.65	11.67	1.62	17.92	11.03	1.87	
	67	22.98	17.29	0.93	21.69	16.71	1.07	20.35	16.11	1.23	18.95	15.49	1.41	17.47	14.85	1.61	15.89	14.18	1.86	
	62	20.58	20.54	0.92	19.62	19.62	1.06	18.62	18.62	1.22	17.58	17.58	1.40	16.46	16.46	1.61	15.25	15.25	1.85	
750	72	20.96	20.96	0.92	19.62	19.62	1.06	18.62	18.62	1.22	17.58	17.58	1.40	16.46	16.46	1.61	15.25	15.25	1.85	
	67	18.62	14.44	0.96	24.57	13.88	1.09	23.07	13.30	1.25	21.50	12.70	1.42	19.85	12.08	1.63	18.09	11.43	1.87	
	62	23.28	17.98	0.94	21.96	17.39	1.08	20.59	16.78	1.23	19.16	16.15	1.41	17.65	15.49	1.62	16.04	14.81	1.86	
800	72	21.39	17.24	0.93	20.16	16.65	1.07	18.88	16.04	1.22	17.55	15.42	1.40	16.14	14.77	1.61	14.65	14.08	1.85	
	67	21.10	21.10	0.93	20.12	20.12	1.07	19.09	19.09	1.22	18.01	18.01	1.40	16.85	16.85	1.61	15.60	15.60	1.86	
	62	21.10	21.10	0.93	20.12	20.12	1.07	19.09	19.09	1.22	18.01	18.01	1.40	16.85	16.85	1.61	15.60	15.60	1.86	
800	72	26.32	14.88	0.95	24.84	14.31	1.10	23.31	13.72	1.25	21.71	13.12	1.43	20.03	12.49	1.63	18.23	11.83	1.88	
	67	23.55	18.66	0.95	22.20	18.05	1.08	20.80	17.43	1.24	19.34	16.79	1.42	17.81	16.13	1.62	16.18	15.42	1.87	
	62	21.64	17.87	0.93	20.38	17.27	1.07	19.08	16.66	1.23	17.72	16.02	1.41	16.29	15.36	1.61	14.78	14.65	1.86	
800	62	21.60	21.60	0.93	20.58	20.58	1.07	19.52	19.52	1.23	18.40	18.40	1.41	17.21	17.21	1.62	15.92	15.92	1.86	
	57	21.60	21.60	0.93	20.58	20.58	1.07	19.52	19.52	1.23	18.40	18.40	1.41	17.21	17.21	1.62	15.92	15.92	1.86	

Figure 5.2: Data Entry Error in Carrier’s SEER 21 Line

Figure 5.2 shows the EPT for the high and low speed of a Carrier SEER 21 unit. In this case both the high and low speed tables have the same range of CFM values (700, 750, and 800). This makes this table completely unusable due to the lack of knowledge regarding the actual CFM for the different speeds.

Figure 5.3 shows the EPT for the low speed of a York SEER 15 unit. This figure shows an example of erroneous data entry for the power consumption of the unit. Note that the 80/62 point for both 700 and 800 CFM show very large power consumption. This is clearly an example of error in the data entry by the manufacturer. These types of data error were not frequent (\approx 5-7 instances of similar errors), yet it is worth noting that this type of error does exist. It is also noteworthy that the data evaluation process caught these errors in the EPTs and that these cases were not used in the research.

COOLING PERFORMANCE DATA - HIGH CFM 2-STAGE OPERATION																
OUTDOOR UNIT MODEL NO.		CZE02411(C)														
INDOOR COIL MODEL NO.		FC/MC36B + MV12B														
CONDENSER ENTERING AIR TEMPERATURE	ID CFM	700					800					900				
	ID DB (°F)	80	80	75	80	80	80	80	75	80	80	80	80	75	80	80
	ID WB (°F)	57	62	62	67	72	57	62	62	67	72	57	62	62	67	72
65	T.C.	24.4	25.4	24.4	27.1	28.8	25.2	25.7	24.8	27.4	29.1	26.0	26.0	25.2	27.8	29.3
	S.C.	24.4	23.9	19.6	19.7	15.7	25.1	24.7	20.3	20.3	16.1	25.9	25.6	21.0	21.0	16.4
	K.W.	1.3	24.1	1.3	1.4	1.4	1.3	12.7	1.3	1.4	1.4	1.3	1.3	1.3	1.4	1.4
75	T.C.	23.7	24.2	23.3	26.0	27.5	24.4	24.6	23.7	26.3	27.7	25.1	25.1	24.1	26.6	27.9
	S.C.	23.6	23.1	19.0	19.2	15.2	24.3	24.0	19.7	19.9	15.6	25.0	24.8	20.4	20.5	15.9
	K.W.	1.5	16.7	1.5	1.5	1.6	1.5	9.1	1.5	1.5	1.6	1.5	1.5	1.5	1.5	1.6
85	T.C.	23.0	22.9	22.2	24.9	26.1	23.6	23.5	22.6	25.1	26.3	24.2	24.1	22.9	25.4	26.6
	S.C.	22.9	22.2	18.4	18.8	14.6	23.4	23.2	19.1	19.4	15.1	24.0	24.1	19.8	20.1	15.5
	K.W.	1.7	9.2	1.7	1.7	1.8	1.7	5.5	1.7	1.7	1.8	1.7	1.7	1.7	1.7	1.8
95	T.C.	22.3	21.7	21.2	23.8	24.8	22.8	22.4	21.5	24.0	25.0	23.3	23.2	21.8	24.2	25.2
	S.C.	22.1	21.4	17.9	18.4	14.1	22.6	22.4	18.5	19.0	14.6	23.0	23.4	19.2	19.6	15.0
	K.W.	1.9	1.8	1.9	1.9	2.0	1.9	1.9	1.9	1.9	2.0	1.9	1.9	1.9	1.9	2.0
105	T.C.	21.1	20.4	19.7	22.1	23.0	21.6	21.1	20.1	22.4	23.2	22.1	21.7	20.3	22.7	23.4
	S.C.	21.0	20.4	17.0	17.5	13.5	21.4	21.2	17.6	18.1	13.9	21.8	22.0	18.3	18.7	14.3
	K.W.	2.2	2.1	2.2	2.2	2.3	2.2	2.2	2.2	2.2	2.3	2.2	2.2	2.2	2.2	2.3
115	T.C.	20.0	19.2	18.4	20.6	21.2	20.5	19.8	18.7	20.9	21.5	20.9	20.2	19.0	21.1	21.7
	S.C.	20.0	19.5	16.1	16.7	13.0	20.3	20.1	16.8	17.3	13.3	20.7	20.6	17.4	17.8	13.7
	K.W.	2.5	2.4	2.5	2.5	2.6	2.5	2.5	2.5	2.5	2.5	2.5	2.5	2.5	2.5	2.5
125	T.C.	18.9	18.0	17.0	19.0	19.5	19.3	18.4	17.3	19.3	19.8	19.7	18.8	17.6	19.6	20.0
	S.C.	18.9	18.6	15.2	15.9	12.4	19.2	18.9	15.9	16.5	12.7	19.5	19.3	16.6	17.0	13.0
	K.W.	2.8	2.7	2.7	2.8	2.8	2.8	2.7	2.7	2.8	2.8	2.8	2.8	2.8	2.8	2.8

NOTE: ALL CAPACITIES ARE NET (KBTUH) WITH INDOOR FAN HEAT ALREADY DEDUCTED AT 1250 BTUH/1000 CFM.

Figure 5.3: Data Entry Error in York's SEER 15 Line

5.2.2 Calculation of Bypass Factor

The discussion of the EnergyPlus modeling algorithm (see chapter 4) demonstrated the significant role that the bypass factor (BF) plays in the way that sensible and latent performance is modeled. The ADP/BF model is used to define the sensible capacity of the unit at each time step. The sensible capacity determines the run time of the unit due to the fact that air conditioners and heat pumps are generally controlled using thermostats which are sensible-only devices (humidity control was not considered in this research). Due to the central role of the ADP/BF model in determining performance and energy consumption, the BF was calculated for each of the points reported by the manufacturer. It was considered important to know both the relative consistency of BF across models/manufacturers and to be able to evaluate the constant BF assumption that is central to the EnergyPlus model. Calculation of the BF is possible due to the fact that the data provided in the expanded performance tables provides complete knowledge of the entering

conditions, total capacity, and sensible capacity. For a detailed description of the BF calculation see 4.1.1.

Calculation of the BF led to some unexpected results. There were a large number of points that were not able to be calculated due to the fact that the predicted exiting conditions were past the 100% saturation curve on the psychrometric chart. This leads to calculation of a negative bypass factor. There were other cases where the line through the entering and exiting conditions never intersected the 100% saturation curve. This makes it impossible to converge on an ADP, therefore drawing an error in the BF calculation. These two cases are outlined on a psychrometric chart in Figure 5.4.

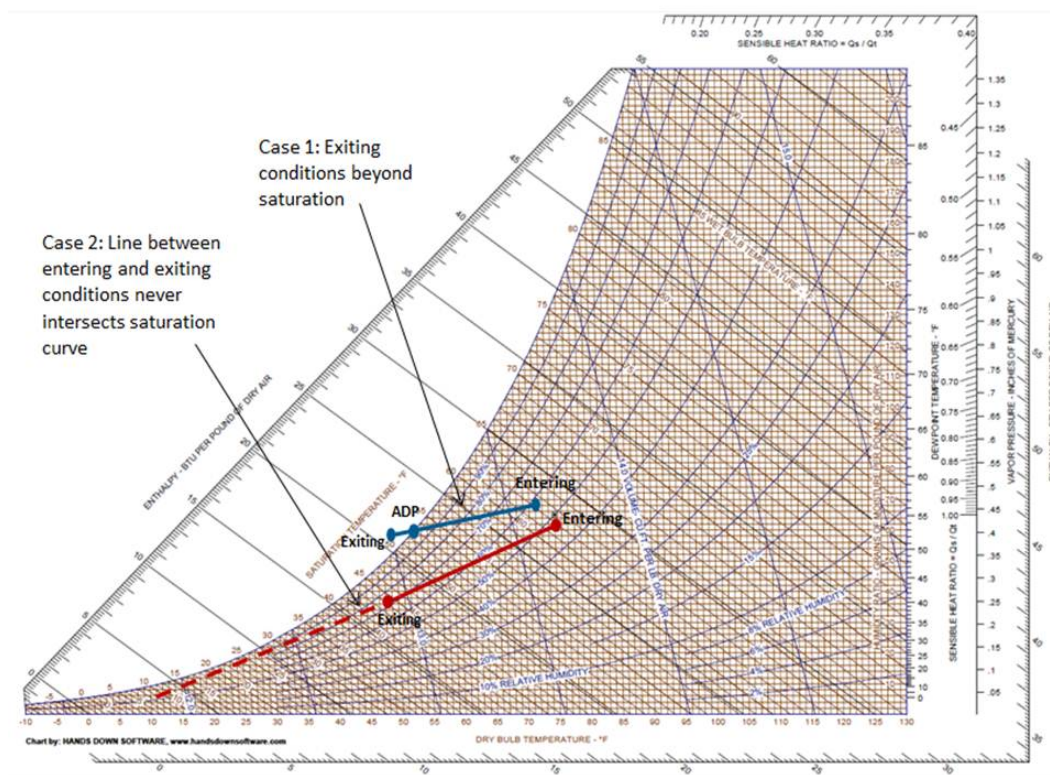


Figure 5.4: Two Common Errors in the BF Calculation

The percent of total data points where these two situations occurred is listed by manufacturer in Table 5.1. Note the consistently large number of points that are calculated to have exiting conditions past the saturation curve.

Both of these cases are physically impossible and bring the validity of the data into question. The case of exiting conditions past the saturation curve is clearly impossible due to the fact that supersaturated air

Table 5.1: Errors in calculated exiting conditions

	Carrier	Goodman	Lennox	York	Trane
Percent of Exiting Conditions Past Saturation	15.5%	16.5%	25.3%	9.7%	5.25%
Percent of Exiting Conditions w/ Undefined ADP	0.6%	0.9%	0.0%	0.6%	0.0%

does not exist under normal atmospheric conditions. The second case has a more complicated explanation. The second case is not possible due to the fact that the air cannot get colder than the surface temperature of the coil. In order to reach that temperature, the entire air mass would need to be cooled to the saturation point and then have water removed until the air was fully saturated at the coil surface temperature (the definition of ADP conditions). The humidity cannot be removed from the air in any other way than through saturation and condensation; a desiccant would allow for another form of moisture removal yet that is not present in a the traditional vapor compression cycle. Since the coil surface temperature defines a lower limit, and the dehumidification must occur through condensation, this defines the ADP conditions which must lie on the saturation curve. Therefore the lower limit for the slope through the entering and exiting conditions is the line through the entering conditions and tangent to the saturation curve. It is also true that there is no humidification process in the vapor compression cycle of an air conditioner unit. This implies that sensible cooling along a constant humidity ratio line is the upper limit with regards to humidity for vapor compression cooling. These physical constraints define the region of the psychrometric chart where the exiting conditions can exist. This region is defined in Figure 5.5.

The number of data points with exiting conditions outside of this region was significant for all manufacturers. The portion of the total data points that were either past the saturation curve or never intersected an ADP temperature are shown for each manufacturer in Table 5.1.

This discovery prompted a discussion with Lennox regarding the validity of their data and how their internal model was calculating these points. This discussion was informative with regards to the testing procedures and how their testing informed the model generated data. It was made clear that only the highest sales volume model received testing. The testing was performed on two separate units (of the exact

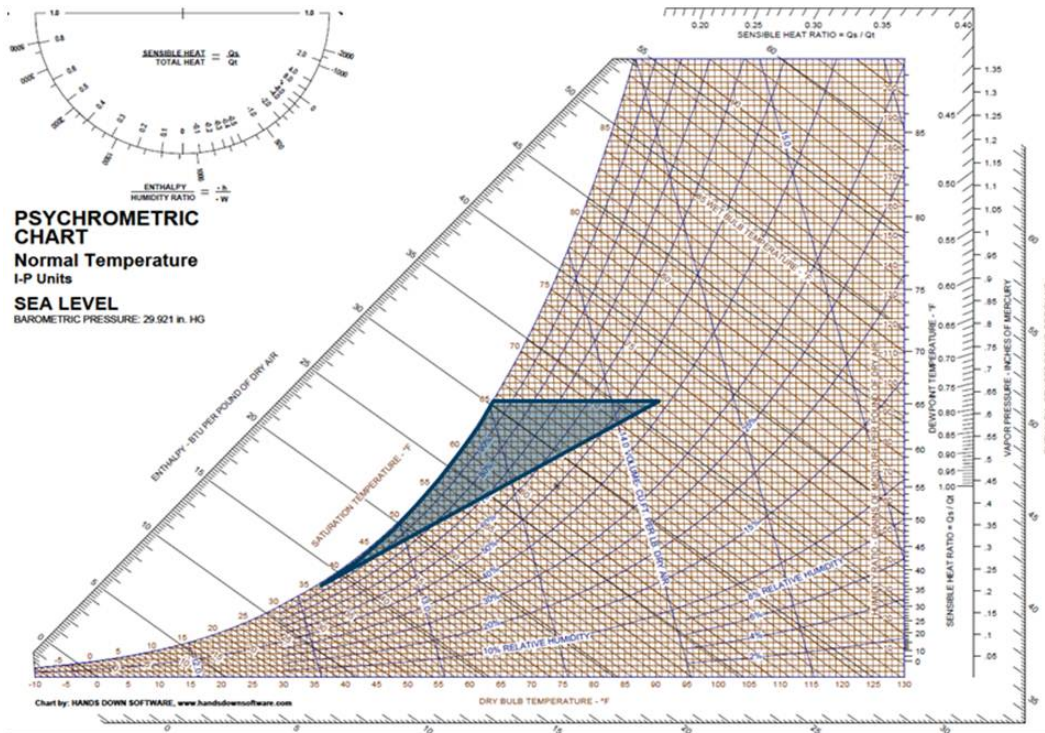


Figure 5.5: Region of the Psychrometric Chart for Air Conditioner Exiting Conditions

same model). If the test results from the two models were within a certain percent error of each other, it had satisfied the AHRI testing and then their in-house model was calibrated with those test results. This model was then used to generate the EPTs for all the other mix and match. Knowing that all of the other mix and match data was purely model generated led to the decision to only input the data from the highest sales volume units into the database. It was also made clear that sensible capacities did not receive a lot of attention during model calibration. From the manufacturer's standpoint, the sensible heat ratios are important to know for accurate sizing in different climates, yet they can be a few percentage points off and still be accurate enough for the sizing purpose they are generated for. These same couple of percentage points can change the slope of the SHR line on the psychrometric chart significantly enough to produce some of the physically impossible results that were observed.

These results were concerning with regards to the overall accuracy of the manufacturer's models. With regards to whole-building modeling however, the fact that EnergyPlus uses the rated BF approach limits

the amount of impact that this data variability has on the model. DOE-2 on the other hand still requires a BF curve as a function of outdoor dry bulb and entering wet bulb. This provides yet another reason to limit the use of DOE-2 for accurate simulation. It was still important to quantify the effect that EnergyPlus's constant BF approach would have on the predicted sensible capacities of the air conditioner and heat pump units. To this end, EnergyPlus's model was implemented in an EES model.

5.2.3 Replication of the EnergyPlus Algorithms Through Engineering Equation Solver (EES)

The fact that EnergyPlus utilizes a constant BF model limits the impact of the erroneous individual BF calculations that were discussed in the previous section. This led to the question of what EnergyPlus would predict for the sensible capacities of the unit at off-rated conditions, and how these capacities would compare with the manufacturer's data. Even though it was suspected that some of the reported sensible capacities were not accurate, it was still important to quantify the amount of variability that the EnergyPlus algorithm would introduce.

In order to evaluate this variability, an EES program was written that simulated the EnergyPlus ADP/BF approach. This model took in the operating conditions, total capacity, and the SHR at rated conditions. From this set of inputs, a BF was calculated at the rated conditions. This BF was then fixed and used (along with the total rated capacity) to calculate the sensible capacities for all of the other reported entering conditions. This replicated exactly how EnergyPlus would calculate the sensible capacity during a simulation. The calculated sensible capacities could then be compared with the manufacturer's reported sensible capacities.

Table 5.2 shows the EPT SHRs alongside the EES calculated SHRs for a Carrier SEER 14 unit. Table 5.3 shows SHR comparison for a Goodman SEER 14 unit. These tables only show the SHRs for a single capacity and only for a set of CFM points in the EPT (600 for Carrier and 800 for Goodman). It can be seen that the EnergyPlus algorithm led to very low errors between calculated SHRs and EPT SHRs for the Carrier unit. The Goodman unit showed larger errors, especially at low outdoor dry bulbs where the SHR was overestimated by the EnergyPlus algorithm. The other manufacturers fell somewhere in-between Carrier

and Goodman, with Trane and Lennox being closer to Carrier and York having similar error to Goodman. The higher SHRs calculated by the EnergyPlus algorithm may result in slightly reduced run time due to the higher sensible fraction. This will cause an underestimation of the annual energy production.

The only cases where the EES program was not **exactly** replicating the EnergyPlus calculations were cases where the rating point itself was calculated to be beyond the saturation curve. This occurred in very few cases. When it did occur the EES program was capable of calculating the negative BF and then continuing to calculate the rest of the SHRs. EnergyPlus on the other hand would produce a fatal error if the BF was calculated to be negative. To avoid these fatal errors a regression was generated that correlated CFM/Ton and the upper limit SHR that would allow EnergyPlus to run.

$$SHR_{MAX} = 0.3821066 + 0.001050652 * CFM/TON_{Rated} - 0.01 \quad (5.6)$$

This correlation is based on BF/ADP theory and is used to ensure a BF_{rated} can be calculated. The effect that this correlation had on the SHRs was also evaluated using the EES program. For those cases where the rated BF was negative, the SHR resulting from the correlation in (5.6) was input as the rated SHR to the EES program and the SHR values were then compared to the EPT values. To demonstrate the difference between these two cases (EES program run with SHR_{Rated} from the EPT and EES program run with SHR from (5.6)), table 5.4 is presented below. The table contains EES SHRs (using SHR_{Rated}) and EES SHRs using the correlation. It also presents the percent difference between each of these cases and the SHRs reported in the EPT.

Table 5.2: Comparison of SHR Calculated by EES Program to EPT SHR (for Carrier SEER 14)

EDB [°F]	ODB [°F]	EWB [°F]	EPT SHR [frac]	EES SHR [frac]	% Difference [%]
80	75	72	0.52	0.51	-2.9%
80	75	67	0.71	0.71	0.0%
80	75	62	0.93	0.94	1.9%
80	75	57	1.00	1.00	0.0%
80	85	72	0.53	0.52	-2.9%
80	85	67	0.73	0.73	0.0%
80	85	62	0.95	0.97	2.1%
80	85	57	1.00	1.00	0.0%
80	95	72	0.54	0.53	-3.0%
80	95	67	0.75	0.75	0.0%
80	95	62	0.99	1.00	0.4%
80	95	57	1.00	1.00	0.0%
80	105	72	0.55	0.54	-3.2%
80	105	67	0.77	0.77	0.0%
80	105	62	1.00	1.00	0.0%
80	105	57	1.00	1.00	0.0%
80	115	72	0.57	0.55	-3.2%
80	115	67	0.79	0.79	0.1%
80	115	62	1.00	1.00	0.0%
80	115	57	1.00	1.00	0.0%
80	125	72	0.58	0.57	-3.3%
80	125	67	0.83	0.83	0.2%
80	125	62	1.00	1.00	0.0%
80	125	57	1.00	1.00	0.0%

Table 5.3: Comparison of SHR Calculated by EES Program to EPT SHR (for Goodman SEER 14)

EDB [°F]	ODB [°F]	EWB [°F]	EPT SHR [frac]	EES SHR [frac]	% Difference [%]
80	65	71	0.5	0.546	9%
80	65	67	0.66	0.707	7%
80	65	63	0.82	0.888	8%
80	65	59	0.87	1	14%
80	75	71	0.51	0.550	8%
80	75	67	0.69	0.714	3%
80	75	63	0.85	0.897	5%
80	75	59	0.9	1	11%
80	85	71	0.53	0.554	5%
80	85	67	0.71	0.722	2%
80	85	63	0.87	0.909	4%
80	85	59	0.93	1	7%
80	95	71	0.54	0.559	3%
80	95	67	0.73	0.73	0%
80	95	63	0.9	0.920	2%
80	95	59	0.96	1	4%
80	105	71	0.57	0.569	0%
80	105	67	0.76	0.748	-2%
80	105	63	0.93	0.947	2%
80	105	59	0.99	1	1%
80	115	71	0.57	0.586	3%
80	115	67	0.76	0.776	2%
80	115	63	0.94	0.987	5%
80	115	59	1	1	0%

Table 5.4: Comparison of EPT SHR to Both Versions of EES Calculations

EDB	ODB	EWB	EPT SHR	EES SHR	% Diff.	EES w/ Adjusted SHR	% Diff.
[°F]	[°F]	[°F]	[frac]	[frac]	[%]		[%]
80	65	71	0.54	0.58	7.0%	0.57	4.7%
80	65	67	0.72	0.76	5.7%	0.74	2.7%
80	65	63	0.89	0.97	8.1%	0.93	4.8%
80	65	59	0.95	1.00	5.1%	1.00	5.1%
80	75	71	0.56	0.58	4.3%	0.57	1.9%
80	75	67	0.75	0.77	2.8%	0.75	-0.2%
80	75	63	0.92	0.98	6.2%	0.95	2.8%
80	75	59	0.98	1.00	2.0%	1.00	2.0%
80	85	71	0.57	0.59	3.5%	0.58	1.0%
80	85	67	0.77	0.78	1.3%	0.76	-1.8%
80	85	63	0.94	0.99	5.4%	0.96	1.9%
80	85	59	1.00	1.00	0.0%	1.00	0.0%
80	95	71	0.59	0.60	1.0%	0.58	-1.5%
80	95	67	0.79	0.79	0.0%	0.77	-3.1%
80	95	63	0.97	1.00	3.0%	0.97	0.2%
80	95	59	1.00	1.00	0.0%	1.00	0.0%
80	105	71	0.61	0.61	-0.1%	0.59	-2.8%
80	105	67	0.82	0.81	-1.1%	0.79	-4.3%
80	105	63	1.00	1.00	0.0%	1.00	0.0%
80	105	59	1.00	1.00	0.0%	1.00	0.0%
80	115	71	0.62	0.63	1.6%	0.61	-1.2%
80	115	67	0.83	0.85	2.0%	0.82	-1.4%
80	115	63	1.00	1.00	0.0%	1.00	0.0%
80	115	59	1.00	1.00	0.0%	1.00	0.0%

Table 5.4 demonstrates the good agreement between the predicted sensible values (including the adjusted SHR_{Rated}) and the SHRs from the EPT. This agreement does not discount the fact that there are large numbers of sensible performance errors (invalid exiting conditions) in the EPTs (table 5.1). This is still a significant concern which places the data quality of the EPTs into question. The good agreement shown in tables 5.2 and 5.4 simply demonstrates that the SHR values that EnergyPlus will use in its simulations will be similar to the values given in the EPTs. Perhaps more importantly, the strong agreement shows that the BF value does not have a large impact on the predicted SHR. It was seen that small amounts of error in the sensible performance can lead to large changes in calculated BF (causing the BF to range from negative to over 1). The EES program replicated EnergyPlus's assumption that the BF is constant for all of the different operating conditions, and therefore did not allow that BF variation to occur. This assumption was shown to not have a large impact on the resulting SHR. Therefore the BF can be seen to be sensitive to SHR variation, yet it does not have a large impact on the results.

It was hoped that evaluation of calculated BF would lend insight into the validity of the constant BF assumption (with respect to ambient temperatures) used in EnergyPlus. This was not achievable due to the suspect quality of the data available. The constant BF assumption is based on accepted theoretical models of cross flow heat exchangers. Therefore, without significant measured data to the contrary, this assumption is assumed to be valid for this model.

5.2.4 Visualization of the Generated Curve Fits

The process of generating the necessary EnergyPlus inputs (see section 5.1) produced curve coefficients for four curves per air conditioner (and heat pump) unit. Each of these curves has either three or six coefficients. This results in 18 different coefficients per air conditioner unit. It is very difficult to assess the consistency and/or physical validity of the different curves by any sort of coefficient comparison. To facilitate comparison of these curves across different models and different manufacturers, each of the curves were visualized in an excel spreadsheet. Excel macros were written so that the graphs could be efficiently cycled through. These macros enabled effective visualization and comparison across four different manufacturers and across all of the units simply by clicking a button to scroll through the different curves. This ability

to look at all of the curves in quick progression enabled observation of trends and outliers as well as some specific data inconsistencies that will be outlined below.

The graphs in figure 5.6 show the biquadratic curves for capacity (column 1) and EIR (column 2) for four different manufacturers (the four rows in the table). The biquadratic graphs were evaluated across different outdoor dry bulbs along the x-axis, and across different entering wet bulbs via different series in the graph (see figure 5.6). The solid lines represent the curve fit values and the dots represent the data from the EPTs. The fact that some of the EPT data extends past the curve fit results is a reflection of different ranges reported by the manufacturers and the fact that the curves were only visualized for the range 75 to 115 °F.

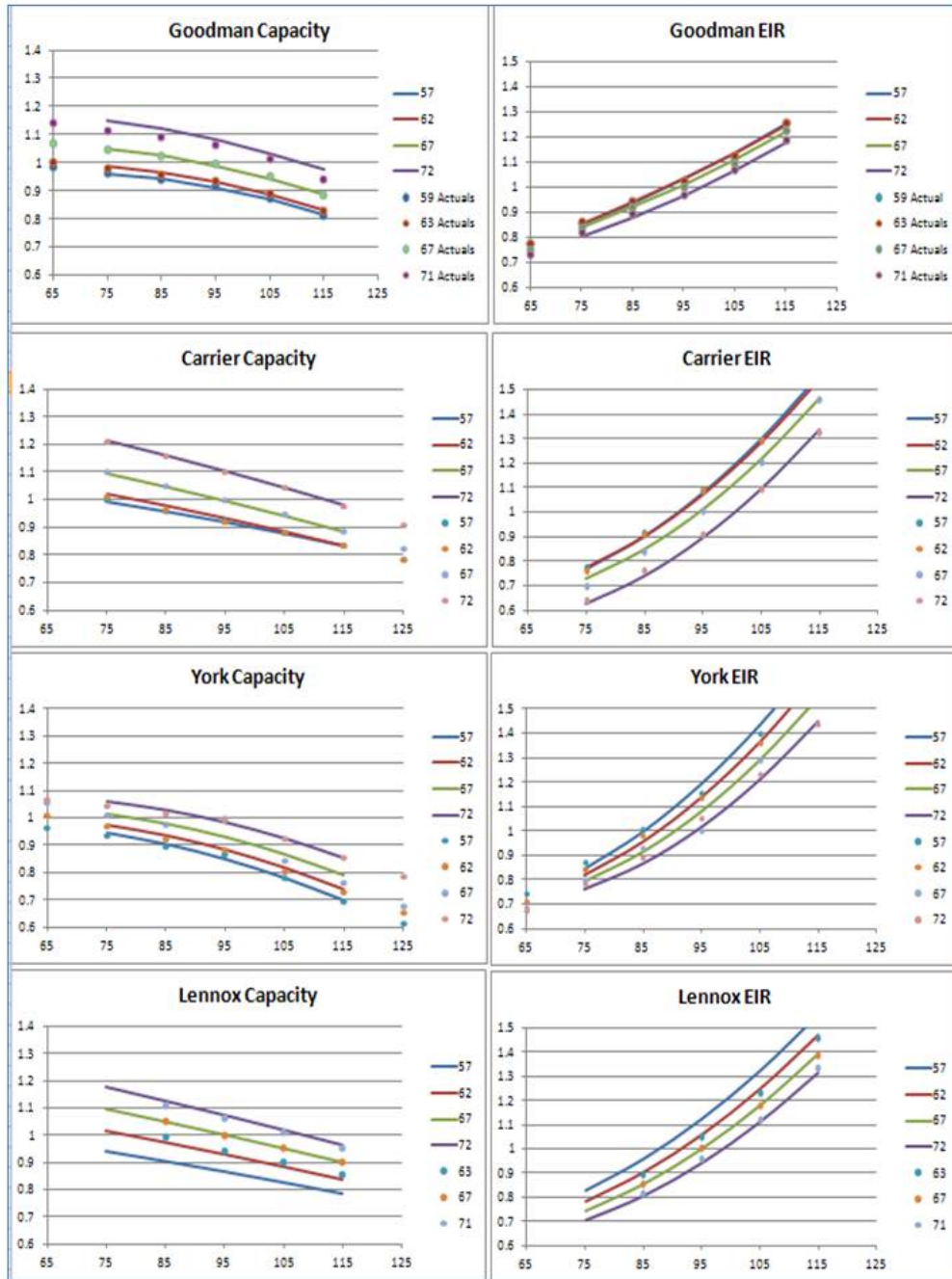


Figure 5.6: Visualization of Biquadratic Curves: Four Manufacturers

It is also worth noting that all of these curves are normalized to the AHRI A-test rating point of 95/80/67. This can be seen by the fact that the 67 series (from the EPT data) evaluated at 95°F is always exactly 1. The fact that the curve fit is not necessarily 1 at 95°F on the 67 series is due to the fact that the

values from the EPT are normalized prior to the least squares regression. Thus the 95/80/67 point will be divided by itself (resulting in the 1 value), yet the curve fit evaluated at 95/67 can yield slightly different results due to the influence of the regression through all of the other data points.

The fit of these regression curves to the manufacturers' data was very good across all of the manufacturers. It can be seen in 5.6 that the curve fit lines lie almost directly on top of the actual data series and very high R^2 values were observed in all cases. This indicated that the performance modeled in the simulation engines would very closely match the performance outlined in the expanded performance tables.

The good agreement between the normalized data and the curve output did not carry out in all cases. When evaluating the York data, it was observed that the general trend of the data was captured very accurately, yet a single data point deviated significantly from the regression fit. The 67 series from the EPT data has been highlighted in figure 5.7. It can be noted that the entire series (as well as the other wet bulb series) trends very closely on top of the curve fit results. The only outlier is the 95/80/67 rating point. It is assumed that the in-house model predicted performance that did not correspond with the AHRI test results. In this case, instead of recalibrating the model itself, the single rating point in the EPT was overwritten with the test results. This one deviation is insignificant to the process of least squares regression and the remainder of the data is fit very accurately. This data manipulation brought the York data under question. The variability of Yorks data is persistent and is discussed in further sections of the thesis.

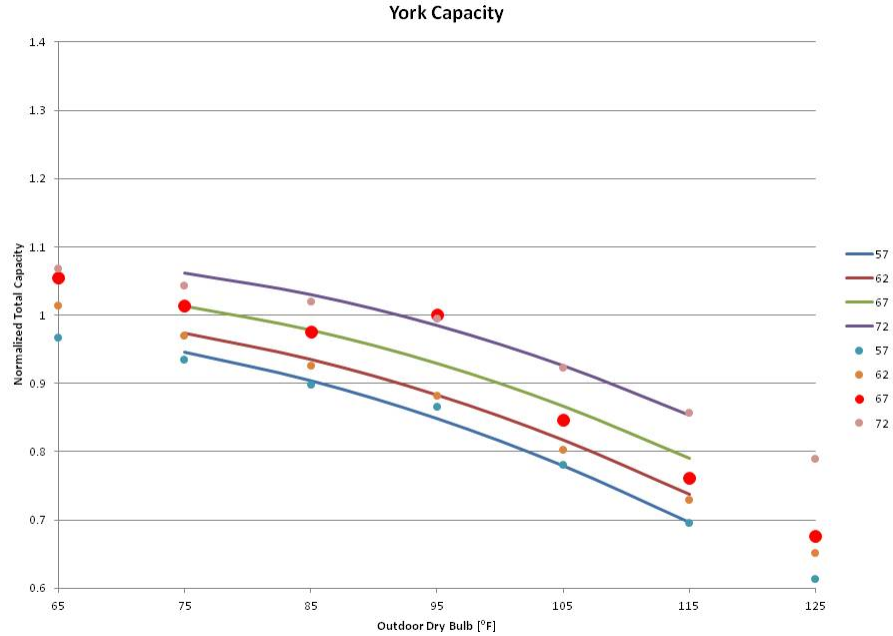


Figure 5.7: Alteration of the Rating Point in York Capacity Curve

In general, the curve visualization process showed more variability in the curve shape between manufacturers. Within a specific manufacturer, the curves would shift slightly between one unit and the next, but the differences were not as significant as between the separate manufacturers. The differences from manufacturer to manufacturer begs the question of whether the variation is due to physical differences in how the manufacturers build their units, or if the variation is due to the different in-house models that generate the expanded performance tables.

5.3 Conclusions From Data Evaluation

It was initially envisioned that this research effort would generate a set model of inputs for all currently available air conditioner and heat pump models. This effort was successful; the database discussed in section 3.3 was utilized to generate full sets of EnergyPlus inputs for each individual model in the database. One possible scenario for accurate modeling of air conditioners and heat pumps would then be to make that database/model inputs available to users. Yet, the thorough inspection of the data that was outlined in this

chapter led to many questions regarding the accuracy of this approach to air conditioner and heat pump modeling (in the current simulation engines). This was due to the significant number of issues present in the manufacturer's data. Some of these issues were:

- (1) Data entry error
- (2) Invalid exiting conditions
 - (a) Past saturation curve
 - (b) Undefined ADP
- (3) Manipulated data points in the tables (adjusted rated values)
- (4) Wide variation in curve shape across manufacturers

This is not to say that all of the data was deemed unacceptable or discarded. At this point, these issues were noted and used to inform later sections of the research. The data issues did raise the following important questions:

- (1) Which inputs are the most sensitive to error/variation?
- (2) Given the fact that there are errors present in the available data, how will this affect the predicted performance of air conditioner and heat pump units?
- (3) What would be the best approach to limit the effects of data variability while capturing the central parts of the unit's performance?
- (4) What set of model inputs will best predict unit performance?

The answers to these question were investigated and the results are presented in Chapter 6.

Chapter 6

Sensitivity Study on Model Inputs

The previous chapter outlined the success achieved through utilizing the SQLite database that was created as part of this research effort to generate the required simulation engine inputs for all 260 air conditioners and 200 heat pumps. Chapter 5 also outlined a number of issues that were encountered when evaluating the data contained within that database. This really highlighted one of the main questions outlined in the methodology section (1.3): can we provide more accurate modeling through a full database of inputs representing all current make/models? or are we better served by utilizing the database to inform a model with reduced complexity and better overall accuracy? The data issues that came up during the evaluation of the inputs made it seem less likely that a database of inputs would support robust and accurate modeling practices. The alternate approach of a more generalized model with reduced inputs would reduce the potential impact of the data variability. In order to provide a generalized model, it was necessary to evaluate the how all of the model inputs effected the simulation results and to what degree.

This chapter will look at the results of simulating all of the different units that were compiled into the database. The initial simulation results will be followed by a sensitivity study on the different model inputs. Results from that sensitivity study will be presented and finally some recommendations for improved modeling procedures will presented.

Most of the sections in this chapter will focus on single stage units. This is for two reasons: the methodology is very similar between the single stage and two stage units, and the single stage results are more easily described. The differences between the single stage and two stage approaches will be described in section 6.5 and key results will be presented. A similar study was also done for heat pumps; results for

the heat pumps study are presented in chapter 8.

6.1 Batch Run Methodology

6.1.1 Generating the Input Files

One of the goals of this research was to compare annual energy use across different air conditioners and heat pumps. Once the model inputs had been generated it was possible to start the comparison process through batch runs in EnergyPlus. To execute these batch runs effectively, the development version of BEopt 2.0 was utilized. BEopt 2.0 contains a script called the RunMgrTest which pulls XML input files and calls BEopt using those XML files. In BEopt 2.0, the input file generated at the beginning of a simulation will be an XML file which contains all of the information about the modeled building. That XML file is then processed by a file called “sim.py” which translates the information in the XML file into the inputs that the simulation engines expect. Finally, two separate Python files (energyplus.py and doe2.py) generate the actual input files used by the respective simulation engines.

For the batch runs in this study, a python script was written that would take a single building file (in XML format), delete the current air conditioner or heat pump object, insert a new air conditioner or heat pump object, output that file, and repeat using a loop. The rest of the building file would remain untouched. The air conditioner/heat pump object consists of the simulation inputs that were generated from the database. Therefore, this script allowed the creation of hundreds of XML input files with exactly the same house geometry, schedules, appliances, etc., yet distinct air conditioner or heat pump units. The creation of all of these different XML input files allowed for the use of the RunMgrTest capability to call EnergyPlus repetitively (using multiple processors). The RunMgrTest will write out all of the annual energy consumption output to a single excel file. It will also store all of the .idf files and the .csv files from each run in an output folder. These two capabilities allow for these multiple runs to occur without losing any of the important data that is generated during the process.

This process was executed four different times to create sets of input file for four different US cities: Houston, Phoenix, Atlanta, and Chicago. For each of these different cities it was necessary to generate input

files with the correct climate file location included in the XML. These files could then be simulated at these different locations around the country, thus capturing performance differences due to different annual load distribution and different latent to sensible ratios.

6.1.2 Description of Building Used in the Input File

The four different cities that the air conditioner and heat pump units were simulated in (Houston, Phoenix, Atlanta, and Chicago) each required their own template building file that the units were placed into. This was due to the fact that the location needs to be described in the input file itself, requiring a different set of files for each specific city. The building geometry in the input files was also altered slightly from location to location. This was done to represent the predominant foundation formation in each location. For example, the predominant construction practice in Phoenix is slab-on-grade, whereas in Atlanta it is more common to have houses with an uninsulated crawlspace.

Beyond the slight changes to foundation design, all of the input files used the same house design. The house was a two floor, 2500 ft² design compliant with IECC 2009 building codes. For the air conditioner and heat pump comparison runs, the ducts were removed from the building. This was done so as to not confuse duct losses and different duct characteristics with the performance of the unit itself. For each of the different climates, the air conditioner or heat pump was sized according to Manual J, 2008.

6.1.3 Removing Nominal Capacity from the Picture

The expanded performance data that was gathered for the different units contained a separate expanded performance table for every different capacity unit. Full simulation inputs were generated for each of these different capacity units. One of the research questions that could be asked was whether the capacity of the unit had any influence on its performance. Essentially, it was desired to compare all of the different capacities and SEER lines in this study. In order to carry out this comparison, it was necessary to normalize all of the units to the same capacity. This would allow for EnergyPlus or DOE-2 runs in the exact same building, as described in section 6.1.1.

The normalization had already been performed in all of the curves that were generated. The simulation

engines require that the curves be normalized to be unity at the AHRI rating point of 95/80/67 (cooling) or 47/70/60 (heating). This takes all of the capacity effects out of the curve inputs. The COP and SHR inputs are non-dimensional numbers that contain no effects of capacity. The only input that actually defines the capacity of the unit (regardless of the “nominal” capacity that the expanded performance table was based on) is the rated capacity input. Therefore, the Manual J capacity for the building was input into the XML file as the rated capacity for each respective climate.

This approach is equivalent to retaining the actual rated capacity from the unit and scaling the loads imposed on the system to be proportional to the capacity. Though this approach is perhaps more intuitive initially, it would have been extremely hard to implement into the simulation engines. It would not be sufficient to simply scale up the size of the house to match larger capacity units. This is due to the fact that the internal loads do not scale directly with the square footage of the house. Therefore, it would have been necessary to synthesize the loads entirely. The approach outlined above accomplishes the same effect, but with the ability to use the exact same building for every simulation.

6.1.4 Part Load

For all of the batch run simulations, part load effects were not modeled. The part load curve for EnergyPlus was set to be constant at 1. This effectively models only steady state performance and power consumption.

This was done for two principal reasons. The first and most significant reason was the fact that there does not exist any published data on specific C_d values for the individual units. Neither AHRI or the manufacturers provide any data on the outcome of the cycling test. Therefore any part load performance curves that were introduced into the simulations would be based on estimates. This was not desirable due to the fact that it would mask some of the impacts that the inputs generated from actual data were having on the results. The other main reason for not including part load losses was to eliminate any impact that the sizing routine would have on the annual simulation results. With no part load losses, the size of the unit would not have an impact on the performance. The goal of these runs was to evaluate performance variation as influenced by the specific inputs generated from the database. The role that sizing algorithms play in

affecting the performance was not one of the variables that was evaluated in the batch runs.

The fact that part load effects are modeled completely separately from steady state performance allowed this disaggregation. As discussed in section 4.1.1, part load performance is modeled by extending the runtime at steady state operation for each timestep (dependent on the sensible load to capacity ratio). Thus, if the steady state performance of the unit is modeled correctly, the part load effects can be added on relatively easily.

6.2 Initial Results

This section presents the results from the initial batch runs that utilized the methodology described above. A metric was developed to evaluate the performance of the units in the various climates simulated. This metric is an annual average, steady-state, net COP: $\overline{COP}_{net,ss}$. Essentially, this metric adds up all of the cooling energy delivered throughout the year and divides that cooling energy by the energy consumed in order to deliver the cooling. The metric is steady-state due to the elimination of part load effects (discussed above, 6.1.4). It is a net COP because the indoor fan heat was subtracted from the gross cooling power delivered that is reported by EnergyPlus, and the indoor fan power was added to the cooling energy required by compressor and outdoor fan. For cooling the equation is as follows:

$$\overline{COP}_{net,ss,c} = \frac{\sum_{i=1}^{8760} Q_{cool} - P_{fan}}{\sum_{i=1}^{8760} P_{cool} + P_{fan}} \quad (6.1)$$

The equivalent metric was defined for heating as follows:

$$\overline{COP}_{net,ss,h} = \frac{\sum_{i=1}^{8760} Q_{cool} + P_{fan}}{\sum_{i=1}^{8760} P_{cool} + P_{fan}} \quad (6.2)$$

The only difference between (6.1) and (6.2) is that the fan heat is added to the net capacity in (6.2) (heating) instead of being subtracted. This is to account for the increased capacity provided by the fan heat in heating mode.

The benefit of the $\overline{COP}_{net,ss}$ metric is that it allows comparison across climates and across capacities without any of the confusion that a “total annual cooling energy” type metric would have. It is expected that there is some variation between climates (due to different sensible portions and different ambient conditions),

but there will not be the large disparity that an absolute number would have; this will make comparison across climates easier to achieve. Similarly, there will be no difference in the total cooling energy of a 2-ton unit and a 5-ton unit (other than the variation inherent in the performance data that generated the inputs).

Figure 6.1 shows the initial run of all the different single stage air conditioner units in Houston. The five different graphs indicate the five different manufacturers that were represented in the database: Carrier, Goodman, Lennox, Trane, and York. The different nominal SEER values are indicated by the color of the bars. The units within a specific manufacturer are separated into groupings by the different model-lines that were represented, and lastly the different bars within a model-line grouping represent the different units (capacities) within that model-line. It should be noted that this set of simulations represents how these units would “theoretically” be modeled, according to EnergyPlus. All of the inputs were generated as per the requirements of the simulation engine, and then each unit was modeled with its own set of inputs that correlated directly to the manufacturer data for that unit.

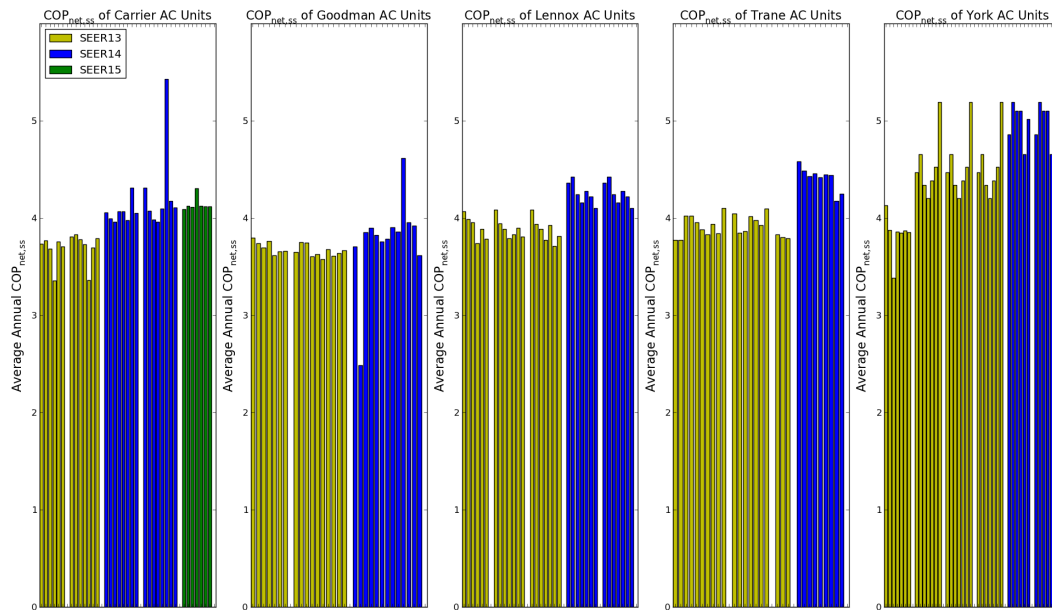


Figure 6.1: $\overline{COP}_{net,ss}$ of all single stage air conditioners evaluated

A number of interesting trends/issues were immediately apparent after this initial set of runs:

- Variation within a model-line (yet without a consistent trend)
- Significant outliers within most manufacturers
- Differences in $\overline{COP}_{net,ss,c}$ for the same nominal SEER rating (within a manufacturer - see York, SEER 13)
- Differences in $\overline{COP}_{net,ss,c}$ for the same nominal SEER rating (between manufacturers - see York vs. Trane vs. Goodman, SEER 14)
- Minimal increase in $\overline{COP}_{net,ss,c}$ between SEER values (within a manufacturer - see Carrier, SEER 14 vs. SEER 15)
- Lack of consistent trend of $\overline{COP}_{net,ss,c}$ with SEER value

Figure 6.2 shows the initial run of all the different two stage air conditioner units in Houston. These were all of the units that had available manufacturers data and were included into the database. Trane did not make performance data available for their two stage units, so there are only four bar charts in the two stage figures. The nominal SEER lines represented here are: SEER 16, SEER 17, SEER 18, and SEER 21.

The initial results from the two stage simulations were even more varied than the single stage units. There was significant variation across manufacturers, to the point where nominal SEER values 2-3 points apart were predicted to have similar $\overline{COP}_{net,ss}$ (depending on the unit considered). There was also more of a trend with the nominal capacity of the unit for two stage air conditioners. The two stage results highlighted the concerns listed above and led to further concerns with accuracy of modeling these systems simply as they are directed to be modeled by the simulation engine documentation.

All of these issues directly impact the goal of the study to provide accurate representation of the annual energy consumed by air conditioners and heat pumps. The data analysis that was performed prior to these simulations (see chapter 5) led to some skepticism regarding the dependability of the data used to generate the inputs. These factors, taken together, raised a series of interesting questions:

- (1) Is the observed variation representative of actual performance?

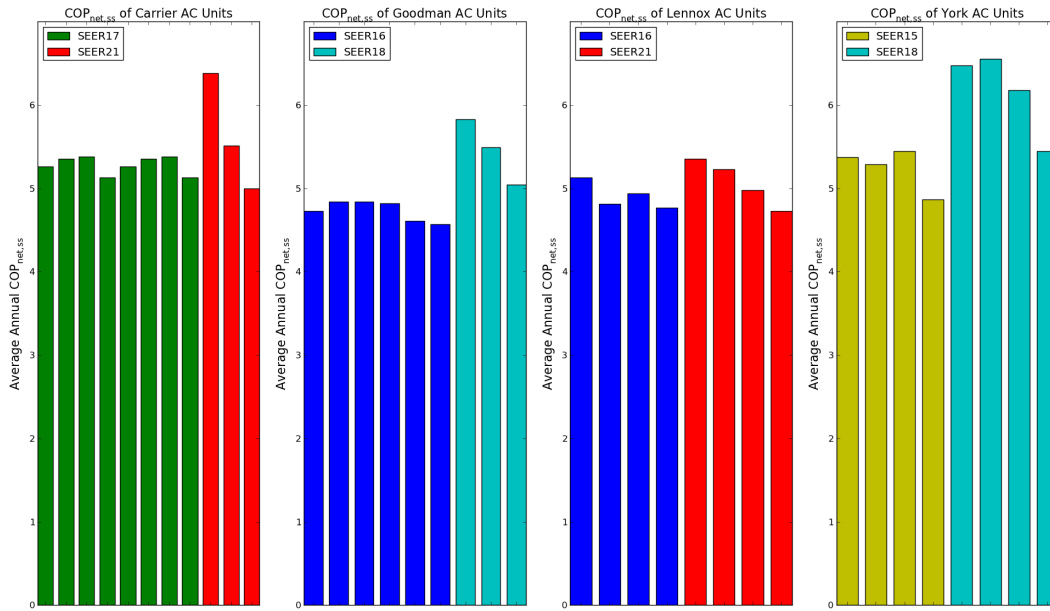


Figure 6.2: $\overline{COP}_{net,ss}$ of all two stage air conditioners evaluated

- (2) Does the variation stem from the different in-house models used to generate the expanded performance tables?
- (3) What model inputs are driving this variation?

Questions 1 and 2 listed above were critical to the results of the research, yet to accurately answer them it was important to understand the answer to question 3. It was necessary to understand which of the various inputs that were generated from the database were having the largest impact on the variation shown in figure 6.1.

In order to answer this question, a sensitivity study was performed on the various inputs to the model to determine which input/s were driving the variation. If the source of variation was determined it would be possible to evaluate that data directly, determine the validity of the variation, and formulate a solution to the modeling problem.

6.3 Sensitivity Study

The sensitivity study was undertaken to understand exactly how the different inputs were effecting the annual simulation results. This would be accomplished by holding a portion of the inputs constant, while letting only a selection of the inputs vary from unit to unit (as calculated from the database). To fix the inputs, the curves would be set to be constant and the rated values would take a single, average value. The first goal of the sensitivity study was to organize a way to proceed through the variables. Given the fact that there are eight different steady state inputs (four rated values, and four curve fits), to exhaustively test all combinations of the variables would have required 246 different combinations of input variables (Note: $\binom{n}{k}$ for $n = 8$ and $k = 1, \dots, n$). Seeing as each one of these combinations necessitated running over 200 different simulations, it was clear that all different input combinations could not be run. Therefore a methodology was developed to most efficiently test the crucial combinations.

The first step in dividing up the study was to determine that the curve fit inputs would be tested first. This decision was made due to the fact that the curve fits:

- (1) Contain the most information from the performance tables
- (2) Are the most complicated to calculate
- (3) Theoretically have less impact than the rated values

This last point is not immediately clear, yet the fact that all of these curves are normalized at the rated values implies that all they do is scale the rated values depending on the current state of the independent variables for the given curve.

The absolute (trivial) basecase was where every air conditioner or heat pump had the exact same inputs. This would result in the exact same energy consumption for the year, therefore being unimportant to simulate. On top of this basecase the different curve fits were introduced to see the relative, and eventually, total impact of the four steady-state, curve inputs. The order in which the different curves were introduced was informed by the theoretical impact of the curves based on knowledge of the simulation algorithms. The progression of the sensitivity study is shown in a flow chart in figure 6.3.

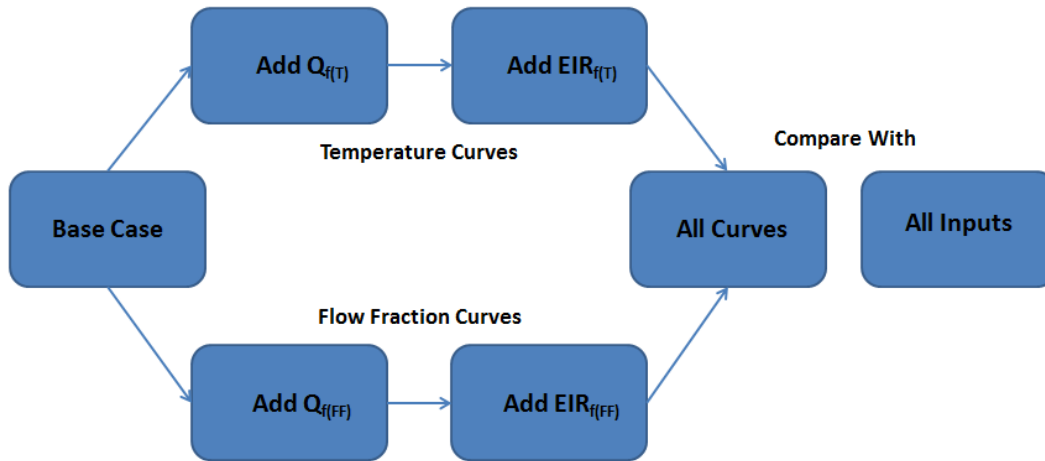


Figure 6.3: The progression of the curve sensitivity study

One important item to note is that both the temperature curves, $Q_{f(T)}$ and $EIR_{f(T)}$ were generated at a certain CFM/Ton. This is the rated CFM/Ton input that is required as one of the EnergyPlus inputs. The rated CFM/Ton is not the actual flow rate of the indoor fan, it is used to adjust the capacity and EIR temperature curves from the CFM/Ton where they were rated to the actual CFM/Ton being delivered by the fan. The rated CFM/Ton is also used as the rating point for the flow fraction curves. The curves then adjust capacity and EIR from the CFM/Ton where they were rated to the actual CFM/Ton of the fan. Due to the fact that the rated CFM/Ton input is integrally related to the curves, and does not have any other impact on the simulations it was always allowed to vary to be the unit specific rated flow rate and was never fixed in the sensitivity study.

6.3.1 Curve Sensitivity Results - Temperature Curves

The first curve that was introduced was the $Q_{f(T)}$ curve. This curve was the first to be selected because without part load effects the capacity of the unit would theoretically have very little impact on the simulation. At most it should have some secondary effects on the way the runtime is calculated. The results from letting only the $Q_{f(T)}$ curve vary using the unit specific curves are shown in figure 6.4.

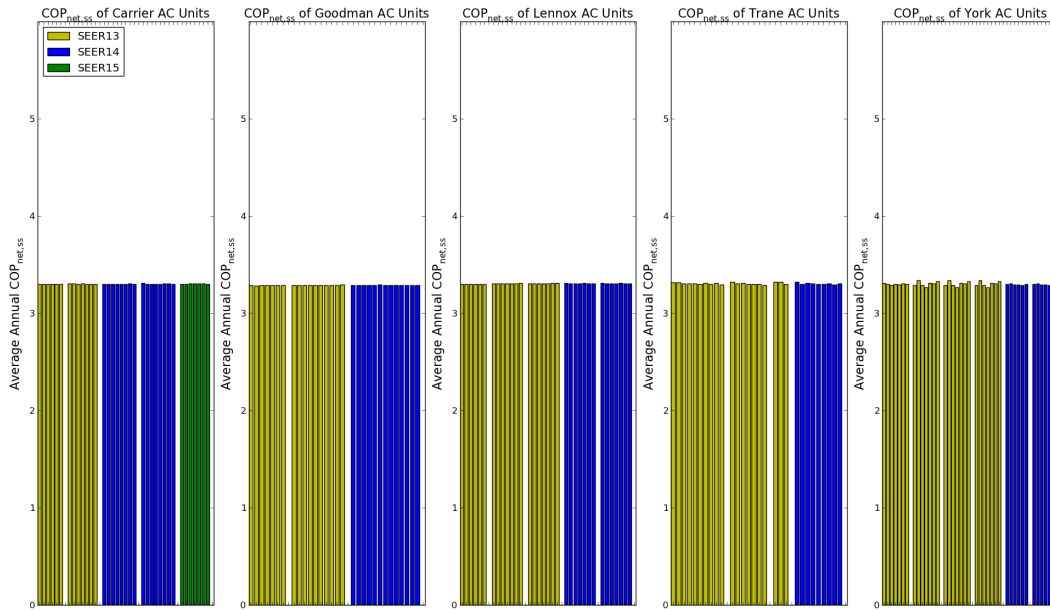


Figure 6.4: Effects of letting only $Q_{f(T)}$ vary

It is clear from the constant $\overline{COP}_{net,ss,c}$ that the theorized impacts of the $Q_{f(T)}$ curve were correct; the curve had almost no effects at all. The next curve to be simulated was the $EIR_{f(T)}$ curve. Seeing as the effects of the $Q_{f(T)}$ curve were so minimal, the next set of simulations that were run included both $EIR_{f(T)}$ and $Q_{f(T)}$. Having both of the curves varying in these simulations allowed for the evaluation of the cumulative effects of the temperature dependent curves. These results are presented in figure 6.5.

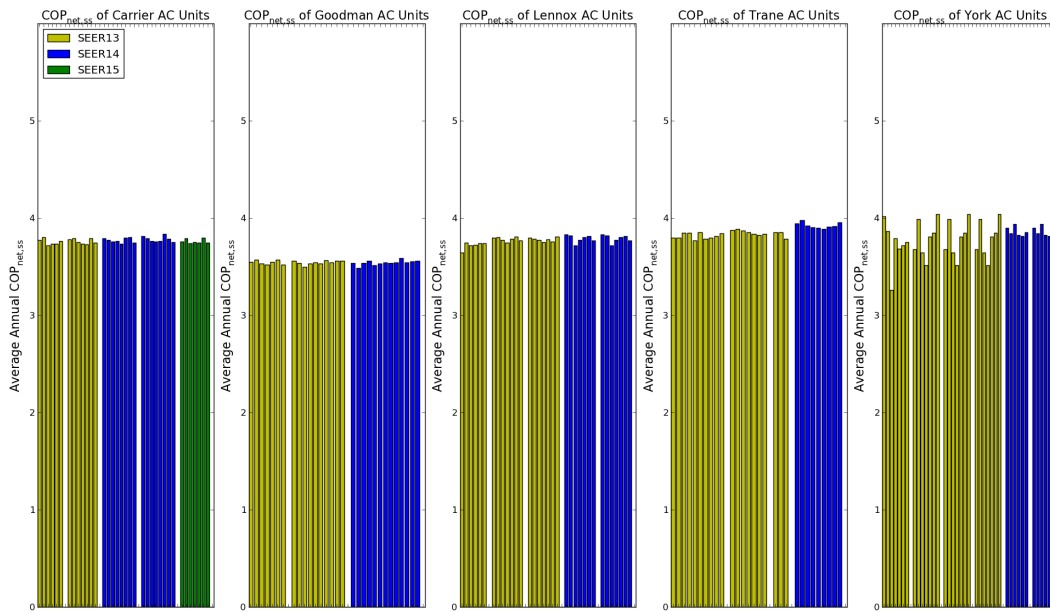


Figure 6.5: Effects of letting both $Q_{f(T)}$ and $EIR_{f(T)}$ vary

The effects of the $EIR_{f(T)}$ curve are more noticeable than just the $Q_{f(T)}$ curves. Some of the variation between manufacturers starts to become apparent. Yet, the variation within a specific manufacturer is very limited (with the exception of York). There is still almost no variability between different SEER values (rated COP is still held constant) or different units within a model line.

6.3.2 Curve Sensitivity Results - Flow Fraction Curves

The next curves that were tested were the flow fraction curves. In order to test the effects of these curves it was necessary to take a slightly different approach than with the temperature curves. The temperature curves were exercised due to the inherent variation in the climate files. The different outdoor temperatures and relative humidities within the space varied throughout the year and therefore the curves were evaluated at a variety of conditions. With the flow fraction curves this had to be done manually by changing the constant flow rate of the fan. The general range for volumetric flow rates is 350-450 CFM/Ton. Most of the rated CFM/Ton values were approximately 400 CFM/Ton; this was also the default flow rate in BEopt. To effectively see the impact of the flow fraction curves, a full set of simulations were run with

actual flow rates of 350 CFM/Ton and 450 CFM/Ton. So, for each flow fraction curve two separate graphs will be presented.

Again, the first flow fraction curve that was varied was the $Q_{f(FF)}$ curve. This curve was selected first for the same theoretical reason as with the temperature curves; the effects from capacity are very secondary effects in the simulation algorithm. The results from the batch run at a fixed flow rate of 350 CFM/Ton are presented in 6.6, and the results for the batch run at 450 CFM/Ton are presented in 6.7.

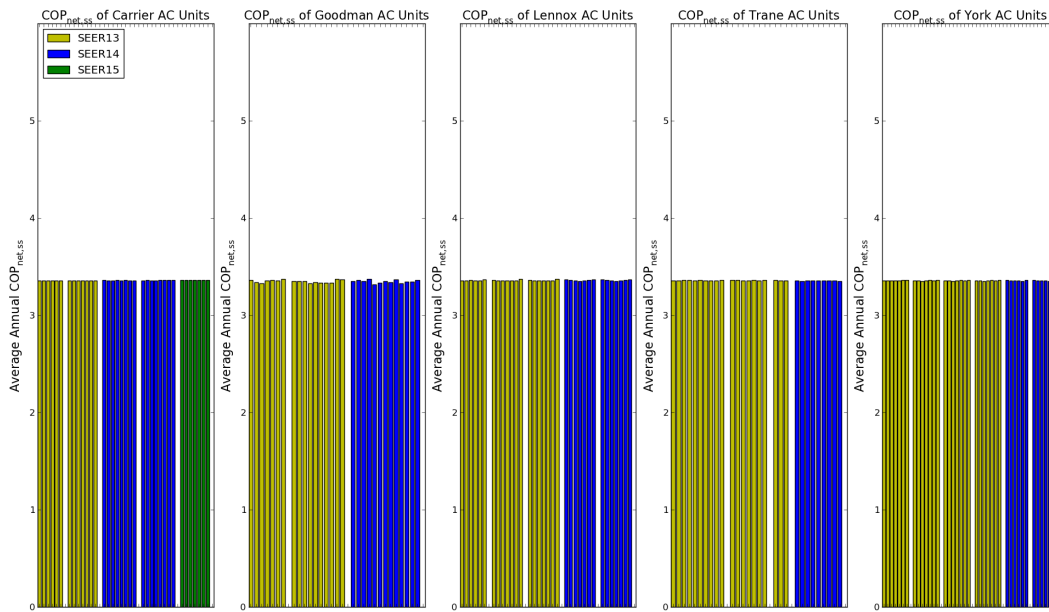


Figure 6.6: Effects of letting only $Q_{f(FF)}$ vary - fixed fan speed of 350 CFM/Ton

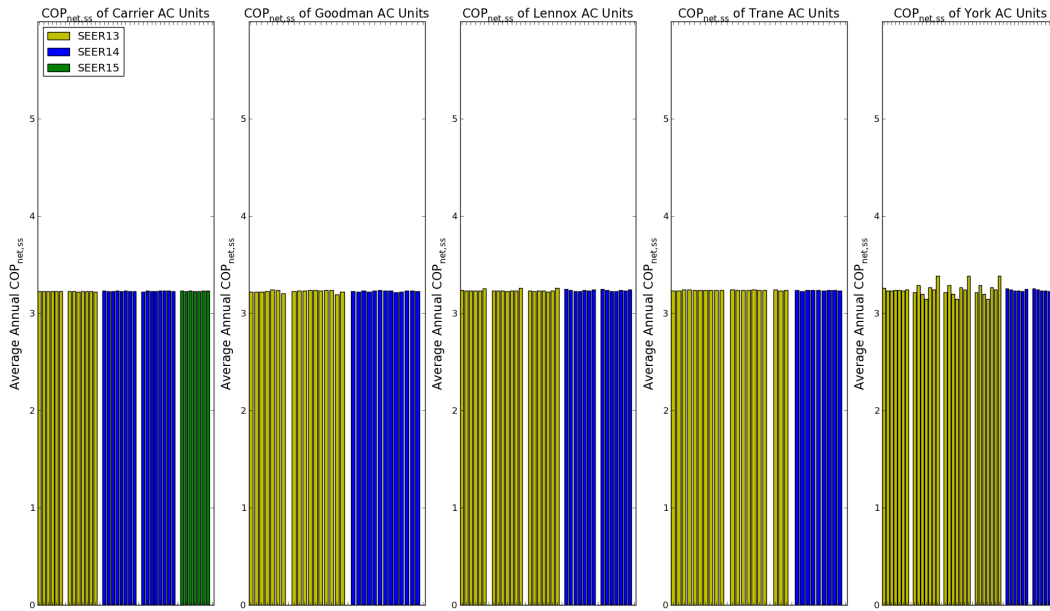


Figure 6.7: Effects of letting only $Q_{f(FF)}$ vary - fixed fan speed of 450 CFM/Ton

The $Q_{f(FF)}$ does not show much variation at all. The results are very similar to the $Q_{f(T)}$ curve sensitivity result. For a single fan speed there is almost no variation, between manufacturers or within a single manufacturer. There is slightly more variation to the $Q_{f(FF)}$ curve than the $Q_{f(T)}$ due to the fact that the curves were generated at different rated CFM/Ton values (whereas all of the $Q_{f(T)}$ curves were generated at the same rating point, 95/80/67). This will make the difference between the fixed flow rate (either 350 or 450) greater or smaller, depending on how far off of 400 CFM/Ton the flow fraction curve was rated at. It can also be noted that the 350 CFM/Ton results show a slightly increased $\overline{COP}_{net,ss,c}$ in general. This is a slightly unexpected result, in that a higher flow rate would usually provide more sensible cooling. Due to the fact that the unit runtime is determined by the sensible load and sensible capacity, this would imply that the 450 CFM/Ton case should consume slightly less energy. In this case, the fact that the metric is a net value introduces the higher fan energy consumed (and lower net capacity) from the higher flow rate. These small differences aside, the annual results show very little sensitivity to the $Q_{f(FF)}$ curve.

Similar to the introduction of the $EIR_{f(T)}$ alongside the $Q_{f(T)}$, the $EIR_{f(FF)}$ was next allowed to

vary alongside of the $Q_f(FF)$ curve. The results from these simulations are shown in figures 6.8 and 6.9.

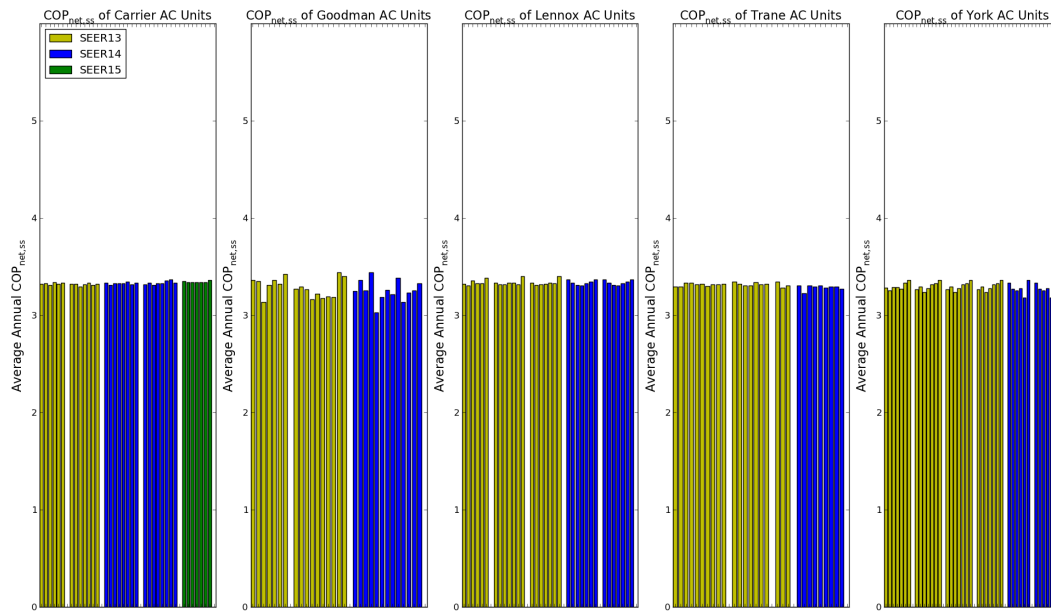


Figure 6.8: Effects of letting both flow fraction curves vary - fixed fan speed of 350 CFM/Ton

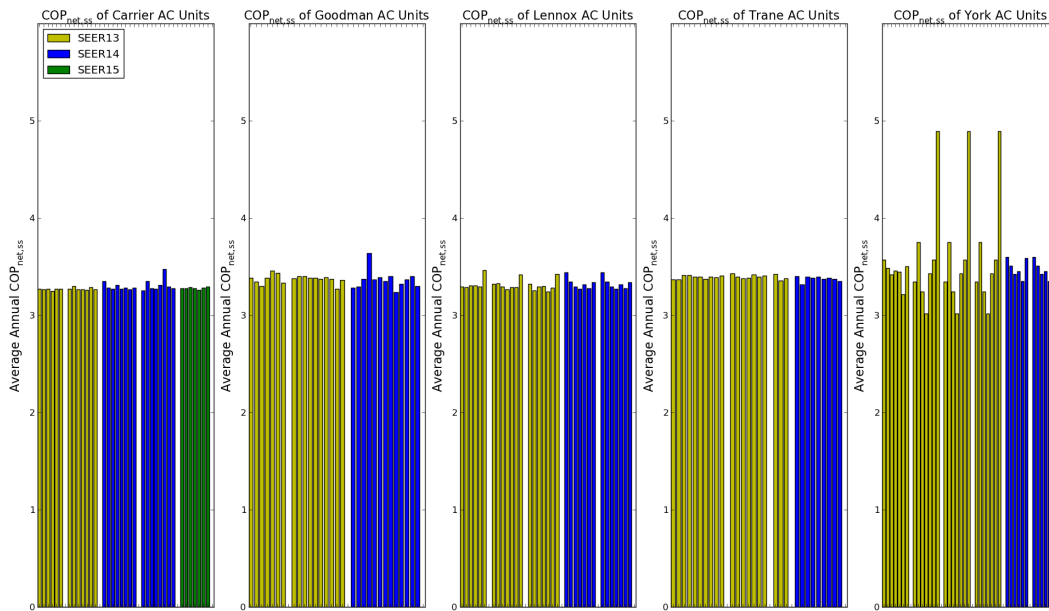


Figure 6.9: Effects of letting both flow fraction curves vary - fixed fan speed of 450 CFM/Ton

The variation induced by the two flow fraction curves was not as significant as the two temperature dependent curves. It can be noted that certain manufacturers demonstrated larger variability at the 350 CFM/Ton flow rate than at the 450 CFM/Ton (or vice versa). This was most likely due to the curves having rated values closer to one of those extremes or the other. For instance, the three significant outliers in the York graph in 6.9 each had rated values of approximately 365. Therefore the variability in the curve is really exposed when evaluating the curve at a much different flow rate (450 CFM/Ton). As noted before, most of the curves used ≈ 400 as the rated value.

Finally, figure 6.10 shows the effects of all of the four curves being the unit specific curve inputs. This simulation was run with a fixed flow rate of 400 CFM/Ton. If figure 6.10 is compared to 6.1, it can be seen that the large majority of the variation exhibited in 6.1 is not due to the curves being allowed to vary. This indicates that the rated values have a large impact on the annual simulation results.

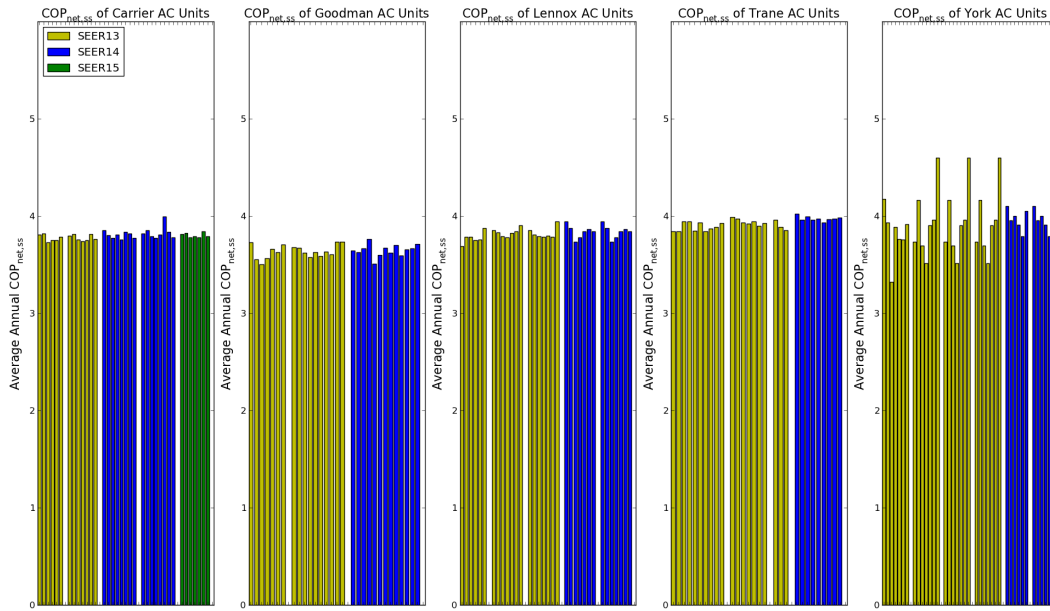


Figure 6.10: Effects of having all units use their unit specific curve inputs (all curves vary)

6.4 Summary of Curve Sensitivity Results

The results from sections 6.3.1 and 6.3.2 demonstrated that the various curve inputs do not have a large impact on the $\overline{COP}_{net,ss,c}$ of an air conditioner. This was especially true within each specific manufacturer; the effect of letting all of the curve inputs be unit specific during the simulations did not result in much overall variation in predicted $\overline{COP}_{net,ss,c}$. This was generally true across manufacturers as well, there were some slight differences (especially in the $EIR_{f(T)}$ curve) but they were not nearly as dramatic as with the rated COP and SHR included in the simulations.

It was made evident from these simulations that having curve inputs is important; this can be noted from the large shift in average $\overline{COP}_{net,ss,c}$ that occurred when introducing the different curves. Yet the specific shape of the curves (the coefficients used) did not appear to have a large impact on the annual simulation results. This led to a critical question regarding the potential simplification of the problem of modeling split system units:

→ Could a single set of curves could be used for all units?

- (1) Within a manufacturer?
- (2) Across manufacturers?

To answer this question it was necessary to evaluate the effects of fixing a single set of curves for different climates and different fixed flow rates. It was decided to look at four different climates: Houston, Phoenix, Atlanta, and Chicago, and at three different air flow rates 350, 400, and 450 CFM/Ton. This parametric study would provide the variation of the curves inputs necessary to evaluate the impact that a fixed set of curve inputs would have. The study would have to be run twice: once with a selected set of representative curves for each manufacturer (answering item 1 above), and a second time with a single set of curves for all manufacturers (answering item 2 above).

To perform the aforementioned parametric study it was necessary to select the representative set of curves for each manufacturer and the set of curves that would be used across all manufacturers. The process of selecting the representative curves is outlined in section 6.6. Before the description of the curve selection process, a brief summary of the two stage sensitivity is presented in 6.5.

A similar study was also done for heat pumps both in cooling mode and in heating mode. The heat pumps showed similar results as those demonstrated for air conditioners. These results are discussed in chapter 8.

6.5 Two Stage Sensitivity

The initial results of the two stage simulations, shown in figure 6.2, showed wide variation in the predicted $\overline{COP}_{net,ss}$ for the different units and different nominal SEER values. To determine the source of the variation, a similar study as the sensitivity outlined above was performed for the two stage models. The notable differences are outlined here and some key results are discussed.

From the discussion of the two stage model in EnergyPlus (see section 4.1.2), it was observed that the performance at different stages was modeled by defining a different set of inputs for each stage. The required inputs were exactly the same from stage to stage. Therefore the initial question that needed answering for the two stage units was: were there significant differences between the database generated inputs for low

stage and high stage. To answer this question the two stage units were modeled as if they were single stage units. That is to say, the low stage inputs were used to define a single stage unit and the high stage inputs were used to define a second single stage unit. This resulted in two theoretical single stage “units” per actual two stage unit. The predicted performance of the low stage units was then compared to that of the high stage units. The results are shown in figure 6.11.

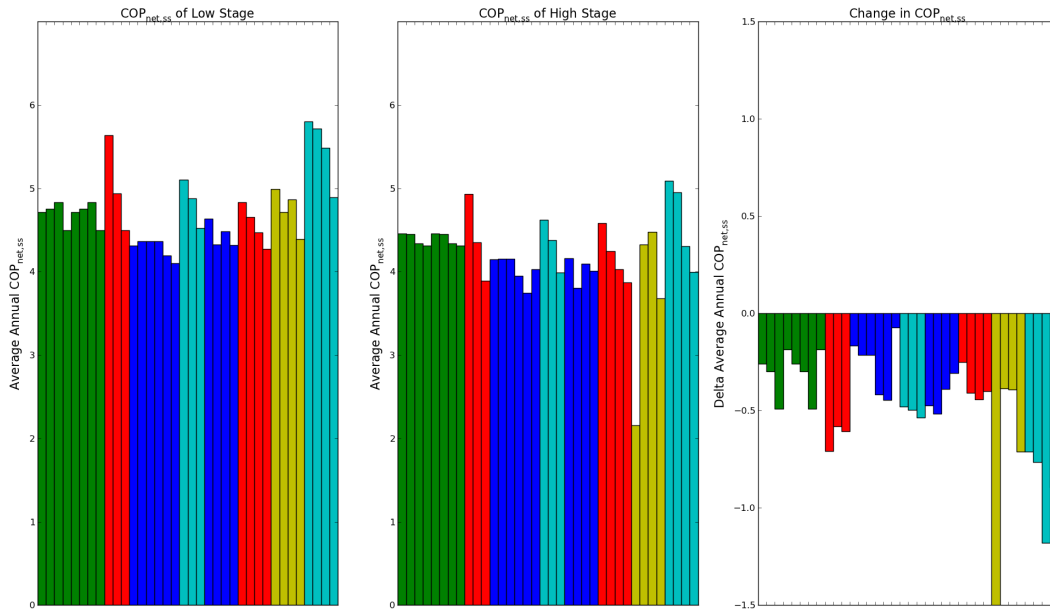


Figure 6.11: Comparison of low stage to high stage performance

It can be noted that the predicted $\overline{COP}_{net,ss}$ of the low stage units was higher than the predicted $\overline{COP}_{net,ss}$ of the high stage units for all of the units modeled. This results follows from the fact that two stage units achieve their higher efficiency through improved performance at the low stage. The individual manufacturers and nominal SEER values were not listed because this figure was important in that it demonstrated that high stage inputs had different results than low stage inputs across the board. This indicated that it was necessary to provide two separate sets of curves (one set for low and one set for high stage).

To perform the curve sensitivity study the stages were kept separated and were continued to be modeled as two different single stage units (per actual two stage unit). Since this simplified the problem

to exactly that of the single stage sensitivity outlined in 6.3, this process will not be discussed in further detail here. The process of selecting a representative set of curves was also identical to single stage selection. Results for the variation due to fixed curves for two stage units will be presented along with the single stage units in section 6.7.

6.6 Selecting Representative Curves

The goal of selecting a set of representative curves was to minimize the variation due to utilizing one set of fixed curves for all the different units (both within a manufacturer and across manufacturers). The process of selecting a set of curves for each individual manufacturer will be outlined first. This will be followed by a brief discussion of the process of selecting a single set of curves that would be suitable for all units in the study.

Within a Manufacturer

The selection process aimed to minimize the variation due to fixed curves by breaking the evaluation down into two parts. First, the variation due to the temperature curves and second the variation due to the flow fraction curves. For the temperature curves, the results were used from the annual simulations with all inputs fixed except for the two temperature curves. The $\overline{COP}_{net,ss,c}$ was averaged across all of the units (for each individual manufacturer). Then the difference between the unit specific $\overline{COP}_{net,ss,c}$ and the average of all $\overline{COP}_{net,ss,c}$'s was calculated.

$$Min(|\overline{COP}_{net,ss,ave} - \overline{COP}_{net,ss,i}|) \quad \forall i \in units \quad (6.3)$$

The process was slightly different for evaluating the flow fraction variation. This was due to the fact that it was not important to calculate the variability within a certain flow rate, but rather to capture the effect of varying flow rates. To accurately capture this variation, the average $\overline{\Delta COP}_{net,ss,c}$ was calculated by taking the difference of the $\overline{COP}_{net,ss,c}$ from the batch run at 350 CFM/Ton and the batch run at 450 CFM/Ton. The average of the $\overline{\Delta COP}_{net,ss,c}$ was then calculated and the difference between that average and the unit specific delta was minimized:

$$Min(|\overline{\Delta COP}_{net,ss,ave} - \overline{\Delta COP}_{net,ss,i}|) \quad \forall i \in units \quad (6.4)$$

Finally, the unit whose curves were used as the representative curves was selected by combining equations (6.3) and (6.4) as shown in equation

$$\text{Min}((\overline{\Delta COP}_{net,ss,ave} - \overline{\Delta COP}_{net,ss,i})^2 + (\overline{COP}_{net,ss,ave} - \overline{COP}_{net,ss,i})^2) \quad \forall i \in \text{units} \quad (6.5)$$

Across Manufacturers

The selection of a single set of curves to be used across manufacturers was a more difficult task. This selection process utilized a lot of the data evaluation results discussed in chapter 5, and information gained from discussions with different manufacturers. There were essentially two possible approaches to this selection process:

- (1) Use the process outlined above for all 169 units and select the curves that provide the average performance across all modeled units
- (2) Select a manufacturer that provides the best data and use the set of curves that provides the average performance within that manufacturer

Ideally, the first option would be the path selected, yet the data issues that came up in chapter 5 highlighted the possibility that some manufacturers' models and data entry procedures were providing less than ideal performance maps. The evaluation of the data investigation led to the selection of a single manufacturer. Within that manufacturer the single set of curves was selected by the exact process and equations outlined above.

6.7 Impact of Using Fixed Curves

The process outlined in section 6.6 resulted in representative sets of curves for each manufacturer: one set for single stage units, and two sets for two stage units (one for low stage, one for high stage). To evaluate the impact of fixing the curves, two sets of simulations were run. One with **all** of the inputs being unit specific and one with the representative curves being used for all units (yet letting the rated COP and SHR be unit specific). When quantifying the impact of fixing the curves, the percent difference in annual cooling energy was used as a metric. The percent difference of annual cooling energy was used due to the

fact that energy consumption was the focus in improving the modeling procedures. The fact that percent difference was used also makes it comparable across climates. Figure 6.12 gives a visualization of this process for a single case (400 CFM/Ton in Houston and for a single manufacturer: Carrier single stages).

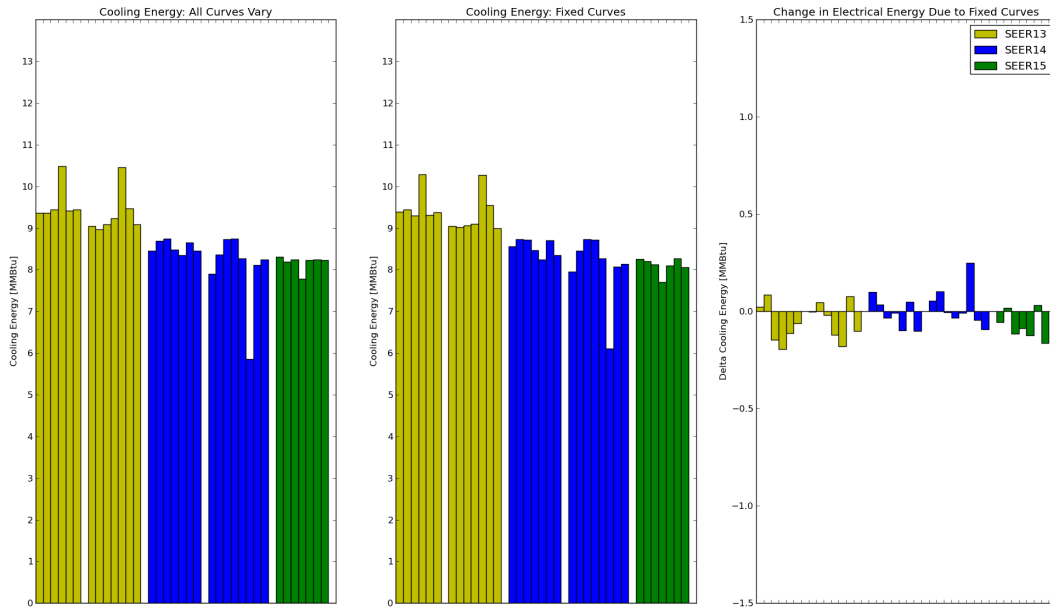


Figure 6.12: Change in Cooling Energy Due to Using Fixed Curves - Carrier, Houston, 400 CFM/Ton

The first bar chart shows the predicted annual cooling energy for each unit when letting all of the inputs vary. The second chart shows the predicted cooling energy when the curves are fixed. The final chart shows the difference between those two cases for each unit simulated.

The differences between all varying and fixed curves were then converted into percent differences. The average percent difference was calculated along with the standard deviation for the entire set of errors (the normality of the distribution was verified with the R statistics package using the Shapiro-Wilk normality test). The average percent difference value demonstrates whether this sets of curves generally shifted the values up or down. The two-sided 95% confidence interval shows how much error above and below that average can be expected (with 95% confidence).

This was done for single and for two stage units. When evaluating the variation due to fixed curves

for two stage units, they were modeled as two stage units in EnergyPlus (the selected curves for high and low were implemented into a two stage model). This showed the cumulative effect of fixing both the high and low stage curves for the two stage case. Tables 6.1 to 6.4 show the results for single stage for five different manufacturers in all four climates and across the three different fixed fan speeds. Tables 6.5 to 6.8 show the resulting variation from using a single set of curves for all of the single stage units.

Table 6.1: Error due to using a single set of curves for each manufacturer - Houston

	350					400					450				
	Carrier	Good.	Lennox	Trane	York	Carrier	Good.	Lennox	Trane	York	Carrier	Good.	Lennox	Trane	York
Average Error	0.2%	1.1%	-0.1%	0.4%	-2.6%	0.3%	0.2%	0.4%	0.5%	-0.7%	-0.7%	1.0%	0.8%	0.6%	-2.9%
95% Confidence (± around average)	1.6%	4.3%	2.1%	3.3%	9.7%	1.8%	2.0%	2.4%	3.6%	11.0%	3.5%	5.0%	3.4%	3.7%	21.6%

Table 6.2: Error due to using a single set of curves for each manufacturer - Atlanta

	350					400					450				
	Carrier	Good.	Lennox	Trane	York	Carrier	Good.	Lennox	Trane	York	Carrier	Good.	Lennox	Trane	York
Average Error	0.1%	1.1%	0.0%	0.4%	-2.8%	0.3%	0.2%	0.4%	0.5%	-1.0%	-0.7%	1.1%	0.8%	0.6%	-3.2%
95% Confidence (± around average)	1.7%	4.3%	2.3%	4.0%	10.4%	1.9%	2.1%	2.6%	4.2%	11.7%	3.6%	4.9%	3.5%	4.4%	21.7%

Table 6.3: Error due to using a single set of curves for each manufacturer - Phoenix

	350					400					450				
	Carrier	Good.	Lennox	Trane	York	Carrier	Good.	Lennox	Trane	York	Carrier	Good.	Lennox	Trane	York
Average Error	1.2%	1.1%	-0.4%	0.6%	-8.5%	0.9%	0.1%	0.1%	0.0%	-6.6%	0.4%	1.0%	0.5%	0.1%	-9.2%
95% Confidence (± around average)	2.0%	4.5%	1.8%	3.7%	11.8%	1.5%	1.9%	1.8%	0.9%	12.4%	2.7%	5.2%	3.0%	1.2%	23.4%

Table 6.4: Error due to using a single set of curves for each manufacturer - Chicago

	350					400					450				
	Carrier	Good.	Lennox	Trane	York	Carrier	Good.	Lennox	Trane	York	Carrier	Good.	Lennox	Trane	York
Average Error	0.1%	1.0%	-2.6%	0.4%	-2.0%	0.4%	-0.1%	-2.2%	0.4%	-0.2%	-0.7%	0.8%	-1.7%	0.5%	-2.4%
95% Confidence (± around average)	2.2%	4.8%	2.8%	4.9%	11.6%	2.5%	2.0%	3.0%	5.3%	12.9%	4.1%	5.2%	3.9%	5.6%	22.1%

Table 6.5: Error due to using a single set of curves all manufacturers - Houston

	400				
	Carrier	Goodman	Lennox	Trane	York
Average Error	-0.3%	-5.1%	-3.6%	3.3%	3.2%
95% Confidence (\pm around average)	1.8%	2.2%	2.1%	3.2%	12.8%

Table 6.6: Error due to using a single set of curves all manufacturers - Atlanta

	400				
	Carrier	Goodman	Lennox	Trane	York
Average Error	-0.3%	-5.5%	-3.8%	0.6%	3.4%
95% Confidence (\pm around average)	1.9%	2.3%	2.3%	3.7%	13.1%

Table 6.7: Error due to using a single set of curves all manufacturers - Phoenix

	400				
	Carrier	Goodman	Lennox	Trane	York
Average Error	0.9%	5.8%	-2.3%	0.6%	1.5%
95% Confidence (\pm around average)	1.6%	2.5%	1.7%	3.7%	13.6%

Table 6.8: Error due to using a single set of curves all manufacturers - Chicago

	400				
	Carrier	Goodman	Lennox	Trane	York
Average Error	0.4%	-8.3%	-2.2%	4.3%	2.7%
95% Confidence (\pm around average)	2.5%	2.2%	3.0%	5.0%	13.5%

The tables above present the average error and a 95% confidence interval around that average error for both cases: representative curves for each manufacturer and one set of representative curves across all manufacturers. It can be seen that the average error is very small when using a single set of curves per manufacturer ($\approx \pm 1\%$), with error bands of $\approx \pm 4 - 5\%$ (both excluding York which has consistently shown extreme amounts of variability when compared to the other four manufacturers). The average error when using a single set of curves across the manufacturers was slightly higher, indicating a shift (upward or downward) for all of the units within a given manufacturer. However the error band stayed relatively small for all manufacturers ($\approx 2 - 5\%$). This indicates good agreement across the different units once the average shift has occurred.

It is also important to consider the error inherent in both the data used to generate these inputs and the uncertainty in the data that this modeling is trying to reproduce. Section 5.2 discusses the error inherent in the manufactures data that is being used to generate these model inputs. Section 3.2.3 discusses

the fact that AHRI allows for $\pm 5\%$ error between the testing results and the reported values. It is therefore not expected that any modeling error less than 5% can be quantified as “error” rather it is within the uncertainty of the data it is being compared against. It is therefore been shown that average error incurred by utilizing one set of curves for all units is within the uncertainty of the data (except for one city in the case of Goodman). This approach achieves very good agreement across all modeled units and is combined with a large reduction in the complexity of modeling the units. The next set of tables shows the same statistics for two stage units.

Table 6.9: Error due to using fixed low and high curves for each manufacturer - Houston

	350				400				450			
	Carrier	Goodman	Lennox	York	Carrier	Goodman	Lennox	York	Carrier	Goodman	Lennox	York
Average Error	0.8%	-3.1%	-2.8%	3.4%	-1.0%	1.9%	-1.5%	-1.2%	1.0%	-2.0%	-1.5%	1.1%
95% Confidence (± around average)	3.4%	5.8%	13.4%	8.9%	3.6%	4.1%	7.1%	7.0%	3.6%	4.2%	7.1%	6.8%

Table 6.10: Error due to using fixed low and high curves for each manufacturer - Atlanta

	350				400				450			
	Carrier	Goodman	Lennox	York	Carrier	Goodman	Lennox	York	Carrier	Goodman	Lennox	York
Average Error	-1.1%	2.6%	-2.6%	2.7%	-1.3%	1.7%	-1.3%	1.9%	-0.7%	1.1%	0.8%	-3.2%
95% Confidence (± around average)	3.9%	5.1%	12.0%	6.9%	4.1%	3.9%	6.3%	4.8%	3.6%	4.9%	3.5%	21.7%

Table 6.11: Error due to using fixed low and high curves for each manufacturer - Phoenix

	350				400				450			
	Carrier	Goodman	Lennox	York	Carrier	Goodman	Lennox	York	Carrier	Goodman	Lennox	York
Average Error	1.3%	2.8%	-2.1%	5.5%	1.1%	1.7%	-0.8%	4.9%	1.1%	0.5%	-0.2%	3.4%
95% Confidence (± around average)	2.1%	5.3%	11.3%	10.1%	1.9%	3.8%	5.5%	8.0%	1.9%	2.3%	2.2%	6.4%

Table 6.12: Error due to using fixed low and high curves for each manufacturer - Chicago

	350				400				450			
	Carrier	Goodman	Lennox	York	Carrier	Goodman	Lennox	York	Carrier	Goodman	Lennox	York
Average Error	-2.0%	-0.8%	-0.5%	4.8%	-1.5%	-1.2%	-0.8%	4.9%	-0.8%	-0.3%	-1.9%	2.0%
95% Confidence (± around average)	5.2%	1.4%	3.2%	6.4%	5.9%	2.4%	3.1%	9.7%	7.5%	3.5%	4.2%	18.1%

The sensitivity study described in this chapter has shown that the curve fit inputs do not have a large effect on the predicted performance for split systems. A methodology for selecting a representative set of curves has been outlined. Finally results showing the expected variation due to utilizing that selected set of curves (for each manufacturer and across all five) have been presented.

This procedure has demonstrated the ability to use a single set of curves for all single stage units and two sets of curves (low and high) for two stage units. This will significantly cut down on the difficulty of modeling split system air conditioners and heat pumps. It will also limit the amount of error introduced from the variable data encountered in the expanded performance tables.

6.8 Curve Coefficients for Energy Modeling (SI and IP)

Tables 6.13 to 6.18 contain the coefficients for the curves that were selected through the process described in section 6.6 in both IP and SI units (EnergyPlus requires SI and DOE-2 requires IP). Tables 6.13 and 6.14 contain the curves selected for air conditioners. Tables 6.15 and 6.16 contain the curves selected for heat pumps in cooling mode, and tables 6.17 and 6.18 contain the curves selected for heat pumps in heating mode . The associated CFM/Ton_{Rated} is included as well. This is due to the fact that the curves are generated at a specific CFM/Ton and that value needs to be input into the simulation engine for the curves to be evaluated appropriately.

Table 6.13: Curves coefficients for air conditioners (IP units)

Stage	Input	Const.	EWB (FF)	EWB ² (FF ²)	ODB	ODB ²	EWB*ODB
Single	$Q_{f(T)}$	3.67027	-0.09865	0.00096	0.00655	-0.00002	-0.00013
	$EIR_{f(T)}$	-3.30270	0.13787	-0.00106	-0.01257	0.00021	-0.00015
	$Q_{f(FF)}$	0.71861	0.41010	-0.12871			
	$EIR_{f(FF)}$	1.32300	-0.47771	0.15471			
	CFM/Ton _{Rated}	386.11637					
Low	$Q_{f(T)}$	3.94019	-0.10472	0.00102	0.00647	-0.00001	-0.00016
	$EIR_{f(T)}$	-3.87753	0.16457	-0.00127	-0.01996	0.00026	-0.00013
	$Q_{f(FF)}$	0.65673	0.51647	-0.17289			
	$EIR_{f(FF)}$	1.56295	-0.79186	0.23003			
	CFM/Ton _{Rated}	423.91023					
High	$Q_{f(T)}$	3.10946	-0.08552	0.00086	0.00863	-0.00002	-0.00014
	$EIR_{f(T)}$	-1.99071	0.09397	-0.00073	-0.00906	0.00017	-0.00010
	$Q_{f(FF)}$	0.69033	0.46438	-0.15451			
	$EIR_{f(FF)}$	1.31565	-0.48247	0.16624			
	CFM/Ton _{Rated}	355.18837					

Table 6.14: Curves coefficients for air conditioners (SI units)

Stage	Input	Const.	EWB (FF)	EWB ² (FF ²)	ODB	ODB ²	EWB*ODB
Single	$Q_{f(T)}$	1.55090	-0.07505	0.00310	0.00240	-0.00005	-0.00043
	$EIR_{f(T)}$	-0.30428	0.11805	-0.00342	-0.00626	0.00070	-0.00047
	$Q_{f(FF)}$	0.71861	0.41010	-0.12871			
	$EIR_{f(FF)}$	1.32300	-0.47771	0.15471			
	CFM/Ton _{Rated}	386.11637					
Low	$Q_{f(T)}$	1.66458	-0.08039	0.00330	0.00124	-0.00003	-0.00052
	$EIR_{f(T)}$	-0.42738	0.14191	-0.00412	-0.01406	0.00083	-0.00043
	$Q_{f(FF)}$	0.65673	0.51647	-0.17289			
	$EIR_{f(FF)}$	1.56295	-0.79186	0.23003			
	CFM/Ton _{Rated}	423.91023					
High	$Q_{f(T)}$	1.36788	-0.06257	0.00280	0.00504	-0.00007	-0.00045
	$EIR_{f(T)}$	0.04232	0.07892	-0.00238	-0.00304	0.00053	-0.00032
	$Q_{f(FF)}$	0.69033	0.46438	-0.15451			
	$EIR_{f(FF)}$	1.31565	-0.48247	0.16624			
	CFM/Ton _{Rated}	355.18837					

Table 6.15: Curves coefficients for heat pumps - cooling (IP units)

Stage	Input	Const.	EWB (FF)	EWB ² (FF ²)	ODB	ODB ²	EWB*ODB
Single	$Q_{f(T)}$	3.68638	-0.09835	0.00096	0.00584	-0.00001	-0.00013
	$EIR_{f(T)}$	-3.43736	0.13666	-0.00105	-0.00794	0.00019	-0.00014
	$Q_{f(FF)}$	0.71866	0.41797	-0.13664			
	$EIR_{f(FF)}$	1.14349	-0.13944	-0.00405			
	CFM/Ton _{Rated}	394.21000					
Low	$Q_{f(T)}$	3.99842	-0.10873	0.00106	0.00751	-0.00001	-0.00016
	$EIR_{f(T)}$	-4.28291	0.18102	-0.00136	-0.02631	0.00033	-0.00020
	$Q_{f(FF)}$	0.65524	0.51166	-0.16689			
	$EIR_{f(FF)}$	1.63911	-0.99895	0.35985			
	CFM/Ton _{Rated}	411.80000					
High	$Q_{f(T)}$	3.46681	-0.09148	0.00090	0.00416	-0.00001	-0.00011
	$EIR_{f(T)}$	-3.55776	0.11274	-0.00073	0.01318	0.00013	-0.00034
	$Q_{f(FF)}$	0.61828	0.56906	-0.18734			
	$EIR_{f(FF)}$	1.57077	-0.91415	0.34338			
	CFM/Ton _{Rated}	344.10000					

Table 6.16: Curves coefficients for heat pumps - cooling (SI units)

Stage	Input	Const.	EWB (FF)	EWB ² (FF ²)	ODB	ODB ²	EWB*ODB
	$Q_{f(T)}$	1.557360	-0.074448	0.003099	0.001460	-0.000041	-0.000427
	$EIR_{f(T)}$	-0.350448	0.116810	-0.003400	-0.001226	0.000601	-0.000467
	$Q_{f(FF)}$	0.718664	0.417974	-0.136638			
	$EIR_{f(FF)}$	1.143488	-0.139440	-0.004048			
	CFM/Ton _{Rated}	394.210000					
Low	$Q_{f(T)}$	1.658788	-0.083453	0.003424	0.002433	-0.000045	-0.000534
	$EIR_{f(T)}$	-0.582916	0.158101	-0.004398	-0.020335	0.001080	-0.000640
	$Q_{f(FF)}$	0.655240	0.511655	-0.166895			
	$EIR_{f(FF)}$	1.639108	-0.998954	0.359846			
	CFM/Ton _{Rated}	411.800000					
High	$Q_{f(T)}$	1.472738	-0.067222	0.002920	0.000052	-0.000030	-0.000359
	$EIR_{f(T)}$	-0.488196	0.099162	-0.002370	0.019503	0.000430	-0.001097
	$Q_{f(FF)}$	0.618281	0.569060	-0.187341			
	$EIR_{f(FF)}$	1.570775	-0.914152	0.343377			
	CFM/Ton _{Rated}	344.100000					

Table 6.17: Curves coefficients for heat pumps - heating (IP units)

Stage	Input	Const.	EWB (FF)	EWB ² (FF ²)	ODB	ODB ²	EWB*ODB
Single	$Q_{f(T)}$	0.508860	-0.000068	-0.000018	0.010632	0.000061	-0.000013
	$EIR_{f(T)}$	0.815861	0.002662	0.000193	-0.009462	0.000228	-0.000316
	$Q_{f(FF)}$	0.719015	0.468781	-0.187796			
	$EIR_{f(FF)}$	1.744516	-1.162934	0.418418			
	CFM/Ton _{Rated}	417.324242					
Low	$Q_{f(T)}$	0.435682	0.000439	-0.000015	0.011645	0.000062	-0.000024
	$EIR_{f(T)}$	0.386442	0.012884	0.000168	-0.008515	0.000242	-0.000386
	$Q_{f(FF)}$	0.804722	0.331862	-0.136585			
	$EIR_{f(FF)}$	2.023042	-1.632826	0.609783			
	CFM/Ton _{Rated}	407.208877					
High	$Q_{f(T)}$	0.251646	0.005801	-0.000063	0.012564	0.000064	-0.000022
	$EIR_{f(T)}$	1.143611	-0.008911	0.000315	-0.007436	0.000334	-0.000459
	$Q_{f(FF)}$	0.826793	0.275436	-0.102171			
	$EIR_{f(FF)}$	1.901372	-1.457820	0.556407			
	CFM/Ton _{Rated}	380.014418					

Table 6.18: Curves coefficients for heat pumps (SI units)

Stage	Input	Const.	EWB (FF)	EWB ² (FF ²)	ODB	ODB ²	EWB*ODB
Single	$Q_{f(T)}$	0.876825	-0.002955	-0.000058	0.025335	0.000196	-0.000043
	$EIR_{f(T)}$	0.704658	0.008767	0.000625	-0.009037	0.000738	-0.001025
	$Q_{f(FF)}$	0.719015	0.468781	-0.187796			
	$EIR_{f(FF)}$	1.744516	-1.162934	0.418418			
	CFM/Ton _{Rated}	417.324242					
Low	$Q_{f(T)}$	0.846130	-0.002279	-0.000047	0.026703	0.000201	-0.000079
	$EIR_{f(T)}$	0.551837	0.020380	0.000546	-0.009638	0.000785	-0.001250
	$Q_{f(FF)}$	0.804722	0.331862	-0.136585			
	$EIR_{f(FF)}$	2.023042	-1.632826	0.609783			
	CFM/Ton _{Rated}	407.208877					
High	$Q_{f(T)}$	0.818223	0.001981	-0.000203	0.028703	0.000207	-0.000071
	$EIR_{f(T)}$	0.815840	-0.006150	0.001021	-0.001301	0.001083	-0.001487
	$Q_{f(FF)}$	0.826793	0.275436	-0.102171			
	$EIR_{f(FF)}$	1.901372	-1.457820	0.556407			
	CFM/Ton _{Rated}	380.014418					

One issue that was not fully explored in this study was the apparent differences in two stage curves. It can be noted that both the average error and the 95% confidence interval are larger for the two stage models. This indicates that there may be some significant differences for two stage units. It is conceivable that there are larger differences for the higher end units in their performance at off-rated conditions; the SEER 13, 14, and 15 units are generally commodity products at this point in air conditioner development and therefore it is not too surprising that their off-rated performance can be modeled by a single set of curves. This was confirmed during a webinar on these results that included engineering staff from: Carrier, Trane, Lennox, Rheem, York, and AHRI. The two stage units on the other hand may actually require further investigation to determine the validity of the variation at off-rated conditions shown from the larger degree of error. Until further data is presented, it is considered more beneficial to limit the difficulty of input generation by presenting a set of representative curves for use with all two stage units. This will also limit the error in modeling due to generating curves from a unit with poor data in the expanded performance table.

The converse of the results shown in this section - that the curve inputs do not have a large impact on predicted performance - is that the rated values do have a large impact on performance. The rated values (rated COP and rated SHR) are the only inputs that have not been fully tested, therefore it is clear that they are responsible for the vast majority of the variation that was shown in the initial batch runs (figures 6.1 and 6.2). Chapter 7 evaluates the rated values that were generated from the expanded performance tables database and compares those values to the rated values listed by AHRI.

Chapter 7

Rated Values - SEER/HSPF Comparisons

From the results presented in chapter 6 it is clear that the rated values, especially rated COP, have a large impact on the predicted energy use of air conditioners and heat pumps. This was an important result that clarified where the focus needed to be directed to improve the accuracy of the split system modeling. The results presented in chapter 6 did not resolve the issues that were observed in figures 6.1 and 6.2. The variation that was observed when modeling all of the different units in the database (as dictated by the simulation engines) was not resolved by the selection of representative curves; the representative curves just simplified the problem and indicated the real source of the variation - the rated values. Therefore, the next step in the process of identifying accurate modeling procedures was to evaluate the rated values from the database of expanded performance table data.

To evaluate the validity of the rated values that were generated from the database it was necessary to utilize the AHRI data that was discussed in section 3.2. The AHRI data was utilized during this section of the analysis for the following reasons:

- (1) It represents actual testing data (not the manufacturer model generated data that is in the performance tables)
- (2) AHRI reports data that facilitates the comparison with manufacturers rated values(A-test point, unrounded SEER values)
- (3) It is desirable to compare the predicted energy use to the nominal SEER values of the units being modeled

The most important of the three points listed above is item 1. The data published by AHRI is representative of actual testing data where the test procedures are clearly defined and monitored by AHRI [1]. This provides some validation against the rated values that were gathered from the manufacturers' performance tables. This would be a relatively simple validation if AHRI published the results for all of the tests that they require in the SEER rating process. The issue with the AHRI data is that they do not report all of these test results; in fact they only report the results of the A-test point. This brings us to item 2 noted above. The fact that they publish the unrounded SEER values along with the A-test point facilitates the inference of some of the other testing points for further comparison. Finally, item 3 addresses the fact that this research hopes to facilitate comparison between the industry metrics SEER and HSPF and annual simulation results. This section will evaluate the correlation between simulation predicted efficiency and the SEER/HSPF efficiencies that are reported by AHRI.

This chapter will be split into two sections: single speed rated values, and two speed rated values. This is mostly due to the fact that the SEER rating process for single speed and two stage units are completely different (see appendix B), thus requiring different methods of comparison.

7.1 Single Speed Rated Values

The single speed rated values were evaluated in two different ways: direct comparison of EER_A values between the AHRI data and the expanded performance database values, and evaluation of the EER_B point and C_d values using the SEER equation and the AHRI unrounded SEER values.

When gathering the AHRI data for the single speed units it was not possible to actually use the actual AHRI website for data acquisition. This was due to the enormous quantity of indoor/outdoor combinations (mix and match) that were reported on the AHRI website. For a single outdoor unit, there was on the order of 700-2,000 different tested combinations. This made it very difficult to locate the mix and match that corresponded to the combination for which the expanded performance tables were generated. Instead of using the AHRI website, it was noted that most of the expanded performance pdfs contained a section where they listed AHRI combination ratings for a smaller subset of the total mix and match. It was therefore possible to locate the corresponding AHRI data with less manual searching.

Once the EER_A results and unrounded SEER values had been collected for all of the single speed units in the database it was possible to compare that AHRI data with the data that was contained in the expanded performance database. The first comparison that was made was the direct comparison of EER_A values. This comparison is shown for all five manufacturers in figure 7.1. This graph shows a scatter plot comparing the database EER_A values to the AHRI EER_A values. A perfect correlation would result in all of the data points lying exactly on the $y = x$ line. The larger the difference between the two values, the farther off of that line the data would fall. Lines demonstrating the $\pm 5\%$ error range were also plotted on the graph to give sense of the percent difference between points.

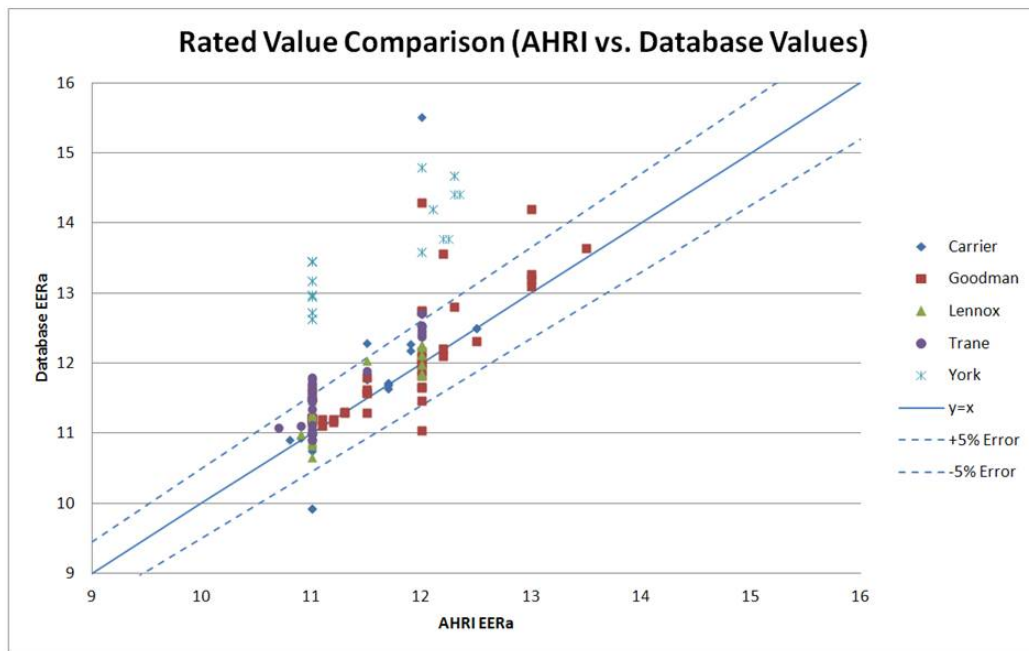


Figure 7.1: Comparison of EER_A - AHRI versus database values

It can be noted that there were a large number of points outside of the $\pm 5\%$ error band, especially on the plus side. There were also large numbers of points that were within the $\pm 5\%$ error band, yet were still demonstrating a certain amount of deviation. This was especially true for certain manufacturers. The fact that there are a large number of points that lie directly on the 11 and 12 AHRI EER_A values shows that there was much less variation documented in the AHRI data than was present in the performance tables. The fact

that large numbers of the calculated EER_A points are outside of the $\pm 5\%$ error band shows that this error cannot be explained by the uncertainty inherent in the AHRI data (see section 3.2.3). This indicates that these rated values are not acceptable as modeling inputs and should be avoided for best modeling practices.

The next step in evaluating the rating points was accomplished by utilizing the single speed SEER rating procedure to evaluate the validity of the information in the expanded performance tables. The single speed SEER rating procedure is extremely simple; it consists of a single equation:

$$SEER = PLF(0.5) * EER_B \quad (7.1)$$

Where

- $PLF(0.5) = (1 - 0.5 * C_d)$
- $SEER$ is the annual efficiency metric in Btu/Wh
- EER_B is the efficiency at the B rating point (82/80/67) in Btu/h/W
- C_d is the degradation coefficient of the unit

To effectively use the SEER equation it was necessary to find the EER_B rating point. This was accomplished by using the regression curves that were generated while compiling the necessary model inputs. These equations were evaluated at the B rating point of 82°F outdoor dry bulb and 67°F indoor wet bulb. This was necessary because none of the expanded tables report performance for 82°F outdoor dry bulb. The curve evaluation essentially interpolates in the expanded tables, returning the efficiency for the 82/80/67 point. Once the EER_B point from the expanded tables was generated, it was possible to use this value along with the unrounded SEER value from the AHRI data and equation (7.1) to calculate the C_d . This was helpful in evaluating the rated values for two reasons. First, the C_d value has bounds on the possible values that it can take on. C_d values less than zero are physically impossible and therefore not defined. C_d values greater than 0.25 are not possible due to the fact that AHRI provides a default of 0.25 if the cycling test is not performed. Therefore, no manufacturer would use a C_d greater than 0.25 (even if the cycling test resulted in a higher value). Second, if the C_d values seemed reasonable, it could provide some information on the C_d values that correspond to the units in the study.

Figure 7.2 shows the calculated C_d values using the AHRI unrounded SEER values and the EER_B values calculated from the performance tables database. The shaded band represents the theoretically possible C_d values of 0 to 0.25. The graph is presented without labels for each individual unit. This is because of the large number of units in the study, but also provides a more general view of the ranges that are being calculated for the different manufacturers.

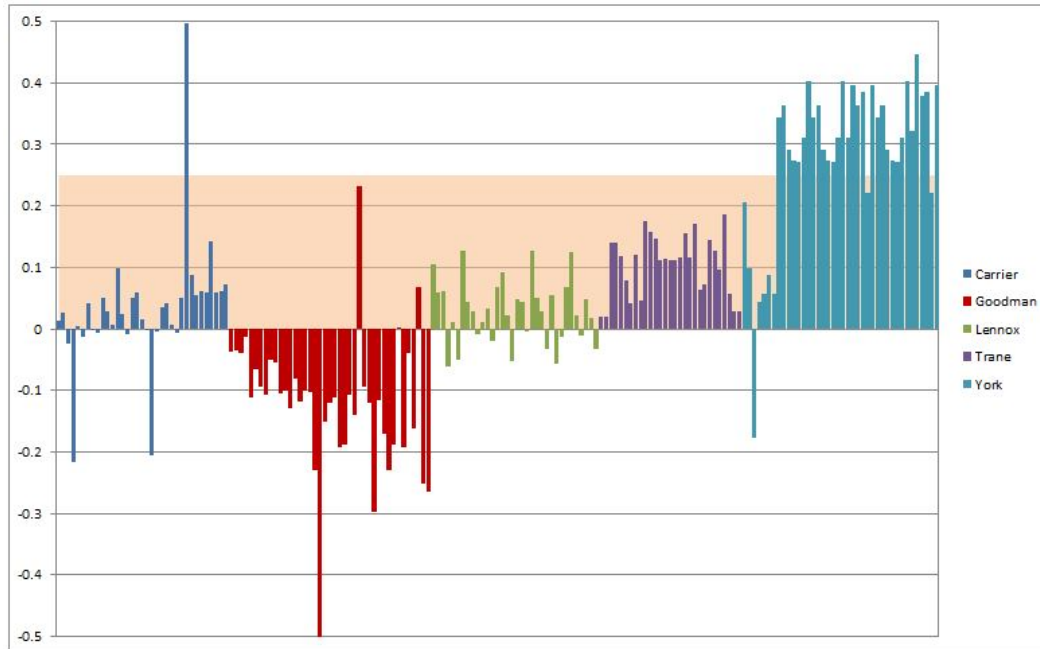


Figure 7.2: C_d values calculated from the SEER equation

The results from the C_d calculations showed a wide variation, from below zero to well above the 0.25 AHRI default value. All but one of the manufacturers contained at least some units that would require a negative C_d value for the EER_B value to result in the reported SEER value. This is not a valid C_d value, which implies that the EER_B value is not valid. This calls the expanded performance data for those units into question. For other units, the C_d was above the AHRI default of 0.25. Again, this implies an invalid EER_B value and therefore questionable rated values from the data included in the expanded performance database.

The combination of the EER_A rating comparison and the calculated C_d results demonstrated significant variability in the single speed rated values. The results from this section did support the earlier

findings that there was significant variability in the simulation results, and that that variability was due to rated values, yet the results do not present a clear picture of how to correct for the this variation. It is not clear how to select a COP that would define a SEER 13 or a SEER 14. Before a discussion of recommended modeling procedures, section 7.2 presents results from a comparable study with two stage models.

7.2 Two Stage Rated Values

For the two stage units it was possible to gather the AHRI rating data directly from the AHRI website. This was due to a much smaller number of mix and match tests listed on the website for the two stage models. Data was gathered for the appropriate mix and match combination that corresponded to the expanded performance tables.

Similar to the single speed case, a direct comparison was made between the A rating point from the AHRI data and the A point in the expanded performance database. This metric was only able to show half of the picture in the two stage case due to the fact that AHRI only publishes the high speed A test (A_2). This test point really only represents part of the picture when dealing with two stage units. If sized appropriately, the unit will be operating much of the year at the low speed. This also only allows a comparison with one of the two rated values used in the simulation engine (high speed). The comparison was made for the available A_2 point and is presented in figure 7.3. Due to the much smaller number of units in the two speed study, it was possible to graph the EER_A values in a line chart with the unit labels on the x-axis. There are two separate lines shown: one for the AHRI data and one for the expanded performance data. In each case they are broken up into each family of units (model line).

Figure 7.3 shows a range of agreement between the AHRI and expanded performance database. Some of the model lines track exceptionally well while others show significant differences. In most cases the trend of EER_A within a model line is pretty well captured, while the actual values may be off across the line.

To get a more complete picture of the other rated values for the two speed units, a comparison was made between the unrounded SEER values from AHRI and the SEER values that would be calculated using the expanded data. This comparison provided both a clearer picture of the discrepancies between the two data sources, and provided a picture of how the different sets of rated values would theoretically compare

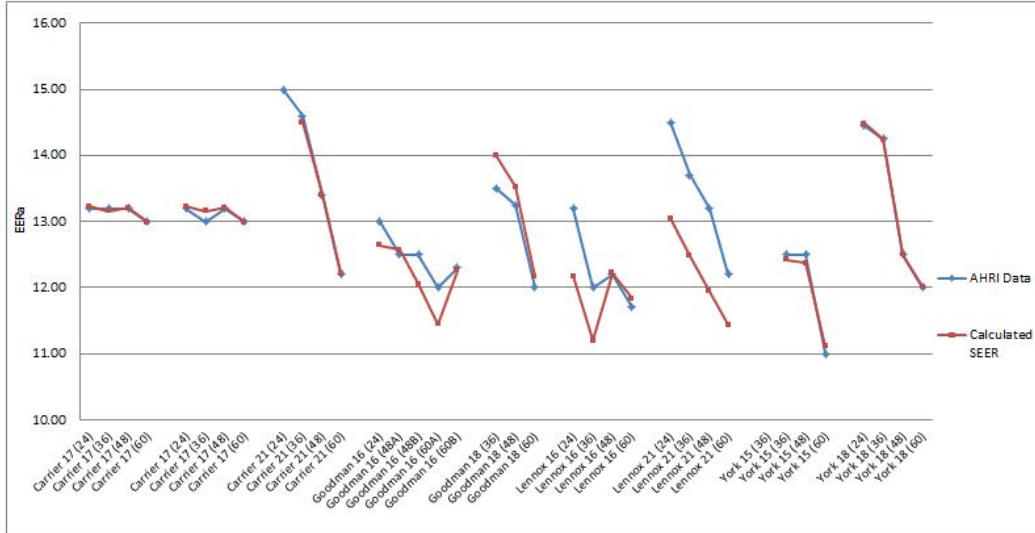


Figure 7.3: Comparison of two stage EER_{A_2} - AHRI versus database values

(on an annual energy basis).

This process was made complicated by the complexity of the two stage SEER rating procedure (see appendix B). The two stage SEER calculation requires knowledge of four different rating points (A_2 , B_2 , B_1 , F_1) and the C_d value. It was possible to calculate all of the different rating points using the same approach as described in section 7.1; evaluating the regression curves at the respective rating conditions. Due to the different “if” statements included in the two stage rating process, it was not possible to use the calculated rating points and the unrounded SEER to back calculate C_d values. It was therefore necessary to assume a C_d value and calculate a SEER value; denoted $SEER_{CALC}$. This $SEER_{CALC}$ could then be compared to the AHRI SEER values (denoted $SEER_{AHRI}$). The C_d value has limited impact in the two stage SEER calculation. This is consistent with the fact that cycling losses are significantly reduced with two speed units. This is due to the fact that the low speed can be used to meet many of the lower loads seen over the course of the year, thus reducing the amount of on/off cycling.

The $SEER_{CALC}$ values were obtained using the exact procedure outlined by AHRI in their rating document, 210/240 [1] and described in detail in appendix B. For each unit, the unit specific curves were utilized to estimate all of the four rating points required to calculate the SEER value. For the first set of

runs, it was assumed that the C_d was always 0.1 (consistent with common values in the literature [9]). To evaluate the impact of the C_d assumption a sensitivity analysis was run with C_d values of 0.01 and 0.25. These two values represent the upper and lower bounds of the possible C_d values outlined by AHRI (see section 2.3.3).

The results are shown in figure 7.4. This figure has three different solid lines, one for the $SEER_{CALC}$ (using best assumption of C_d , 0.1), one for $SEER_{AHRI}$, and one for the nominal SEER value for the model line. The two runs using different C_d values are included in the figure as a shaded band, providing a bounding of the possible error due to different C_d values. A C_d value of 0.01 is the upper limit of the band and a C_d value of 0.25 is the lower limit

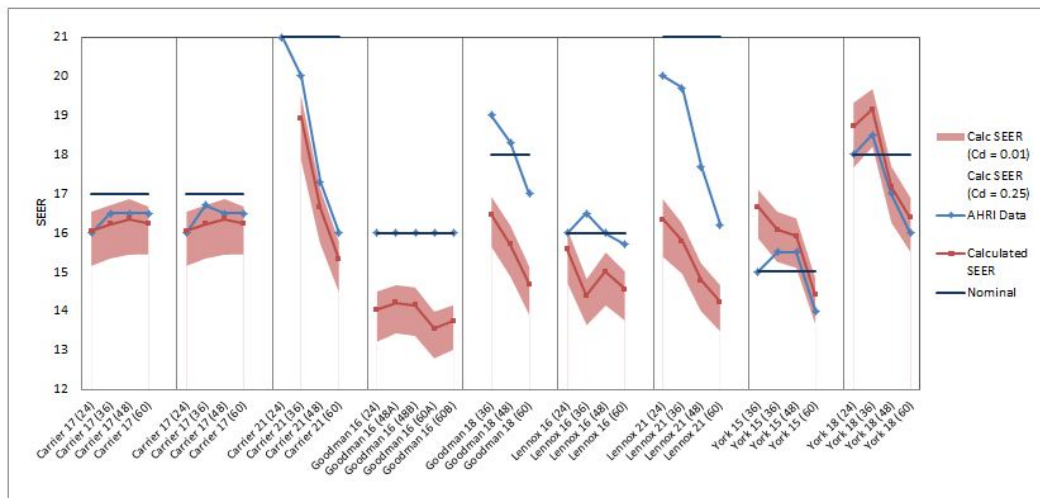


Figure 7.4: Comparison of $SEER_{CALC}$ to $SEER_{AHRI}$ with variation of C_d included

This analysis showed that some of the results could potentially be explained by different C_d values, yet the majority of the units still do not have AHRI SEER values that lie within the bounds laid out in this sensitivity C_d . A change in the assumed C_d value could explain only 14 of the 36 units shown here. The variation demonstrated in this sensitivity study, provides another reason that it would be beneficial to have the manufacturers/AHRI report the C_d values used in generating the expanded performance tables/rated values. It should be noted that, while manufacturers do not report on the fan efficiency used in generating their expanded performance tables, this uncertainty does not affect the calculations shown in Figure 7.4.

This is due to the fact that the same fan efficiency was used in converting the manufacturer's data to gross values that was used to convert back to the net values used in the calculated SEER.

These results showed a number interesting issues with the two stage models. First, and most significantly, there were large discrepancies between $SEER_{CALC}$ and $SEER_{AHRI}$ for the majority of the units. The differences ranged from 0 to over 3.5 SEER points. There were also cases where the $SEER_{CALC}$ did not even match the trend of the $SEER_{AHRI}$ (a new development from the EER_A comparison). The large discrepancy between the two SEER values highlighted the issues that were observed when the two stage units were initially simulated (discussed in section 6.2). The fact that any variation over a single SEER point is outside of the $\pm 5\%$ error band that can be explained by the uncertainty inherent in the AHRI data (see section 3.2.3) again demonstrates that the rated values generated from the manufacturer's EPTs are not acceptable for accurate modeling purposes.

This degree of variation shown in the calculated SEER values was very similar to the variation in the actual simulation results. This connection between the $SEER_{CALC}$ values and the simulation results can be seen by revisiting figure 6.2. Figure 7.5 shows the initial simulation results using all the unit specific inputs juxtaposed with the SEER study shown above. The arrows in the figure point out the correlation between the groups of bars in the simulation results and the model lines (separated by spaces) in the line graph. It should be noted that the trends within each model line match extremely closely between the $SEER_{CALC}$ and the simulation results. The $SEER_{CALC}$ also predicted the relative efficiency of the different units quite well.

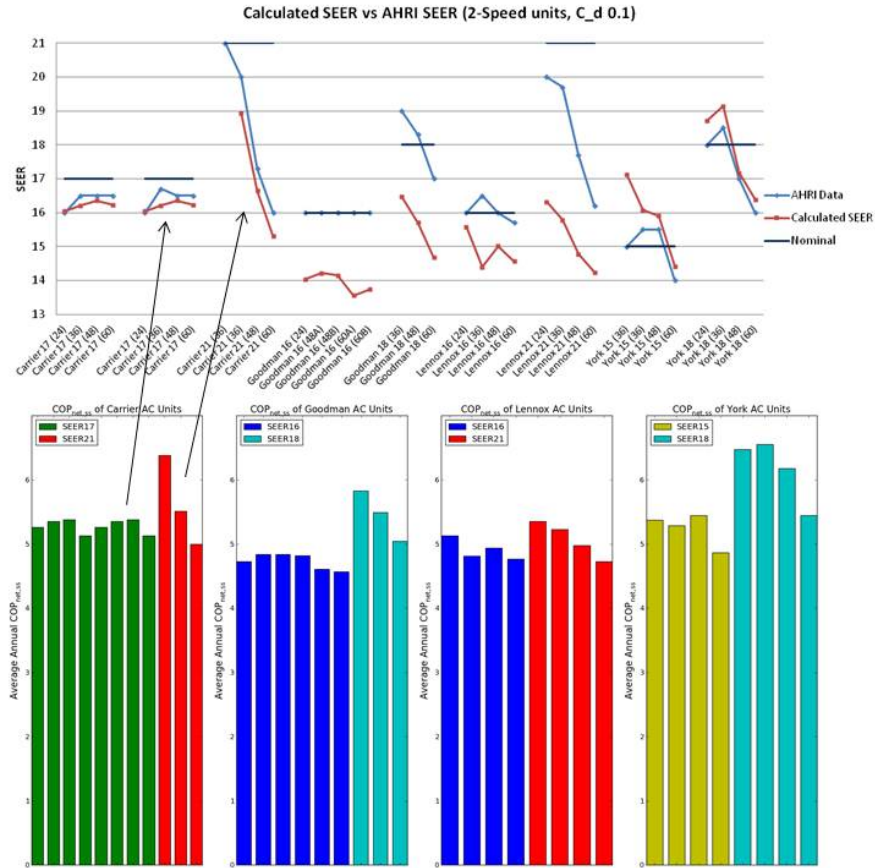


Figure 7.5: Comparison of $SEER_{CALC}$ to Simulation Results

The degree of agreement between $SEER_{CALC}$ and the simulation results indicates that if the actual AHRI test points were used as the rated values that the results would match the $SEER_{AHRI}$ lines (in blue) instead. This would be a preferable correlation due to the fact that all of the $SEER_{AHRI}$ values are based on testing results. The strong correlation between the $SEER_{CALC}$ values and the simulation values demonstrates again the central nature of the rated values in determining the predicted annual energy use. If AHRI began to publish more of the individual test results, this would assist in accurately predicting the annual energy use of air conditioners and heat pumps.

Another significant result of figure 7.4 was the identification of a correlation between SEER and capacity for the highest SEER model lines. Both the $SEER_{CALC}$ and the $SEER_{AHRI}$ demonstrated significant degradation of the SEER value for large capacities in the SEER 18 and SEER 21 model lines. This was

the first example of a consistent trend in the capacity of a model line. The 2-ton capacities for the high (nominal) SEER lines had SEER values that were 3-5 points higher than the 5-ton unit of that same model line. The reason for this SEER degradation with capacity was determined through the collection of physical characteristics data.

Data on the physical characteristics of the unit was collected for all the different units. This data included: face area (outdoor coil), fins per inch, number of rows (outdoor coil), compressor fan CFM, and compressor motor horsepower. The metric that turned out to be most useful was an effective surface area metric, defined as $SA_{eff} = FaceArea * Rows$. This gave an estimate of the size of the outdoor unit. Figure 7.6 shows the SA_{eff} of the different units for all manufacturers with single and two speed units providing information on the physical characteristics. They are shown by model line (groups of bars showing ascending capacities) in ascending nominal SEER values.

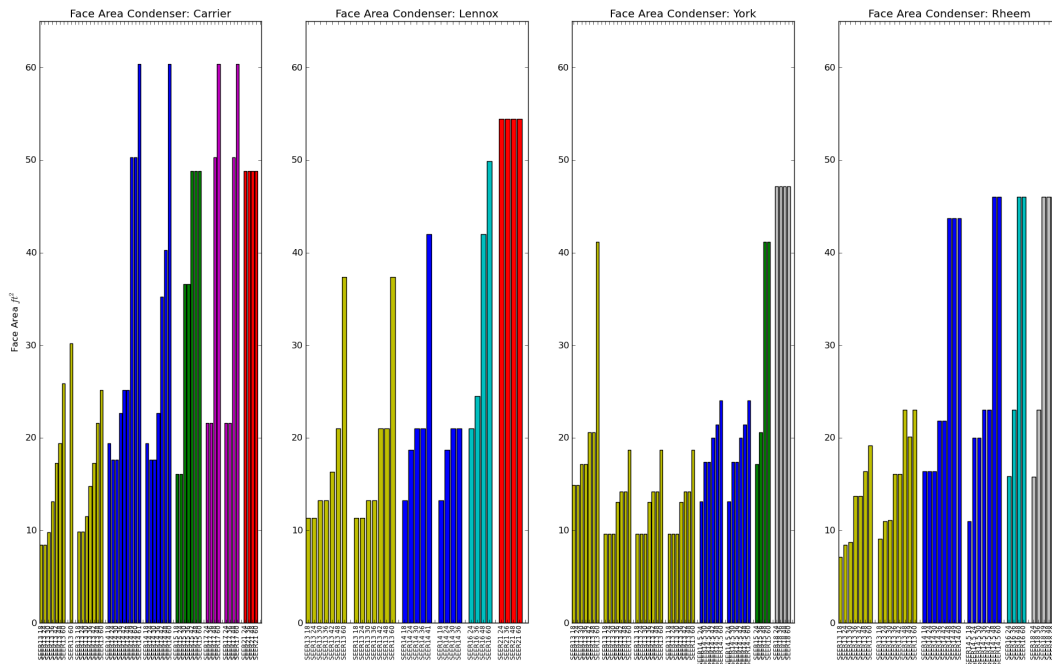


Figure 7.6: SA_{eff} of the different units

Whereas most of the model lines have an increasing SA_{eff} for increasing capacity, the very top SEER model lines (right most grouping in each graph) have a constant SA_{eff} across all capacities. This means

that the manufacturers had reached a physical limit in the size of the outdoor coil; they could not fit a bigger coil into the same cabinet size. This allows them to achieve the extremely high SEER levels at the lowest capacities (due to the over-sized heat exchanger). As the unit is expected to deliver more capacity with the same sized coil, the SEER rating suffers and this results in the degradation with capacity discussed previously. This makes it possible to have a SEER model line advertised as “Up to SEER 21”, when actually the 5-ton unit is rated at a SEER 16. This trend with capacity was only present for the highest efficiency model lines and was confirmed by multiple manufacturers during a webinar presentation on this material that included representatives from: Carrier, Trane, Lennox, York, Rheem, and AHRI.

The trend of decreasing SEER with increasing capacity for the highest SEER model lines should be considered when modeling these units. This could have significant effects during optimization routines (in BEopt for example) where the program is weighing different efficiency options. The ability to downsize the air conditioner not only reduces first costs but also would give a significant reduction in operating costs (due to the improved efficiencies for low capacity units). Knowledge of this SEER trend further incentivizes decreasing the loads on the house and could bring marginal technologies such as increased wall insulation into the picture during optimization.

7.3 Discussion and Modeling Methodology

This chapter highlighted the importance of rated values in accurate modeling of split DX systems. It also demonstrated that the rated values generated from the expanded performance database have a high degree of variability when compared to the testing-based AHRI data. This variability was demonstrated through:

- (1) Direct comparison of rated values (single and two stage)
- (2) Calculation of required C_d values that would result in the $SEER_{AHRI}$ values (single speed only)
- (3) Calculation of $SEER_{CALC}$ and comparison with $SEER_{AHRI}$ (two speed only)

The $SEER_{CALC}$ values for two stage units were then compared to the annual simulation results (modeled with unit specific inputs). The $SEER_{CALC}$ results correlated very closely with the annual simulation

results, even though they were simple SEER calculation results. This indicated that it would be extremely beneficial to use AHRI test results for all of the different rating points. Unfortunately this is not currently feasible. AHRI only publishes the high speed, A_2 test.

With the issues presented in this chapter in mind, it was decided to not utilize specific rated values from the expanded performance database for accurate air conditioner and heat pump modeling. Instead, rated values were selected such that they gave the desired unrounded SEER values. If there is data available from AHRI to further inform these rated value selections (the A point for example), it should be used in conjunction with the unrounded SEER. This approach allows for large amounts of flexibility. A user who is only concerned with a nominal SEER 17 unit can model that directly by using rated values that produce a 17 SEER rating. Also, a user who wants to model a specific make/model/capacity can find that AHRI data and choose the rated points that achieve the unrounded SEER listed there.

To facilitate this process the SEER rating procedure was built in BEopt's option editor so that a user can iterate on the different values included in the SEER calculation until approaching the desired SEER.

These rated values will be used in conjunction with the representative curves that were selected as part of chapter 6. The use of these curves will greatly reduce the number (and complexity) of the inputs without reducing the accuracy of the simulation. The rated value selection process outlined in this chapter will provide the few remaining inputs and facilitate a consistent approach that will reflect the listed SEER ratings more accurately. The SEER and HSPF rating procedures should still be evaluated for consistency (across different modes/speeds/climates) and more work needs to be done with metering actual units over annual operation and comparing those results with the SEER/HSPF results. For current modeling, the approach outlined here will provide results consistent with the AHRI ratings. This will allow for accurate relative ranking of units, and will reflect more closely the testing results that are inherent in the SEER/HSPF ratings.

One of the only inputs that has not been studied in detail here is the part load factor as a function of part load ratio curve (PLF-fPLR). This was due to the fact that C_d values are not provided by AHRI or the manufacturers. It was attempted to calculate the C_d values for single speed units by using the unrounded SEER and EER_B values (section 7.1), yet the results were not considered accurate enough to inform the

PLF-fPLR curves. A physical approach to determining the part load degradation was outlined in [9] and described here in section 2.4. This approach utilizes information on the time constant of the coil and the maximum cycles per hour determined by the thermostat controls, and calculates a PLF curve. Henderson et al. compared the physical approach to the linear form of PLF-fPLR defined in AHRI 210/240 (that uses C_d) with good agreement. In [9], Henderson et al. also provide values for current coil time constants and cycling rates. These values correlated to C_d values of 0.05-0.15. This was consistent with values reported by one of the manufacturers during personal correspondence. Modeling of part load in this research used these C_d values and the linear form of the PLF-fPLR curve ($PLF = 1 - C_d * (1 - PLR)$) to model part load degradation. It was also noted that single stage units were generally on the lower end of this C_d range and two stage units on the higher side.

Increased reporting by AHRI of some already available data would greatly increase the accuracy of annual simulations. This would help inform both the rated values and give actual data on the C_d values. There is currently work being done by both ASHRAE and AHRI on improvements in this arena. This report will ideally be used to inform some of those improvements.

Chapter 8

Heat Pumps - Notable Differences(Curves and Rated Values)

The previous two chapters have focused on single stage and two stage air conditioners. Chapter 6 discussed a sensitivity study that looked at the impact of the regression curve inputs on annual simulation results. Chapter 7 looked at the rated values and compared the rated values from the database to AHRI data. Heat pumps were not discussed during those two chapters to avoid repetition of similar processes and results and to avoid over complication of the procedures described.

Heat pumps were an important portion of the research described here, yet the methodology and research procedures used in investigating heat pump performance was very similar to that of air conditioners. This was due to:

- (1) Similarity between the simulation engines' modeling approach (both in inputs and algorithms)
- (2) Similar data resources
- (3) Consistent results between heating and cooling
- (4) Practically identical results for cooling in heat pumps and cooling in air conditioners (noted through curve visualization and simulation results)

Due to the overlap described above, the present chapter will focus on the differences that were encountered while researching heat pumps and the specific challenges and hurdles that were overcome to improve the understanding and accuracy of heat pump modeling. The cooling component of heat pumps followed an identical path as described in the previous chapters and will not be discussed in further detail.

Before discussing the details of the differences with heat pumps, the initial results of the heat pump batch runs are presented below (for both single and two stage). For the two stage heat pumps, only Carrier, Goodman, and York had available data. The results are broken up into families of units in each model line, and also color coded by nominal SEER value for each model line (similar to air conditioner figures). Even though the results are looking at heating efficiency, the nominal SEER value was used for grouping the units in the graphs seeing as this is how they are divided up by industry. It is also generally the case that increased SEER values correlates with increased HSPF. For evaluation of the HSPF rated values see section 8.2. It can be noted that the results are very comparable to what was initially seen with air conditioner performance. There is significant variation within a manufacturer and across manufacturers.

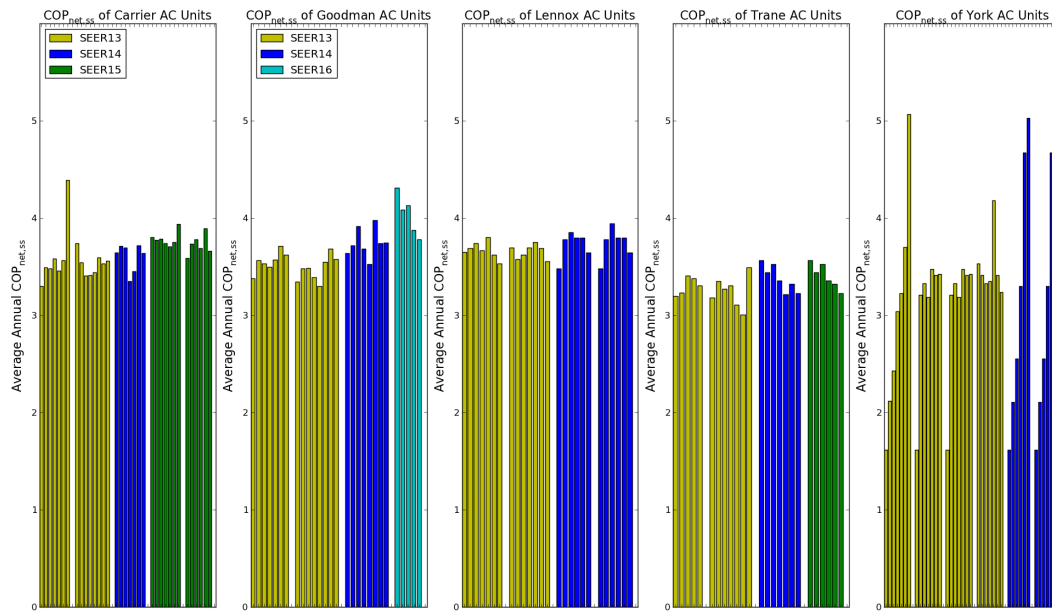


Figure 8.1: Initial results for all single stage heat pumps

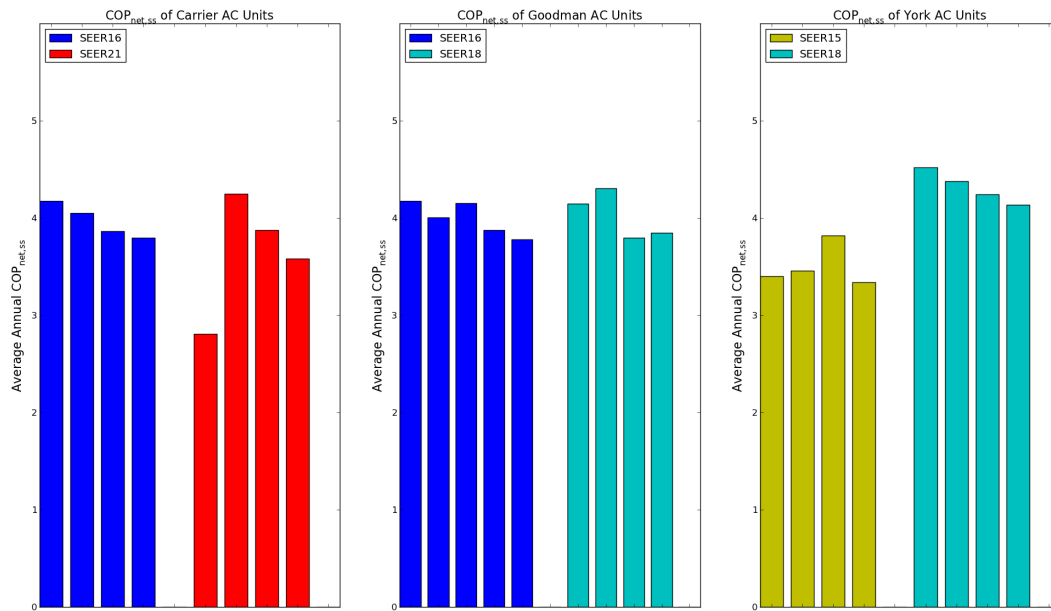


Figure 8.2: Initial results for all two stage heat pumps

8.1 Curve Data

One of the most significant differences between heating and cooling operation was the availability of data for the required model inputs. Item 2 (above) notes the similarity in data resources. This refers to the fact that the data sources are the same for heat pumps and air conditioners (AHRI and manufacturers data). Therefore it was possible to follow a very similar procedure with heat pumps to collect all of the available expanded performance data into a single database. While database construction followed a similar process, the data that was provided for heat pumps proved to be even less consistent than the air conditioner data.

The air conditioner data varied significantly in the manner in which it was reported, yet all of the five manufacturers in the database provided adequate data to inform full sets of model inputs. For heat pumps most of the manufacturers did not provide adequate information to create the full set of curves required by the simulation engines. It can be recalled from section 4.1.3 that the required curve inputs were:

- (1) Total Capacity - function of entering dry bulb and outdoor dry bulb

- (2) Energy Input Ratio (EIR - inverse of COP) - function of entering dry bulb and outdoor dry bulb
- (3) Total Capacity - function of flow fraction
- (4) EIR - function of flow fraction
- (5) Part Load Fraction (PLF) - function of part load ratio (PLR)

It can be seen from observing table 3.6 that of the five manufacturers in the database only three provide data on various entering dry bulbs, and only three report on various CFM/Ton values. This leaves only two manufacturers (Carrier and York) that actually report on both, varying CFM/Ton and varying entering dry bulb. Seeing as York has been the most variable in their reporting procedures and in simulation results, this leaves Carrier as the only reliable source for full sets of simulation inputs. For more details on the variables reported on and in what ranges, please see tables 3.3 to 3.6.

The fact that many of the manufacturers did not publish adequate data provided additional instigation to use a single set of curves for heating operation, (as described for air conditioner modeling in chapter 6). The acceptability of using a set of representative curves was verified by an identical sensitivity study to the one on the curve inputs with air conditioners.

Before describing the sensitivity study, it should be noted that EnergyPlus does not require biquadratic curves (function of entering dry bulb and outdoor dry bulb) for the $Q_{f(T)}$ and $EIR_{f(T)}$ inputs. The documentation states that the inputs can be simply quadratic curve fits (function of outdoor dry bulb only). The impact of using quadratic versus biquadratic inputs was investigated and it was noted that there was a consistent (slight, < 3%) decrease in $\overline{COP}_{net,ss,h}$ when using biquadratic curves instead of quadratic curves. It is hard to determine which of these values would be more accurate. One significant advantage that the biquadratic curves present is the ability to capture the effects of changing indoor temperatures.

Figure 8.3 shows the effects of using a 68°F set point instead of a 71°F set point. The decrease in $\overline{COP}_{net,ss,h}$ can be noted with the higher set point. This effect, while small (only 1-3.5% change in $\overline{COP}_{net,ss,h}$), can not be captured at all without curves that adjust due to entering dry bulb. This will limit the ability to capture the full effects of aggressive set back measures. This effect could be captured only with Carrier and Trane (only manufacturers reporting various indoor dry bulb data).

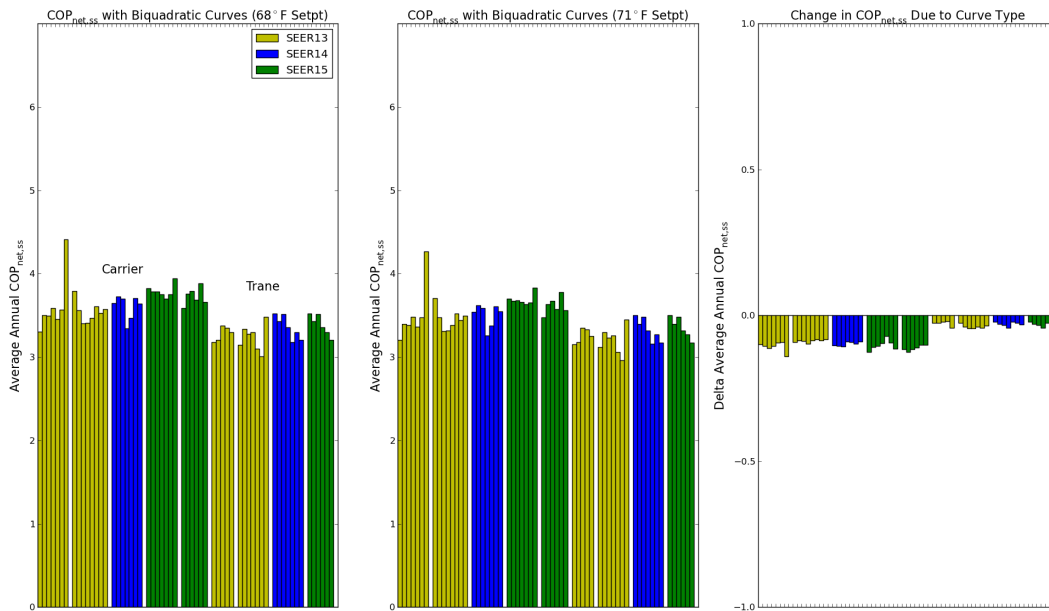


Figure 8.3: Impact on $\overline{COP}_{net,ss,h}$ due to changing the heating set point

The sensitivity study for the curves across all manufacturers was performed with all quadratic curves for equivalent comparison. The sensitivity study followed a very similar format to the one described in chapter 6. Sensitivity to the temperature curves and the flow fraction curves were tested individually. In each case, the capacity curve was introduced initially and then the EIR curve was added into the simulations. To avoid repeating all of the same graphs shown in section 6.3, only the graphs showing the effects of fixing all inputs except for both temperature curves, and the effects of fixing all inputs except for both flow fraction curves are shown here. These results are presented in figures 8.4, 8.5, and 8.6.

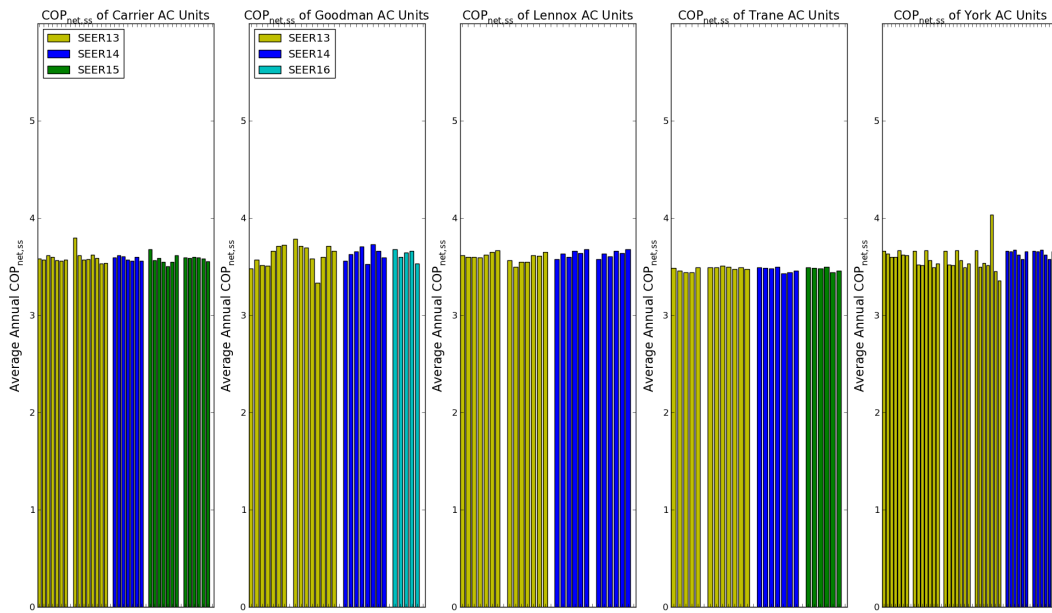


Figure 8.4: Variation due to temperature curves

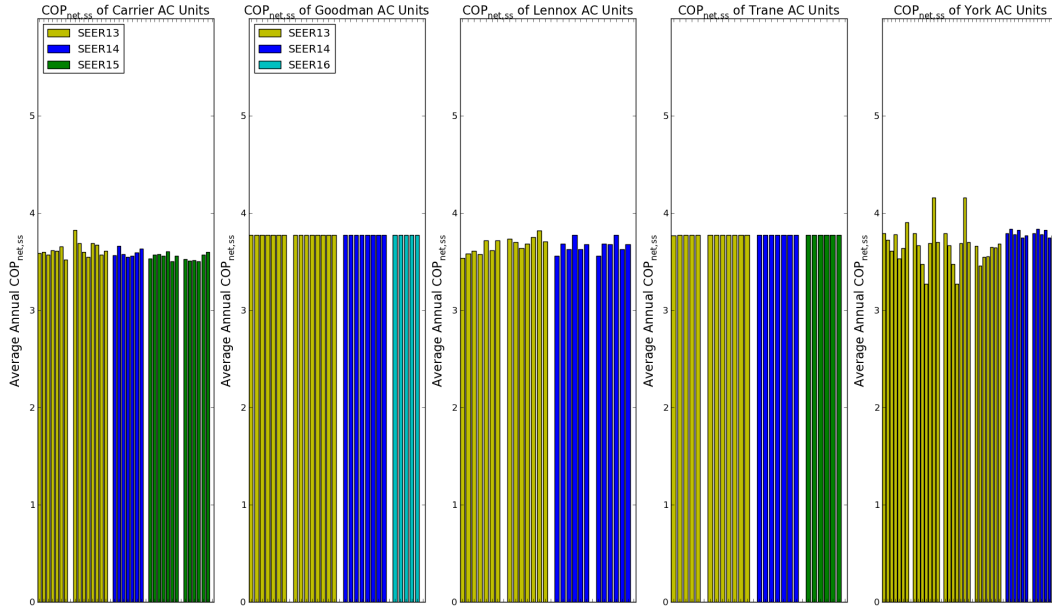


Figure 8.5: Variation due to flow fraction curves (350CFM/Ton)

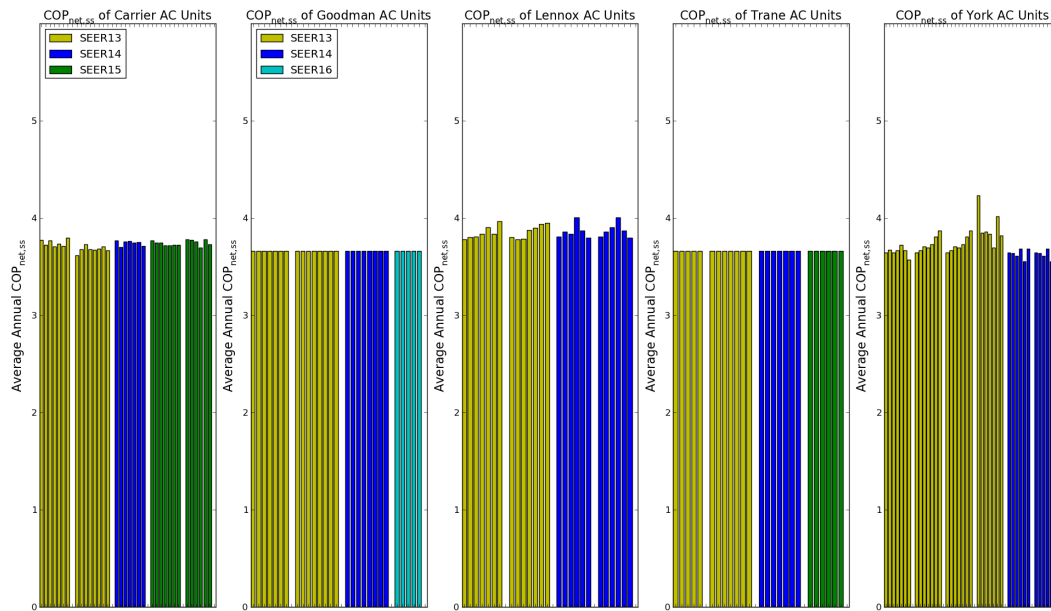


Figure 8.6: Variation due to flow fraction curves (450CFM/Ton)

It is worth noting that the temperature curves were again responsible for only a limited amount of variation in the results. The flow fraction curves showed limited variation as well (though slightly more than in air conditioners). It is clear to see that the Goodman and Trane units did not provide data for flow fraction curves (data not available for various CFM/Ton values). Though there was not a lot of variation due to the flow fraction curves, they definitely inform the model and one can see the change in $\overline{COP}_{net,ss,h}$ due to the different flow rates (8.5, versus 8.6). Without a set of flow fraction curves this could not be captured.

The overall lack of consistency in reported data, and the relatively low impact of the curve inputs indicated that representative curves would again be extremely beneficial in providing consistent, accurate modeling practices. Representative curves were selected by following the same procedures outlined in section 6.6. For heat pumps it was even more clear that a single set of curves (across all manufacturers) was beneficial. Carrier curves were thought to be the most complete and consistent of all manufacturers, providing biquadratic temperature curves and flow fraction curves.

8.2 Rated Values

Rated values were more difficult to verify for heat pumps. This was due to both the complexity of the HSPF calculation procedure and lack of available data. For details on the HSPF calculation, refer to appendix B. To calculate the HSPF for a given unit, the H2 test is required for single speed and both the H2₁ and H2₂ tests are required for two speed. All of the H2 tests are performed at an outdoor dry bulb of 35°F and require a defrost cycle during the test period. These tests therefore report “integrated” capacity and power. Integrated capacity and integrated power include the effects of defrost. As discussed in section 2.3.4, the capacity will decrease significantly during a defrost cycle due to both the off-time of unit and the preceding frost buildup. This is commonly known as the “defrost knee”. This can be seen visually in figure 8.7 where the integrated capacity sags right around 35°F. This figure was extracted from Carrier’s expanded performance document on their 25HBB5 heat pump. Integrated power does not change significantly during defrost due to the fact that the compressor still is required to run (albeit in reverse). The low outdoor temperature allows the compressor to run more efficiently during reverse cycle defrost, thus lowering the electric consumption slightly. The limited power reduction associated with the switch from total to integrated power was confirmed by evaluation of the data provided by Rheem. Power decreases in the order of 2-6% were listed in the Rheem data.

Of all the manufacturers evaluated during this research only Carrier provided data on the integrated capacity, and none of the manufacturers provided data on the integrated power (though it is assumed that this will differ only slightly).

Lack of integrated data makes it impossible to calculate an HSPF ($HSPF_{CALC}$, comparable to the $SEER_{CALC}$ used in the section 7.2), making comparison between the HSPF listed by AHRI ($HSPF_{AHRI}$) and the rated values from the database impossible. The Carrier data was the only data that provided the capability of comparison between $HSPF_{CALC}$ and $HSPF_{AHRI}$. Even this comparison was not perfect due to the lack of integrated power data from Carrier.

$HSPF_{CALC}$ was computed for all of the Carrier units. The single stage HSPF calculation was used for the single stage units and the two stage calculation for the two stage units. When following the HSPF

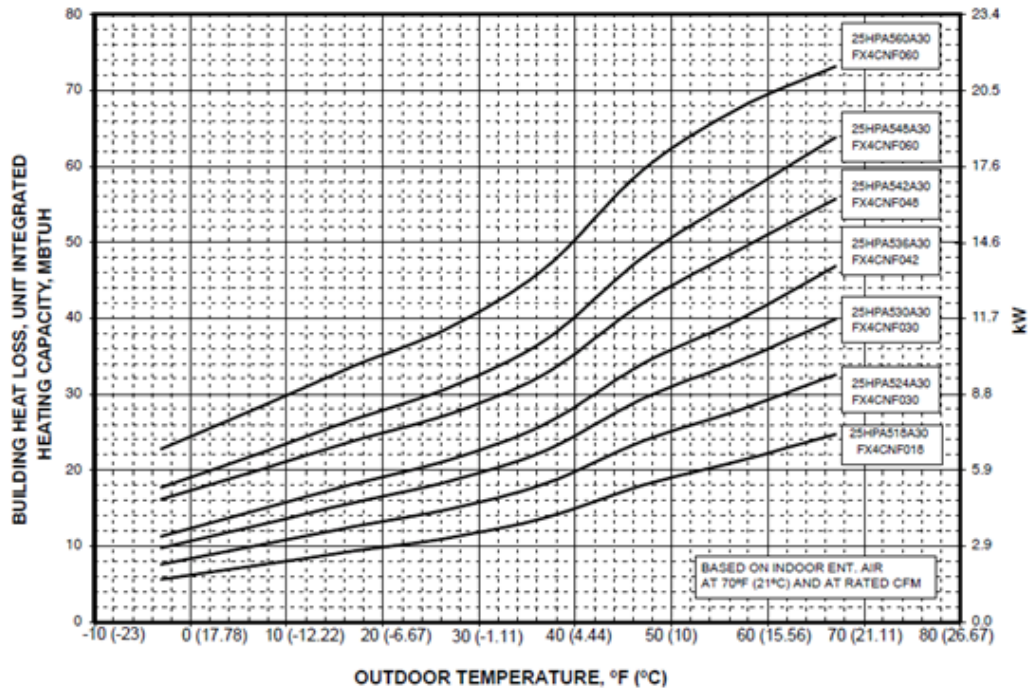


Figure 8.7: Graph depicting integrated capacity as a function of outdoor dry bulb [3]

calculation procedures, the different rating points were calculated by using the curves generated from the expanded performance tables (just as was done for the SEER calculations, section 7.2). Due to quality of fit achieved with the regressions, this essentially amounts to interpolating in the expanded performance tables. The AHRI database was then queried to gather the HSPF reported for the same indoor/outdoor combination. The comparison between $HSPF_{CALC}$ and $HSPF_{AHRI}$ is shown in figure 8.8. The annual simulation results for those same units is shown in 8.9. Similar to the air conditioner results, it can be noted that the trends in the $\overline{COP}_{net,ss,h}$ generally mimic the trend in $HSPF_{CALC}$ values. This indicates that appropriate rated values would result in more accurate simulation results. If the AHRI rating points were used, the simulation results would follow the $HSPF_{AHRI}$ line in figure 8.8 more closely. This would provide a clearer distinction between the relative efficiencies and would more closely replicate the values generated by the regulated testing results of AHRI.

In figure 8.8, the assumed C_d value was varied from 0.15 in the “Calc” series to the bounding values of 0.01 and 0.25. These results are shown in the dashed gray lines and represent a bounding of the potential

error in the C_d assumption.

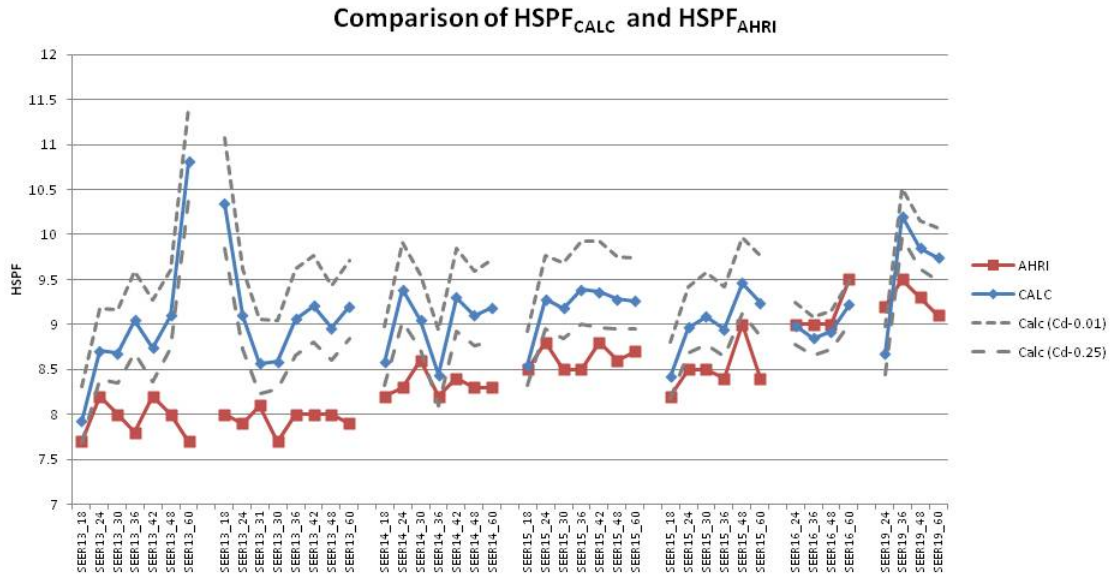


Figure 8.8: Comparison of $HSPF_{CALC}$ and $HSPF_{AHRI}$

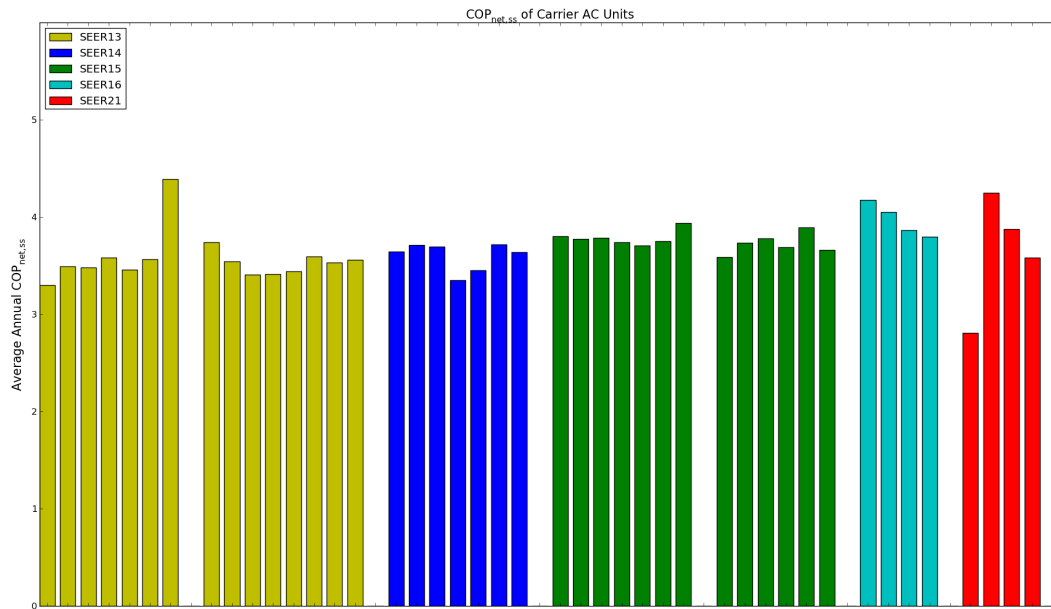


Figure 8.9: Simulation results for the matching Carrier units

It seems that the rated values from the database are generally over calculating the HSPF of the units. They are also generating more constant HSPFs, especially across all of the single stage units. It would improve the modeling of heat pump heating mode calculations if there was better available data on the values for the 17, 35, 47, and 62 rating tests.

The only other way of evaluating the rated values in the database was through COP values listed by certain manufacturers (Carrier, Trane, and York) in the AHRI results sections of their expanded performance tables. Most manufacturers include AHRI results for various mix and match along with the expanded performance tables. The three manufacturers listed above included COP_{47} and COP_{17} along with the HSPF values. These values were compared directly with the COP_{47} and COP_{17} from the database (similar to the A test comparisons in chapter 7). The results of the comparison for COP_{47} is shown in figure 8.10 and for COP_{17} in figure 8.11.

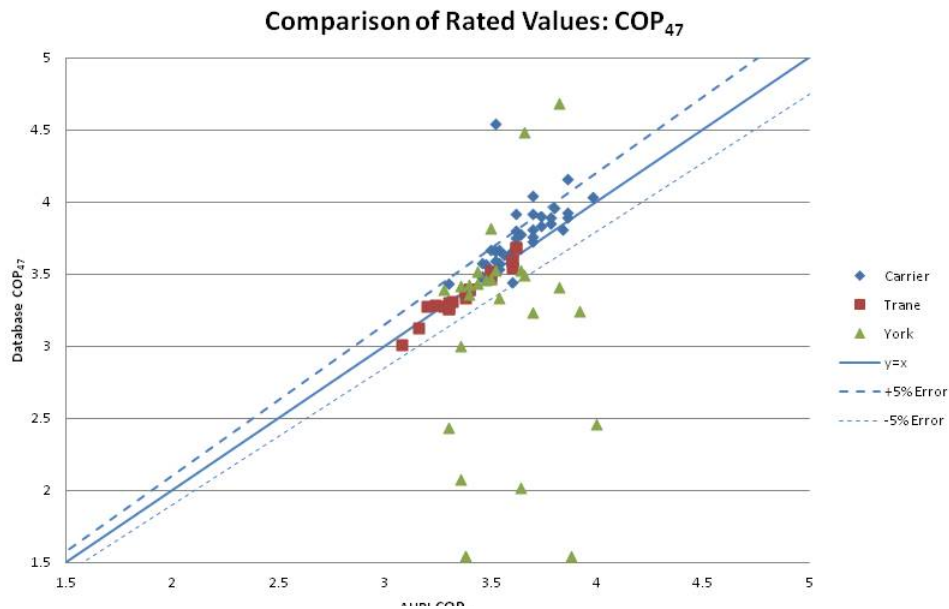


Figure 8.10: Comparison of AHRI and Database COP_{47} values

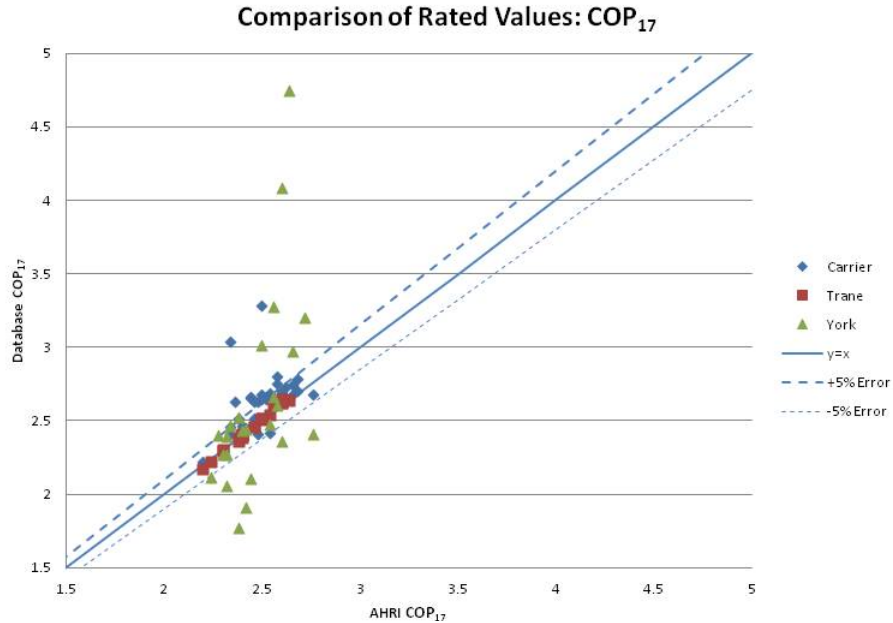


Figure 8.11: Comparison of AHRI and Database COP₁₇ values

The wide scatter of the York COP values shown in these figures clearly accounts for the wide variability that can be seen in figure 8.1. The other manufacturers with available data on the COP values showed better agreement, though there was still some scatter in the data.

8.3 Conclusions From Heat Pumps

This chapter discussed the significant issues dealt with during the evaluation of the heat pumps inputs that were generated from the expanded performance database. Inputs were generated for ≈ 200 heat pumps units. These units were all simulated in a single building. The results of these initial simulations showed significant variation, similar to that discussed in the air conditioner discussion. This led to both a sensitivity study with the curve inputs and an investigation of the rated values and the accuracy of the simulations with regards to HSPF ratings.

There was less complete data sets for the heat pumps than there was for the air conditioners. This helped direct the selection of the representative curves for heat pump heating mode. Overall the modeling of heat pumps will be significantly improved by using these representative curves along with rated values

that generate the HSPF that is desired to be modeled.

Chapter 9

Conclusions and Future Work

9.1 Conclusions

The aim of this research was to provide improved energy prediction of air conditioners and heat pumps by using annual simulation tools. It is thought that with more accurate predictions of split system energy use (across different climates, building, and units) it will be possible to better evaluate policy decisions on efficiency improvements or code upgrades.

This research began by evaluating the simulation engines EnergyPlus and DOE-2 and their algorithms and required inputs. This was accompanied by a survey of the available data on air conditioner and heat pump performance. Once it was determined that the manufacturers' expanded performance tables were the best fit for informing the model inputs, an effort was undertaken to compile the expanded performance tables into a usable format. This effort resulted in a SQLite database that contained ≈ 450 units and was able to be queried in such a manner as to generate all of the necessary model inputs for every one of those 450 units.

The initial annual simulation results using all of the unit specific inputs were not as consistent as was hoped. There were large differences between different units and between different manufacturers. These differences were: wide ranges of predicted efficiency for a single SEER value (both within a single manufacturer and between manufacturers), and significant SEER overlap (lower SEER levels with higher predicted efficiencies than higher SEER units). These inconsistencies prompted analysis of the data that was used for the model inputs as well as analysis of the sensitivity of the models to the different inputs.

The data analysis was carried out through: visual inspection, calculation of exiting conditions and

bypass factors, comparison between calculated bypass factor and the theory of constant bypass factor (as used in the EnergyPlus model), and visualization of the curve inputs and comparison between the different curves. The results of the data evaluation showed significant inconsistencies between the way in which different manufacturers were producing their expanded performance tables. This indicates differences in the in-house models used in table generation. Without actual knowledge of the models being used it is difficult to say which manufacturer is providing the most accurate data. Yet the results of this section of the research raised some concern over the consistency of the data and its applicability to annual simulation inputs.

The data analysis was complemented by a sensitivity study on the curve-fit inputs that are required by the simulation engines. This sensitivity study looked at the variation in predicted efficiency ($\overline{COP}_{net,ss}$) due to introduction of the various curve inputs: one at a time, and in conjunction with one another. This study showed very low sensitivity to the curve inputs in general. It was important to have the inputs, but the specific curves did not have a large impact in predicted efficiency. The impact of fixing the curves was tested by running simulations in Houston, Phoenix, Atlanta and Chicago and at three different fan speeds. The results supported the initial observations that the impact of individual curves was limited (average error of $\approx 2 - 5\%$). This finding was further upheld through evaluation of uncertainty in the AHRI testing data that the expanded performance tables are supposed to expand upon. It was noted that AHRI allows $\pm 5\%$ difference between testing results and the reported efficiency and capacity values. The fact that the average error due to fixed curves was $< 5\%$ in all but one of the tested cases (one manufacturer in one location for single stage units), demonstrates that additional error is very rarely introduced by utilizing the standard curves. Based on this analysis, representative curves were selected and used for each of the individual units. This result had large benefits in that it reduced the complexity of the inputs needed to inform the model; with a representative set of curves users are left with inputs that are more commonly encountered and are more easily calculated (e.g. COP, SHR, flow rate).

The final piece of analysis was an evaluation of the rated values generated from the database and their impact on the annual simulation results. It was clear from the curve sensitivity study that the rated values were driving the large portion of the variation and inconsistency that was seen in the initial simulations. It was therefore necessary to evaluate the quality of the rated values that were being generated from the

database. This was accomplished through comparison with AHRI data. The AHRI data is based on well-regulated testing procedures and is the most consistent data source available. Comparisons were made between AHRI data and the database values by looking at: reported rating points, calculated C_d values, and comparing calculated SEER to the AHRI SEER. These comparisons showed significant differences between the AHRI data and the values in the database. This was concerning due to the fact that these inputs are the most important and influential of all of the simulation engine inputs. This issue could be solved in two different ways: full reporting by AHRI of all required test results, or improved agreement between manufacturer's data and AHRI data.

For current modeling work it is suggested to use the curve fits selected as a result of the sensitivity study (see 6.6) in combination with rated values that produce the SEER or HSPF of the unit that is being modeled. It has been shown that this will both reduce the complexity of the model inputs and increase the agreement with the SEER and HSPF rating procedures.

The research presented here has shown the importance of accuracy in these simulation inputs for accurate representation of current equipment. It has also shown the current shortcomings in data consistency and completeness. It is envisioned that this work can inform future efforts on improved reporting by both manufacturers and AHRI.

This research was disseminated to the manufacturers through a webinar organized by the author and other members of the residential buildings group at NREL. The webinar presented the findings reported here to representatives from: Trane, Carrier, York, Rheem, Lennox, and AHRI. These companies represent 71% of the marketplace as of 2008 as well as the governing body for all certification procedures. There was very positive responses from the attendees and an interest in improved reporting for simulation purposes. ASHRAE has also formed a subcommittee (SPC 205) that is focused on improving HVAC reporting for simulation tools. It was also noted during the webinar that AHRI has recently convened a committee focusing on manufacturer reporting procedures and it was suggested that this thesis be used in informing that committee.

Ideally, the efforts made through the manufacturers webinar, ASHRAE subcommittee SPC 205, and the AHRI committee will gain traction and improve residential HCAV reporting. This work has the potential

to inform this process and facilitate development of accurate and consistent residential HVAC performance reporting.

9.2 Future Work

The most important future work regarding air conditioner and heat pump simulation revolves around improved reporting standards. These standards need to be defined and required by the manufacturers. As mentioned above, this work is already underway with the ASHRAE and AHRI committees and it is hoped that this research will help inform those standards.

Two interesting issues that surfaced during the manufacturers webinar (discussed above) were fan efficiency and C_d values. These are two components of air conditioner and heat pump performance that did not receive complete treatment in this research. This was due to limited data on both of these items; neither value is reported by AHRI or the manufacturers. For this research part load performance was estimated using a physical model discussed in section 2.4. The fan efficiency was assumed to be the default value from AHRI 210/240 of 365 W/ 1000 CFM. This value is what is assumed to be the fan power consumption if the outdoor unit is tested without an indoor fan. It is probable that many of the higher efficiency units utilize more efficient indoor fans to increase their SEER or HSPF ratings (these ratings are calculated with net capacities and efficiencies). Evaluation of the Rheem data provided indicated that this was the case for their high efficiency units. Both the Watts/CFM of the fan and the C_d of the unit play a role in the calculation of the SEER and HSPF for the unit. If better data becomes available regarding these two values it would be very beneficial to investigate any trends that exist for these values. Improved knowledge of these two components could also resolve some of the apparent discrepancies between $SEER_{CALC}$ and $SEER_{AHRI}$ discussed in chapter 7 (and between $HSPF_{CALC}$ and $HSPF_{AHRI}$, discussed in 8.2).

It was also noted that some of the two stage air conditioners and heat pumps showed significant variation with different curve inputs (see section 6.7). This was different from the extremely consistent single speed units. For this research it was recommended to utilize a single set of curves for all two stage units. This was due to lack of reliability in the manufacturer data and a desired consistency in modeling approach. It was considered more beneficial to reduce input complexity and potential error introduction by

means of selecting a single set of curves, yet it is possible that there are actual physical differences being captured by the variation in the curve forms. It would be beneficial to investigate more deeply the physical characteristics of the high efficiency units and determine if the higher degree of variability shown in the curve inputs is warranted or not.

During this thesis work it was not possible to incorporate metered data into the research effort. The testing based SEER and HSPF values were used as a surrogate for full annual metered data for the evaluation of rated values. The modeling methods suggested here provide the capability for good agreement between annual simulation results and the listed SEER and HSPF values. A significant research contribution would be evaluating the correlation between SEER/HSPF values and annual energy use, by collecting actual metered data. This correlation has been evaluated by comparing simulation results and SEER values ([5] and [12]), yet those simulation results were based on the manufacturers' data. This data has been shown here to not correlate very well with the SEER and HSPF ratings. Therefore it would be beneficial to verify the connection between SEER/HSPF and annual energy use through a different method: metered data. If this connection was established, the modeling methodology provided here could be used with even more confidence.

Finally, research into modeling of variable speed compressors would be beneficial to expand the simulation engine capabilities to cover mini-split systems and fully variable speed drives. These systems are becoming more common, and present potentially significant energy reduction measures. Modeling of a variable speed drive is currently achieved in EnergyPlus by modeling four different stages and interpolating between the stages. This does not actually represent the process of a variable speed drive. It would be helpful to quantify the degree of accuracy achievable through the current modeling capabilities and if necessary propose an alternative model for fully variable speed systems. This model could be used to model mini-split systems as well.

Bibliography

- [1] ANSI/AHRI. 2008 standard for performance rating of unitary air-conditioning & air-source heat pump equipment. Technical report, AHRI, Arlington, Virginia, 2008.
- [2] M. Brandemuehl and M. Wassmer. Ashrae 1197-rp: Updated energy calculation models for residential hvac equipment. Technical report, ASHRAE, Atlanta, Georgia, 2009.
- [3] Carrier. Product data - 25hbb5 heat pump. Technical report, 2009. URL http://www.commercial.carrier.com/commercial/hvac/product_technical_literature/1,3069,CLI11_DIV12_ETI4906_MID157_PRD1752,00.html.
- [4] T. Chapp. Expansion valves and ammonia in direct expansion systems. (May), 2011. URL <http://www.danfoss.com/NR/rdonlyres/1444CC08-FFD3-44B4-9101-87A2D306271D/0/DXInstallation.pdf>.
- [5] A. Courtney. Assessing the Effectiveness of SEER as a Predictor of Seasonal Cooling Efficiency. Master's thesis, University of Colorado, 2006.
- [6] Energy Information Administration. 2009 Building Energy Data Book. 2009. URL <http://buildingsdatabook.eere.energy.gov>.
- [7] P. Fairey, D. Parker, B. Wilcox, and M. Lombardi. Climatic impacts on heating seasonal performance factor (hspf) and seasonal energy efficiency ratio (seer) for air-source heat pumps. ASHRAE Transactions, 110(2):178–188, 2004.
- [8] Hugh I. Henderson and Kannan Rengarajan. Model to predict the latent capacity of air conditioners and heat pumps at part-load conditions with constant fan operation. ASHRAE Transactions, 102(1): 266 – 274, 1996. ISSN 00012505.
- [9] Hugh I Henderson, Danny Parker, Florida Solar, and Yu J Huang. Improving doe-2 s resys routine : User defined functions to provide more accurate part load energy use and humidity predictions part load efficiency degradation for cycling equipment. ACEEE Summer Study on Energy Efficiency, pages 113–124, 2000.
- [10] John Hill. personal communication, 2011.
- [11] James J. Hirsch & Associates. Deer residential seer-rated units performance maps. Technical report, Southern California Edison, Irwindale, California, 2005.
- [12] James J. Hirsch & Associates. Eer & seer as predictors of residential seasonal cooling performance. Technical report, Southern California Edison, Irwindale, California, 2005.
- [13] S. Kavanaugh. Limitations of seer for measuring efficiency. ASHRAE Journal, (July):27–29, 2002.
- [14] Ueno Kohta. ECM Efficiency. Home Energy, May/June, 2010. URL homeenergy.org.

- [15] N Kruis. Reconciling differences between residential dx cooling models in doe-2 and energyplus. In Proceedings of IBPSAUSA SimBuild 2010, 2010.
- [16] M. Moran and H. Shapiro. Fundamentals of Engineering Thermodynamics. John Wiley and Sons, 2008.
- [17] US Department of Energy. Energyplus engineering reference. Technical report, 2009.
- [18] Walter Parken, George Kelly, and Robert Beausoliel. Factors Affecting the Performance of a Residential Air-To-Air Heat Pump. ASHRAE Transactions, 83(1):839–849, 1977.
- [19] C K Rice. THE ORNL MODULATING HEAT PUMP DESIGN TOOL MARK IV USER S GUIDE. ISBN 1800553684.
- [20] Iain Walker. Blower Energy Use. URL http://apps1.eere.energy.gov/buildings/publications/pdfs/building_america/ns/b20_blower_energy.pdf.
- [21] M. Wassmer. A Component-Based Model for Residential Air Conditioner and Heat Pump Energy Calculations. Master’s thesis, University of Colorado, 2003.
- [22] Bruce Wilcox, Ken Nittler, Jonh Proctor, and Rick Chitwood. Furnace Fan Watt Draw and Air Flow in Cooling and Air Distribution Modes. Technical report, California Building Energy Efficiency Standards, 2008.
- [23] D. York and C. Cappiello. Doe-2 engineer’s manual: Version 2.1 a. Technical report, Lawrence Berkeley Lab., CA (United States); Hirsch (James J.) and Associates, Camarillo, CA (United States), 1981. URL http://www.osti.gov/energycitations/product.biblio.jsp?osti_id=10147851.

Appendix A

Example Python Script

This appendix includes an example Python script to demonstrate the methods used for extracting the expanded performance tables from the text version of the expanded performance data files. It is important to note that the indent in Python scripting indicates which level of a “loop” or “if” statement that the code is in. This is very different from most programming languages where the loops are terminated by an “end loop” statement (or something of that nature). In Python it is simply a decreased indent that indicates the end of a code structure. One other important aspect of Python’s code structure is the presence of dictionaries as a data structure. Dictionaries are similar to arrays. The difference between them is that arrays are referenced by numerical indices whereas dictionaries are indexed by “keys”. These keys are assigned as the dictionary is being created and they allow one to reference the data in the dictionary by calling the name of the dictionary followed by the key in brackets. Nested dictionaries were used extensively to store different types of performance data about a specific unit within a large dictionary of all models for a given manufacturer. For example one could call `Carrier[ABB_SEER13_18][SHR]` and retrieve the sensible heat ratio for that specific model/capacity from Carrier.

All of the different parsing scripts that were written utilized slightly different methods to extract the necessary data, but the general approach was similar across all. The general approach adopted is outlined below:

- (1) Open the text file and read all of the lines into a list
- (2) Use a “for” loop to go through the list of lines and find certain key phrases or tokens that indicated

the beginning of an expanded performance table

- (3) Model names (indoor and outdoor) were usually found using regular expressions
- (4) Once the expanded table for a certain model was located the data in the table would be looped through and written into a dictionary
- (5) All of the individual dictionaries were placed in a larger dictionary, keyed by unit name and capacity
- (6) Finally, the dictionary keys were looped through and the data was written into comma separated files.

The file below is the data extractor that was written for the Goodman air conditioners. Code for other manufacturers or for SQLite database creation can be requested by contacting the author.

```

'''
Created on Feb 25, 2011

@author: dcutler
'''

from __future__ import division
from util import Psychrometrics
import units
import re

main_dir = "..\..\..\Data\HVAC\Goodman Data\AC units\"
filenames = [main_dir+'SS-SSX14.txt', main_dir+'....']

#Parse data, populate output list
for filename in filenames:

    model_list = []
    outdoor_list = []
    counter = -1

```



```

f = open(filename , 'r')
full_dict = {}
outputdict_low = {}
outputdict_high = {}
outputdict_single = {}
flines = f.readlines()
CFM_list = []
for linenum, fline in enumerate(flines):
    ODBrow = [65,75,85,95,105,115]
    EWBrow = [59,63,67,71]
    # Split line into data by comma
    fdatas = fline.split()
    if fdatas[0] == 'MBh':
        #find model number and capacity
        if flines[linenum-7].split()[1] == "Cooling":
            modelline = flines[linenum-7]
            print modelline
            matchobj = re.match(
                '[a-zA-z\x97\s]*\s(.*\s*)\s*[\s]*', modelline)
            indoor_outdoor = matchobj.group(1)
            modelobj = re.match('([a-zA-Z0-9\s]*).*', indoor_outdoor)
            model = modelobj.group(1)
            print model
            if indoor_outdoor not in model_list:
                model_list.append(indoor_outdoor)
                outdoor_list.append(model)
        elif len(flines[linenum+50].split())>1:
            if flines[linenum+50].split()[1] == "Cooling":
                modelline = flines[linenum+50]

```

```

print modelline
matchobj = re.match(
    '[a-zA-z\x97\s]*\s(.*\s*)\*[.\s]*', modelline)
indoor_outdoor = matchobj.group(1)
modelobj = re.match('([a-zA-Z0-9\s]*).*', indoor_outdoor)
model = modelobj.group(1)
print (model, indoor_outdoor[len(model):])
if indoor_outdoor not in model_list:
    model_list.append(indoor_outdoor)
    outdoor_list.append(model)
else:
    None
counter = counter + 1
#check for 2-stage and store as "stage"
if 'D' in filename[-20:]:
    if float(counter/24) in range(30):
        outputdict_low = {}
        outputdict_high = {}
    if (counter//12)%2 == 0:
        stage = 'low'
    else:
        stage = 'high'
else:
    if float(counter/12) in range(30):
        outputdict_single = {}
    stage = 'single'
Totalrow = flines[linenum]
totals = Totalrow.split()
SHRow = flines[linenum+1]

```

```

SHRs = SHRow.split()

kwrow = flines[linenum+3]

kws = kwrow.split()

if len(flines[linenum-2])==3:
    edb = flines[linenum-2]
    EDB = edb.strip()

elif len(flines[linenum-10])==3:
    edb = flines[linenum-10]
    EDB = edb.strip()

elif len(flines[linenum-18])==3:
    edb = flines[linenum-18]
    EDB = edb.strip()

cfm = flines[linenum-1]

CFM = cfm.strip()

if CFM not in CFM_list:
    CFM_list.append(CFM)

else:
    None

for m in range(4):          #cycle through EWB
    for n in range(6):      #cycle through ODB
        if float(EWBrow[m])>float(EDB):
            None
        else:
            total_net = str(float(totals[4*n+1+m]))
            total = str(float(totals[4*n+1+m])+
                float(CFM)*1.2454/1000)
            SHR = SHRs[4*n+1+m]
            sens = float(totals[4*n+1+m])*float(SHR)

```

```

sens_new = sens + float(CFM)*1.2454/1000
SHR_new = sens_new/float(total)
kw = kws[4*n+1+m]
key = CFM + "-" + str(EWBrow[m]) + "-" + EDB
+ "-" + str(ODBrow[n])
try:
    db_ADP = Psychrometrics.T_adp(float(EDB),
    float(EWBrow[m]), float(CFM), sens_new,
    float(total))
    ldb = Psychrometrics.T_ldb(float(EDB),
    float(EWBrow[m]), float(CFM), sens_new,
    float(total))
    BF = (ldb-db_ADP)/(float(EDB)-db_ADP)
except ValueError:
    BF = 'Error'
if stage == 'low':
    outputdict_low[key] = {'total':total_net,
    'SHR':SHR, 'kw':kw, 'BF':BF}
elif stage == 'high':
    outputdict_high[key] = {'total':total_net,
    'SHR':SHR, 'kw':kw, 'BF':BF}
else:
    outputdict_single[key] = {'total':total_net,
    'SHR':SHR, 'kw':kw, 'BF':BF}
full_dict[indoor_outdoor] = {'low':outputdict_low,
    'high':outputdict_high, 'single':outputdict_single}

f.close()

#Full data dump

```



```
        , float ( full_dict [g][h][key][ 'kW' ])
        , full_dict [g][h][key][ 'BF' ]
    datas . append ( data )

f . write ( 'Model , Indoor , Stage , EDB , CFM , ODB , EWB , Total , SHR , kW , BF ' )
f . write ( "\n" )

for records in datas :
    record = str ( records ) [ 1 : - 1 ]
    f . write ( record )
    f . write ( "\n" )

f . close ( )
```

Appendix B

SEER and HSPF calculations

B.1 SEER Calculation Procedures

B.1.1 Single Stage Units

The calculation of the SEER value for single speed air conditioners is a simple, one-line equation:

$$SEER = PLF(0.5) * EER_B \quad (B.1)$$

Where

- $PLF(0.5) = (1 - 0.5 * C_d)$
- $SEER$ is the annual efficiency metric in Btu/h/W
- EER_B is the efficiency at the B rating point (82/80/67) in Btu/h/W
- C_d is the degradation coefficient of the unit

C_d is defined as:

$$C_d = \frac{1 - \frac{EER_{cyc,dry}}{EER_{ss,dry}}}{1 - CLF} \quad (B.2)$$

Where

- $CLF = \frac{\dot{Q}_{cyc,dry}}{\dot{Q}_{ss,dry} * \Delta\tau_{cyc,dry}}$
- $\Delta\tau_{cyc,dry}$ is the full on/off cycle time in hours.

This calculation contains several assumptions that are worth noting. First is the fact that the SEER value is calculated on the single outdoor dry bulb temperature of 82°F. It is also clear from (B.1) that the rating process assumes a part load factor (PLF) of 0.5 at 82°F. These two assumptions taken together imply that the SEER rating procedure assumes that 82°F is the average operating point for the entire cooling season and that the air conditioner or heat pump experience a PLF of 0.5 at those conditions

One other aspect of the rating procedure that is worth noting is the indoor conditions at which the units are tested. All cooling tests are performed at 80°F indoor dry bulb and 67°F indoor wet bulb. This essentially assumes that the cooling set point is 80°F which is significantly higher than most people keep their thermostats in the summertime. This should not effect the relative rating of units, but it does lead to higher steady state efficiencies than would actually be encountered under more realistic operating conditions.

B.1.2 Two Stage Units

The two stage SEER calculation is very different than the single speed calculation outlined above. The first significant difference is that it uses a temperature binning to describe the climatic temperature distribution (see figure B.1). There are eight different bins with each bin containing 5°F: 67, 72, 77, 82, 87, 92, 97, 102. The bins are referenced as $j = 1, \dots, 8$.

Bin Number, j	Bin Temperature Range °F	Representative Temperature for bin °F	Fraction of Total Temperature Bin Hours, N_j/N
1	65-69	67	0.214
2	70-74	72	0.231
3	75-79	77	0.216
4	80-84	82	0.161
5	85-89	87	0.104
6	90-94	92	0.052
7	95-99	97	0.018
8	100-104	102	0.004

Figure B.1: Binning for SEER rating procedure

The SEER process defines a building load term ($BL(T_j)$) that defines the load the unit is required to

meet as a function of temperature, defined as:

$$BL(T_j) = \frac{(T_j - 65)}{95 - 65} * \frac{\dot{Q}^{k=2}(95)}{1.1} \quad (\text{B.3})$$

Where 1.1 is a sizing factor and $\dot{Q}^{k=2}(95)$ is the capacity at the A₂ test. It can be seen that 95°F is the defined as the design temperature for the SEER process and 65°F is the balance temperature (or zero load temperature). When T_j (the bin temperature) is equal to 65°F the equation evaluates to 0, implying zero load. When T_j equals 95°F the load is equal to the capacity of the unit indicating that this was the temperature designed for at full capacity.

This building load is used to weight the contribution of every temperature bin. This is to indicate the higher demand on the air conditioner unit at higher temperatures, even though there may be more total hours spent at lower temperatures. The combination of building load weighting and bin weighting is shown in figure B.2.

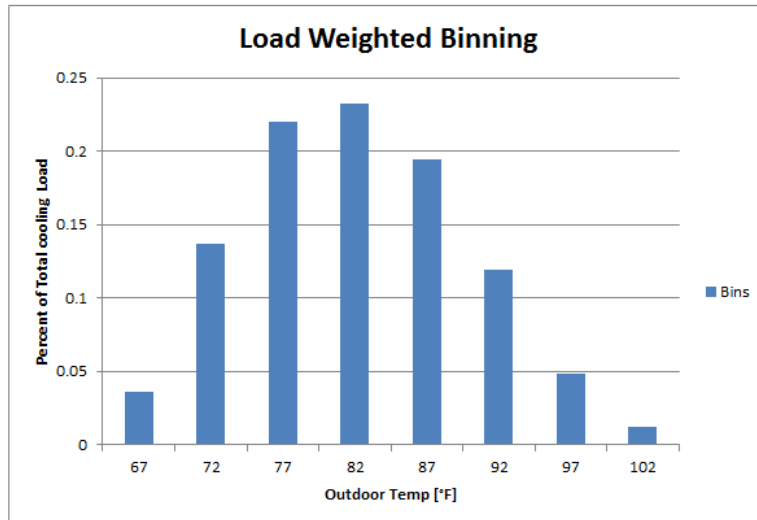


Figure B.2: Hourly weighted load profile for SEER

It can be noted that even though the climate described by the bins in figure B.1 has the highest fractional hours in the 72°F bin, the load is centered at 82°F. This is the same as in the single speed SEER procedure. Both the most common temperature bin and the center of the load distribution are at relatively cool temperatures. This generally skews the efficiencies to higher values than would actually be seen in

hotter climates such as Houston or Phoenix.

The actual two stage SEER value is calculated as:

$$SEER = \frac{\sum_{j=1}^8 q_c(T_j)}{\sum_{j=1}^8 e_c(T_j)} = \frac{\sum_{j=1}^8 \frac{q_c(T_j)}{N}}{\sum_{j=1}^8 \frac{e_c(T_j)}{N}} \quad (\text{B.4})$$

The calculation of the respective terms in (B.4) requires preliminary calculations of the capacity and power consumption at high speed ($\dot{Q}^{k=2}(T_j)$ and $\dot{E}^{k=2}(T_j)$ respectively) and low speed ($\dot{Q}^{k=1}(T_j)$ and $\dot{E}^{k=1}(T_j)$). These calculations are defined below: High Speed:

$$\dot{Q}^{k=2}(T_j) = \dot{Q}^{k=2}(82) + \frac{\dot{Q}^{k=2}(95) - \dot{Q}^{k=2}(82)}{95 - 82} * (T_j - 82) \quad (\text{B.5})$$

$$\dot{E}^{k=2}(T_j) = \dot{E}^{k=2}(95) + \frac{\dot{E}^{k=2}(95) - \dot{E}^{k=2}(82)}{95 - 82} * (T_j - 82) \quad (\text{B.6})$$

Low Speed:

$$\dot{Q}^{k=1}(T_j) = \dot{Q}^{k=1}(67) + \frac{\dot{Q}^{k=1}(82) - \dot{Q}^{k=1}(67)}{82 - 67} * (T_j - 67) \quad (\text{B.7})$$

$$\dot{E}^{k=1}(T_j) = \dot{E}^{k=1}(67) + \frac{\dot{E}^{k=1}(82) - \dot{E}^{k=1}(67)}{82 - 67} * (T_j - 67) \quad (\text{B.8})$$

Where $\dot{Q}^{k=2}(95)$, $\dot{Q}^{k=2}(82)$, $\dot{Q}^{k=1}(82)$, $\dot{Q}^{k=1}(67)$ are the A_2, B_2, B_1 , and F_1 capacity results (the E values correspond to the power consumption values for the same tests).

To define the actual power consumption and capacity, AHRI outlines three different regions of operation:

- (1) Low speed capacity is greater than the building load: $\dot{Q}^{k=1}(T_j) \geq BL(T_j)$ (cycling)
- (2) Building load falls between the high and the low capacity: $\dot{Q}^{k=1}(T_j) \leq BL(T_j) \leq \dot{Q}^{k=2}(T_j)$ (between speeds)
- (3) Building load is greater than high capacity: $BL(T_j) \leq \dot{Q}^{k=2}(T_j)$ (always on)

At each temperature, the building load is calculated and compared to the high and low speed capacities as outlined above. Once the appropriate mode of operation has been selected, $\frac{q_c(T_j)}{N}$ and $\frac{e_c(T_j)}{N}$ are calculated. The mode-of-operation specific methods for calculating $\frac{q_c(T_j)}{N}$ and $\frac{e_c(T_j)}{N}$ are defined below. Then $\frac{q_c(T_j)}{N}$ and $\frac{e_c(T_j)}{N}$ are each summed and SEER can be calculated using (B.4).

1) - Cycling

$$\frac{q_c(T_j)}{N} = X^{k=1}(T_j) * \dot{Q}^{k=1}(T_j) * \frac{n_j}{N} \quad (\text{B.9})$$

$$\frac{e_c(T_j)}{N} = \frac{X^{k=1}(T_j) * \dot{E}^{k=1}(T_j)}{PLF_j} * \frac{n_j}{N} \quad (\text{B.10})$$

Where:

$$X^{k=1}(T_j) = \frac{BL(T_j)}{\dot{Q}^{k=1}(T_j)} \quad (\text{B.11})$$

$$PLF_j = 1 - C_D(1 - X^{k=1}(T_j)) \quad (\text{B.12})$$

and n_j/N are the fractional bin hours defined in B.1.

2)- Between Speeds

$$\frac{q_c(T_j)}{N} = [X^{k=1}(T_j) * \dot{Q}^{k=1}(T_j) + X^{k=2}(T_j) * \dot{Q}^{k=2}(T_j)] * \frac{n_j}{N} \quad (\text{B.13})$$

$$\frac{e_c(T_j)}{N} = [X^{k=1}(T_j) * \dot{E}^{k=1}(T_j) + X^{k=2}(T_j) * \dot{E}^{k=2}(T_j)] * \frac{n_j}{N} \quad (\text{B.14})$$

Where:

$$X^{k=1}(T_j) = \frac{\dot{Q}^{k=2}(T_j) - BL(T_j)}{\dot{Q}^{k=2}(T_j) - \dot{Q}^{k=1}(T_j)} \quad (\text{B.15})$$

3) - Always On

$$\frac{q_c(T_j)}{N} = \dot{Q}^{k=2}(T_j) * \frac{n_j}{N} \quad (\text{B.16})$$

$$\frac{e_c(T_j)}{N} = \dot{E}^{k=2}(T_j) * \frac{n_j}{N} \quad (\text{B.17})$$

The $\frac{q_c(T_j)}{N}$ and $\frac{e_c(T_j)}{N}$ for each appropriate temperature (and building load) can now be summed and equation (B.4) can be used to calculate the two stage SEER value.

B.2 HSPF Calculation Procedures

B.2.1 Single Stage Units

The HSPF calculation procedure for single speed units is much more complicated than the SEER calculation. One significant difference between HSPF and SEER for single, two, or variable speed calculations

is that HSPF contains binning and fractional hours for six different climates. The only climate that is reported on is climate IV, yet the rating procedure does acknowledge that climate plays a significant role in the seasonal energy efficiency.

Region Number	I	II	III	IV	V	VI
Heating Load Hours, HLH	750	1250	1750	2250	2750	*2750
Outdoor Design Temperature, T_{OD}	37	27	17	5	-10	30
j T_j (°F).....	Fractional Bin Hours n_j/N					
1 62.....	.291	.215	.153	.132	.106	.113
2 57.....	.239	.189	.142	.111	.092	.206
3 52.....	.194	.163	.138	.103	.086	.215
4 47.....	.129	.143	.137	.093	.076	.204
5 42.....	.081	.112	.135	.100	.078	.141
6 37.....	.041	.088	.118	.109	.087	.076
7 32.....	.019	.056	.092	.126	.102	.034
8 27.....	.005	.024	.042	.087	.094	.008
9 22.....	.001	.008	.021	.055	.074	.003
10 17.....	0	.002	.009	.036	.055	0
11 12.....	0	0	.005	.026	.047	0
12 7.....	0	0	.002	.013	.038	0
13 2.....	0	0	.001	.006	.029	0
14 -3.....	0	0	0	.002	.018	0
15 -8.....	0	0	0	.001	.010	0
16 -13.....	0	0	0	0	.005	0
17 -18.....	0	0	0	0	.002	0
18 -23.....	0	0	0	0	.001	0
* Pacific Coast Region.						

Figure B.3: Binning for HSPF rating procedure

The HSPF calculation procedure has a similar principal equation as the SEER calculation, in that it is a load met divided by the energy required to meet the load :

$$HSPF = \frac{\sum_{j=1}^J n_j * BL(T_j)}{\sum_{j=1}^J e_h(T_j) + \sum_{j=1}^J RH(T_j)} * F_{def} = \frac{\sum_{j=1}^J [\frac{n_j}{N} * BL(T_j)]}{\sum_{j=1}^J \frac{e_h(T_j)}{N} + \sum_{j=1}^J \frac{RH(T_j)}{N}} * F_{def} \quad (B.18)$$

Where:

- The summations are from $j=1$ to J , where J is the number of bins with non-zero fractional hours (this value changes depending on which climate one is working with)
- $\frac{n_j}{N}$ is the fractional hours for the specific bin j
- $BL(T_j)$ is the building load for that temperature bin [Btu/h]
- $e_h(T_j)$ is the annual electricity consumed by the heat pump during periods when the outdoor temperature was in the bin T_j [W]
- $RH(T_j)$ is the annual electricity consumed by the resistive element during periods when the outdoor temperature was in the bin T_j [W]
- F_{def} is the defrost demand credit (for details see [1])

The main difference with the HSPF rating process is that it is assumed that the building heating load is always met. The load is either met by the heat pump (the $e_h(T_j)$ term) or the backup resistive element (the $RH(T_j)$ term).

The calculation of the individual terms of equation (B.18) will now be defined.

$$BL(T_j) = \frac{65 - T_j}{65 - T_{OD}} * DHR * 0.77 \quad (B.19)$$

Where T_{OD} is the outdoor design temp (see figure B.3), 0.77 is a correction factor, and DHR is the design heating requirement, defined as:

$$DHR_{min} = \dot{Q}_h(47) * \left[\frac{65 - T_{OD}}{60} \right] \quad (B.20)$$

for all regions except region V, and $DHR_{min} = \dot{Q}_h(47)$ for region V. $\dot{Q}_h(47)$ is expressed in Btu/h. The DHR used in equation (B.19) is DHR_{min} rounded to the nearest 5,000 if it is less than 40,000, and rounded

to the nearest 10,000 if it is greater than 40,000. There is also a DHR_{max} , yet this is not used for the reported HSPF.

The energy used by the heat pump and resistive element are defined by the following equations:

$$\frac{e_h(T_j)}{N} = \frac{X(T_j) * \dot{E}_h(T_j) * \delta(T_j)}{PLF_j} * \frac{n_j}{N} \quad (\text{B.21})$$

$$\frac{RH(T_j)}{N} = \frac{BL(T_j) - [X(T_j) * \dot{Q}_h(T_j) * \delta(T_j)]}{3.413 \frac{\text{Btu/h}}{\text{W}}} * \frac{n_j}{N} \quad (\text{B.22})$$

Where:

- $X(T_j) = BL(T_j)/\dot{Q}(T_j)$ or 1, whichever is less
- $PLF_j = 1 - C_D^h * (1 - X(T_j))$
- $\delta(T_j)$, the low temperature cut-out, is 0 if $T_j \leq T_{off}$ or $\frac{\dot{Q}(T_j)}{3.413 * \dot{E}(T_j)} < 1$, is 0.5 if $T_{off} < T_j \leq T_{on}$ and $\frac{\dot{Q}(T_j)}{3.413 * \dot{E}(T_j)} \geq 1$, and is 1 if $T_j > T_{on}$ and $\frac{\dot{Q}(T_j)}{3.413 * \dot{E}(T_j)} \geq 1$ (T_{on} and T_{off} being the outdoor temperature for automatic shut off and turn on if applicable)
- $\dot{Q}_h(T_j)$ and $\dot{E}_h(T_j)$ are the capacity and power consumption respectively at the outdoor temperature T_j in [Btu/h] and [W].

It can be seen that the low temperature cut-out ($\delta(T_j)$) and the load factor ($X(T_j)$) are used in conjunction to determine the portion of load met by the heat pump and the portion met by the backup element. When the instantaneous COP ($\dot{Q}(T_j)/[3.413 * \dot{E}(T_j)]$) is less than 1 or the outdoor temperature bin is less than the automatic cut-out, it is assumed that the heat pump will not operate. This is seen by the $\delta(T_j)$ term zeroing out equation (B.21) and setting equation (B.22) equal to the building load. When the instantaneous COP is above 1 (and the cut-out is above T_{on}) the heat pump meets as much of the load as possible, and the resistive element only being called for when $BL(T_j) > \dot{Q}(T_j)$.

The terms $\dot{Q}_h(T_j)$ and $\dot{E}_h(T_j)$ are calculated as follows:

$$\dot{Q}_h(T_j) = \begin{cases} \dot{Q}_h(17) + \frac{(\dot{Q}_h(47) - \dot{Q}_h(17)) * (T_j - 17)}{47 - 17} & \text{if } T_j \geq 45^\circ\text{F or } T_j \leq 17^\circ\text{F} \\ \dot{Q}_h(17) + \frac{(\dot{Q}_h(35) - \dot{Q}_h(17)) * (T_j - 17)}{35 - 17} & \text{if } 17^\circ\text{F} < T_j < 45^\circ\text{F} \end{cases} \quad (\text{B.23})$$

$$\dot{E}_h(T_j) = \begin{cases} \dot{E}_h(17) + \frac{(\dot{E}_h(47) - \dot{E}_h(17)) * (T_j - 17)}{47 - 17} & \text{if } T_j \geq 45^\circ\text{F or } T_j \leq 17^\circ\text{F} \\ \dot{E}_h(17) + \frac{(\dot{E}_h(35) - \dot{E}_h(17)) * (T_j - 17)}{35 - 17} & \text{if } 17^\circ\text{F} < T_j < 45^\circ\text{F} \end{cases} \quad (\text{B.24})$$

where $\dot{Q}_h(47)$, $\dot{Q}_h(35)$, and $\dot{Q}_h(17)$ are determined by the H1, H2, and H3 tests respectively (similarly for the \dot{E}_h values). This completes the necessary equations for calculation of the single stage HSPF.

B.2.2 Two Stage Units

The calculation of HSPF for two stage heat pumps follows a very similar layout as the two stage SEER calculation. Three different operating regions are defined: cycling (between off and low), between speeds, and full operation at high speed.

For complete details on the calculation procedures, the reader is referred to [1]. The process is not described in full here seeing as most of the insights regarding the calculation procedure have been described either in the discussion of two stage SEER calculation or single stage HSPF calculation.